"NICKEL PRECIPITATION BY OZONE OXIDATION IN A SEMI-BATCH BUBBLE REACTOR"

Luis Enrique Calzado Palomino

Department of Mining, Metals and Materials Engineering
McGill University, Montreal

"A thesis submitted to McGill University in partial fulfillment of the requirements for the degree of Doctor of Philosophy"

May, 2003

ABSTRACT

The research aims to develop the use of ozone in nickel oxidation-precipitation from dilute solutions. The process presents three main steps: ozone transfer from gas to liquid, ozone decomposition by hydroxyl ions, and nickel oxidation-precipitation. Each step was studied using a semi-batch bubble reactor. For ozone gas-liquid transfer, a methodology to calculate the volumetric mass transfer coefficient ("k_La") was developed. Parameters evaluated included: diffuser porosity, volume of liquid and superficial gas velocity. To calculate the mass transfer coefficient ("k_L") interfacial area ("a") is estimated from gas holdup and bubble size measurements. Ozone decomposition by OH^- was examined as a function of pH and two ranges were identified, above and below pH 7.2. A kinetic equation for pH > 7.2 is proposed. Decomposition rate below pH 7.2 is low and considered negligible. Ozone oxidation-precipitation of nickel (II) in aqueous sulfate solution was determined as a function of pH, ozone and nickel concentration. X-ray diffraction (XRD) analysis determined that the products comprised $Ni(OH)_2$, NiOOH, $Ni_3O_2(OH)_4$ and $Ni_2O_2(OH)_4$. From the pattern of ozone consumption and the XRD results the proposed reaction sequence is hydrolysis – precipitation – oxidation rather than oxidation – hydrolysis – precipitation suggested in the literature.

RÉSUMÉ

La recherche a comme but le développement de l'utilisation de l'ozone pour l'oxydation et la précipitation du nickel des solutions diluées. Le procédé présente trois étapes principales: le transfert d'ozone de gaz au liquide, la décomposition de l'ozone par ions hydroxyle et la précipitation et, l'oxydation du nickel. Chaque étape est étudiée en utilisant un réacteur demi-cuvée de bulle. Pour le transfert d'ozone du gaz au liquide, une méthode pour le calcul du coefficient de transfert de masse volumétrique ("k_La") a été développée. Parmi les paramètres évalués, il y la porosité du émulgateur, le volume du liquide et la vélocité du gaz superficiel. Pour le calcul du coefficient de transfert de masse ("k_L"), l'aire interfaciale ("a") est estimée de la retenue du gaz et la mesure de la grandeur de la bulle. L'ozone décomposé par OH^- a été examiné en fonction du pH, et deux intervalles ont été évalués, au-dessus et au-dessous de 7.2. Une équation cinétique pour pH > 7.2 est proposée. La vélocité de décomposition en dessous du pH 7.2 est faible et négligeable. L'oxydation du nickel (II) dans la solution aqueuse du sulfate est déterminée en fonction de pH, concentrations d'ozone et nickel. L'analyse en diffraction de rayon X détermine que les produits sont un mélange de $Ni(OH)_2$, NiOOH, $Ni_3O_2(OH)_4$ et $Ni_2O_2(OH)_4$. Compte tenu des tendances de la consommation d'ozone et des résultats en diffraction X la séquence de réaction proposée est hydrolyse – précipitation – oxydation plutôt qu'oxydation - hydrolyse – précipitation, telle que proposée dans la littérature.

ACKNOWLEDGMENTS

I express my sincere appreciation and gratitude to Professor J. A. Finch for his advice, encouragement and support during the course of this research.

I thank to Professor R. Harris for his moral support, advice and gentleness in answering my questions.

Special thanks are extended to Dr. C. O. Gomez for the invaluable input to this work and for time passed in fruitful discussion and teaching me the different topics of this research.

I thank to Dr. S. R. Rao and Dr. J. Jara for their guidance and recommendations during the period of work.

I thank Inco, Teck-Cominco, Noranda, Falconbridge, Corem and the Natural Sciences and Engineering Research Council of Canada (NSERC) for funding under the NSERC University-Industry Collaborative Research and Development Program.

Thanks at McGill University, mineral processing group, H. B. Kim and members of Department of Mining, Metals and Materials Engineering for their support and their friendship.

To my wife Elena and our children, Luis, Kathia and Lionel.

I express my profound gratitude for they willingness to surrender a lot of hours that properly belonged to them so that this work might be done.

TABLE OF CONTENTS

LIST OF FIGURES

LIST OF TABLES

LIST OF APPENDICES

NOMENCLATURE

a	interfacial area (m^{-1})
C^*_G	equilibrium concentration gas phase (mol L^{-1})
C^*_L	equilibrium concentration liquid phase (mol L^{-1})
C_i	concentration of "i" specie (mol L^{-1})
C_{io}	concentration of "i" specie in the interface (mol L^{-1})
C_G	gas concentration (mol L^{-1})
C_{Gi}	interface gas concentration (mol L^{-1})
C_L	liquid concentration (mol L^{-1})
C_{Li}	interface liquid concentration (mol L^{-1})
c	solute concentration in liquid phase (mol L^{-1})
c*	solute concentration in equilibrium (mol L^{-1})
D	molecular diffusion coefficient ($m^2 s^{-1}$)
D_L	radial dispersion coefficient (m)
d_i	bubble diameter (m)
$d_{3,2}$	Sauter mean diameter (m)
E_L	coefficient of axial dispersion in the liquid phase ($m^2 s^{-1}$)
H	Henry's law constant
J_i	flux with respect to mixture (mol $m^{-2} s^{-1}$)
J_G	superficial gas velocity (cm s^{-1})
k	mass transfer coefficient (m s^{-1})
k'	pseudo first order rate constant for a given pH value (s^{-1})
K	Solubility product
K_La	overall mass transfer coefficient (s^{-1})
k_G	gas film mass transfer coefficient (m s^{-1})
k_Ga	volumetric mass transfer coefficient in gas phase (s^{-1})
k_L	liquid film mass transfer coefficient (m s^{-1})
k_La	volumetric mass transfer coefficient in liquid phase (s^{-1})

k_La_{20}	k_La at 20 °C
k_La_T	k_La at temperature T (°C)
n	power of the molecular diffusion coefficient, varying from 0.5 to 1
[Ni]	nickel concentration (mol L^{-1})
N_i	flux with respect to interface (mol m^{-2} s^{-1})
N_{O3}	ozone flux with respect to interface (mol m^{-2} s^{-1})
$[O_3]$	ozone concentration (mol L^{-1})
$[O_3]_g$	ozone concentration in gas phase (mol L^{-1})
$[O_3]_{g\ in}$	ozone concentration inlet in gas phase (mol L^{-1})
$[O_3]_{g\ out}$	ozone concentration outlet in gas phase (mol L^{-1})
$[O_3]_{l\ (i)}$	ozone concentration in the interface (mol L^{-1})
$[O_3]_l$	ozone concentration in the bulk (mol L^{-1})
$[O_3]_{liq}$	ozone concentration in liquid phase (mol L^{-1})
$[OH^-]$	hydroxide concentration (mol L^{-1})
pO_3	ozone partial pressure (Pa)
pO_2	oxygen partial pressure (Pa)
P_{or}	absolute pressure at the orifice (Pa)
$P_{reactor}$	reactor pressure (Pa)
Q_{or}	orifice reading on site (L/min)
$Q_{reactor}$	gas flow rate to the reactor (L/min)
R	mass transfer flux (mol m^{-2} s^{-1})
R_L	film resistance to mass transfer in liquid phase (s)
R_G	film resistance to mass transfer in gas phase (s)
R_T	total resistance to mass transfer (s)
r	specific mass transfer rate (mol L^{-1} s^{-1})
T_{or}	orifice temperature (K)
$T_{reactor}$	reactor temperature (K)
t	time (s)
U_G	superficial gas velocity (m s^{-1})

U_L	superficial liquid velocity (m s^{-1})
V	solution volume (L)
y	solute concentration in gas phase (mol L^{-1})
W_{O2}	gas mass flow (mol O_2/ min)
Xin	gas inlet ozone concentration (mol O_3 / mol O_2)
Xout	gas outlet ozone concentration (mol O_3 / mol O_2)
z	distance (m)

Greek Letters

ε	fraction of the total volume occupied by the gas
θ	temperature correction factor (1.024)
δ	thickness of the film (m)

CHAPTER 1

Introduction

Heavy metals in aqueous solutions from industrial and mine effluents pose a significant environmental threat. They are commonly precipitated by neutralization using alkaline reagents, usually lime. The product is a voluminous sludge containing unstable metal hydroxides. This material requires continued management to avoid the possibility of re-dissolution by drifts in pH.

To avoid precipitating hydroxides, oxidation technologies are emerging as alternatives in the elimination of metallic ions. Powerful oxidants are used to produce selective oxidation and precipitation of metals. One such oxidant is ozone. Much research on its use has been conducted in the case of municipal waters. A new trend is to apply ozone to remove and recover metals from mining and metallurgical effluents (Sato and Robbins, 2000). The many opportunities to exploit the high oxidation potential of ozone continue to drive applications and concurrent investigations into the reaction mechanisms (Gottschalk et al., 2000).

In this work, I contemplate one application of ozone, the selective precipitation of nickel oxide from dilute solutions generated in mining and processing Ni-ores. Three aspects of such of process need to be considered: mass transfer of gaseous ozone into the aqueous phase, the rate of decomposition of absorbed ozone by reaction with hydroxyl ions and the rate of oxidation and precipitation of nickel. To understand and clarify each aspect, a summary of important related concepts is presented in Chapter 2.

In the experiments conducted, the need to produce and dispose of nickel solutions prompted the use of a semi-batch reactor, i.e., continuous gas and batch liquid. The set up is described in Chapter 3.

The study of ozone gas-to-liquid mass transfer involved devising a methodology suited to the batch reactor to determine the volumetric mass transfer coefficient ("k_La"), and measurement of the specific interfacial area ("a") to derive the mass transfer coefficient ("k_L"). The methodology and test work are presented in Chapter 4.

Possible decomposition of ozone by side reactions in water is an important consideration. Chapter 5 addresses the kinetics of decomposition produced by hydroxide. The decomposition was examined as a function of pH, and two ranges were evaluated, above and below pH 7. The test work included the inhibition effect produced by sodium carbonate.

Chapter 6 concerns the ozonation of nickel in dilute solutions. The required pH to oxidize and precipitate nickel as the oxy-hydroxide was determined. The effect of variation in ozone gas concentration and nickel concentration was examined. The Chapter presents results identifying the role of the precipitate on ozone consumption. The precipitate is characterized by X-ray diffraction.

Chapter 7 outlines the important conclusions, claims to originality, and recommendations for future work.

CHAPTER 2

Literature Review

2.1 Introduction

The traditional method of using lime to precipitate metallic ions from effluents such as acid mine drainage has resulted over the years in the accumulation of significant amounts of sludge (the precipitation product). This accumulated material poses a hazard (hydroxides can re-dissolve by varying the pH) but also represents a possible secondary source of metals. For example, nickel in some sludges in the Sudbury area makes up 5% by weight. To recover the Ni, a two-step process, leaching of the sludge by sulphuric acid followed by selective precipitation as nickel hydroxide or sulphide, has been proposed. A possible alternative precipitation step is by oxidation of nickel to the Ni(III) state using ozone (Nikolic et al., 1978). Demonstration of the technical feasibility, identification of the reaction pathway and characterization of the reaction products are the topics of this thesis. The process involves three stages: ozone mass transfer from gas to liquid, ozone decomposition by side reactions in water, and nickel precipitation as a oxy-hydroxide. In this Chapter, I review the issue of heavy metal contamination and the proposed ozonation process.

2.2 Heavy metals contamination

Heavy metals constitute the group of transition metals, the actinide series (uranium, neptunium, plutonium, and americium), the lanthanide series, and three elements of the metalloids group (arsenic, tellurium, selenium) (Rorrer, 1995). The term heavy metal and transition metal are often used interchangeably.

Heavy metals can exist in either water-soluble or insoluble form. Most common salts of heavy metals are soluble in water, including chloride, sulphate, and nitrate salts (Stephenson, 1987). Heavy metals are hydrolysable and exist in solution as various oxymetal anions and metal hydroxy cations.

Sources of heavy metals in effluents are diverse, but the metals-related industries are the largest contributors. Primary sources include mining and mineral processing operations, which gives rise to so-called acid mine drainage (AMD). Acid is produced by oxidation of sulphide minerals promoted by bacterial action, which in turn dissolves metals (Allan, 1995).

2.3 Technologies for treatment of heavy metals

Available technologies for removal of metallic ions from aqueous solution are given in Figure 2.1 with comparative notes in Table 2.1. The advantages of one process over another are not clear-cut and many process options may initially appear suitable. The destination of the stream can have a significant bearing on the selection of a process. The value, purity, and amount of the recovered metal are other considerations (Reed, 1998).

Water treatment by chemical precipitation with lime is frequently used to treat AMD (Rorrer, 1998). This process generates a concentrated heavy metal sludge that could be considered as a secondary source of metals. The sludges are unstable to pH variations necessitating a costly secured hazardous landfill site. Further treatment is therefore desirable.

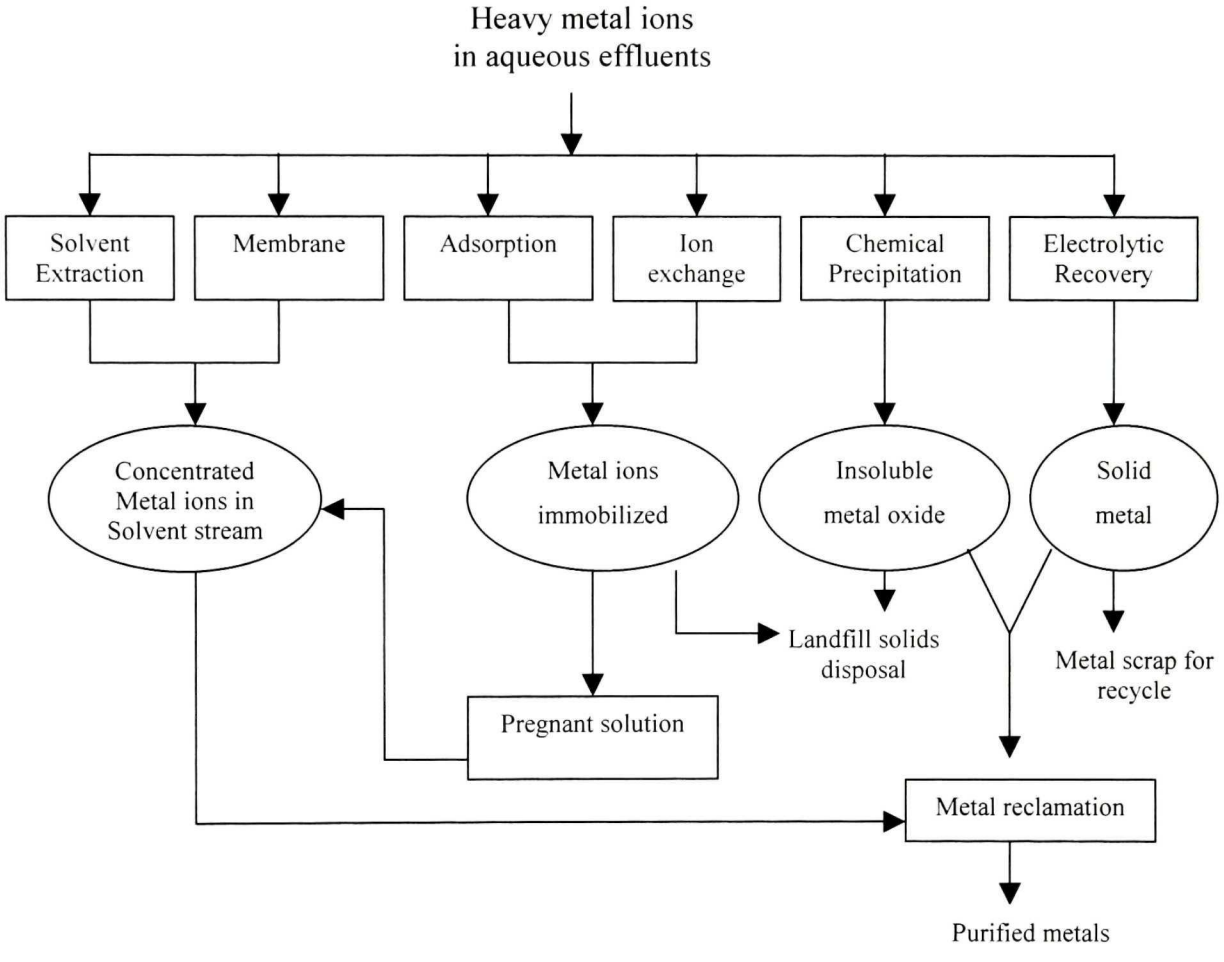

Figure 2.1. Summary of available chemical process technologies for heavy metal ion removal from wastewater (Source Wiley Encyclopedia Series in Environmental Science, Vol. 4, 1998)

Table 2.1. Comparison of chemical process technologies for heavy metal ion removal (Source: Environmental Analysis and Remediation, Vol. 4, 1998)

Process	Chemical/Energy Input	Metal Reclamation	Major Advantages	Major Disadvantages
Chemical precipitation	Precipitant, flocculant, acid base; mixing and fluid handling	Metal sludge	Well established, low effluent concentrations	High chemical dosages, several unit operations
Electrolytic recovery	Electrical power	Solid metal scrap	Well established; direct recovery of solid metal; no chemical consumption	Energy intensive; high capital costs; reduced efficiency at dilute concentrations
Ion-exchange	Regenerated solutions; fluid handling	Concentrated soluble metal stream	Highly selective, effectiveness <100 ppm	Chemical regeneration requirements, adsorbent expense; prone to fouling in mixed waste streams
Disposable adsorbents	Replacement adsorbent; fluid handling	Metal immobilizes on solid adsorbent	Simple metal remove process; low adsorbent cost; effective <100 ppm	Selectivity, recurring cost of new adsorbent, disposal cost of spent adsorbent
Membranes	Extractant for liquid-supported membrane; fluid handling	Concentrated soluble metal stream	Selective; continuous concentrated metal solution recycle	Membrane durability, fouling
Liquid-liquid extraction	Organic solvent/water contact: loading and stripping in mixer and settlers	Concentrated soluble metal stream	Selective; continuous concentrated metal solution recycle	Capital costs; solvent emissions to air/water; solvent disposal

2.4 Ozone as an oxidant

The oxidizing action of ozone involves one of the oxygen atoms being reduced while the other two form molecular oxygen (Bard et al., 1985). The redox reaction of the ozone-water couple is represented by the following reactions:

Acid solutions:

$$O_3 + 2H^+ + 2e^- = O_2 + H_2O \qquad E^o = 2.075\ V \qquad (2.1)$$

Then

$$E_h\ (volts) = 2.075 - 0.059\,pH + 0.0295 \log\left(\frac{pO_3}{pO_2}\right) \qquad (2.2)$$

Alkaline solutions:

$$O_3 + H_2O + 2e^- = O_2 + 2OH^- \qquad E^o = 1.246\ V \qquad (2.3)$$

Then

$$E_h\ (volts) = 1.246 - 0.059 \log[OH^-] + 0.0295 \log\left(\frac{pO_3}{pO_2}\right) \qquad (2.4)$$

An efficient ozone generator using air produces up to 2 volume percent (i.e., $pO_3 = 2.0176 \times 10^3$ Pa), so the practical upper limit of Eh for solution saturated with ozone is given by $E_h\ (volts) \approx 1.78 - 0.059\ pH$. Potential can be increased when ozone is produced using oxygen; in the present work, the range of ozone produced is between 0.567×10^3 Pa (2.5×10^{-4} mol/L O_3) to 2.079×10^3 Pa (9.17×10^{-4} mol/L O_3).

2.5 Ozone potential – pH equilibrium diagram

Depending on ozone pressure and whether the solution is acidic or basic, the potential – pH equilibrium diagram is constructed using Equation (2.2) or (2.4). Figure 2.2 shows the proportion of ozone becomes predominant relative to oxygen at potentials above line (4'); however, the equilibrium pressure O_3/O_2 is high (1.01325×10^{62} Pa).

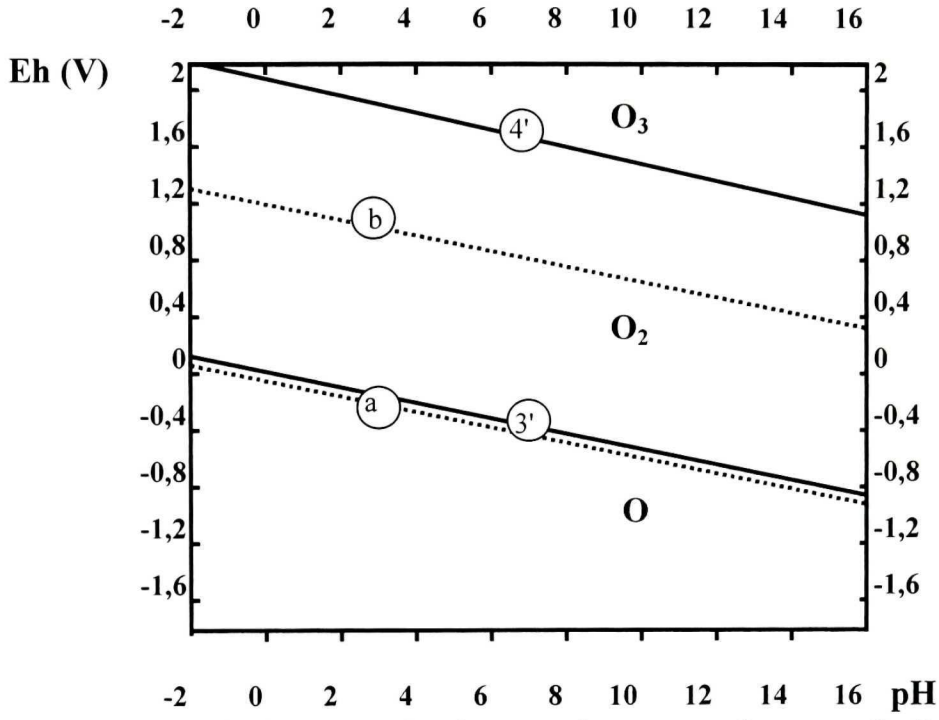

Figure 2.2. Domains of relative predominance of gaseous substances O, O_2 and O_3 at 25 °C (Pourbaix, 1974)

2.6 Ozone mass transfer gas to liquid

When a gas containing a soluble compound is placed in contact with water, resistance to mass transfer will produce a concentration gradient in each phase (Figure 2.3). One of the models proposed to characterize mass transfer assumes that this resistance is equal to the sum of the resistance in each phase (Lewis and Whitman, 1924); this is called the "two-film" theory or "two-resistance" theory (Treybal, 1980).

According to Charpentier (1981), physical and chemical interaction between gas and liquid phases involves diffusional resistance located in the laminar film around the interface. Several models assume negligible resistance in the bulk fluid compared to the resistance in the laminar film.

Fick's first law of diffusion is used to describe mass transfer through the laminar film to the phase boundary (Wesselingh, 1990). Regardless of the boundary conditions

assumed the film mass transfer coefficient is predicted to be proportional to some power of the molecular diffusivity, "D", (Gottschalk et al., 2000); i.e.,

$$k \propto D^n \tag{2.5}$$

Dobbins (1964) claims the "n" value depends on the degree of agitation in the system and will equal 0.5 where the system is turbulent and 1 where it is laminar.

From the two-film theory, it is possible to predict the rate of transfer of a substance from one phase to another. According to Roustan (1982), the equation of transfer may be written:

$$R = k_G (C_G - C_{Gi}) = k_L (C_{Li} - C_L) \tag{2.6}$$

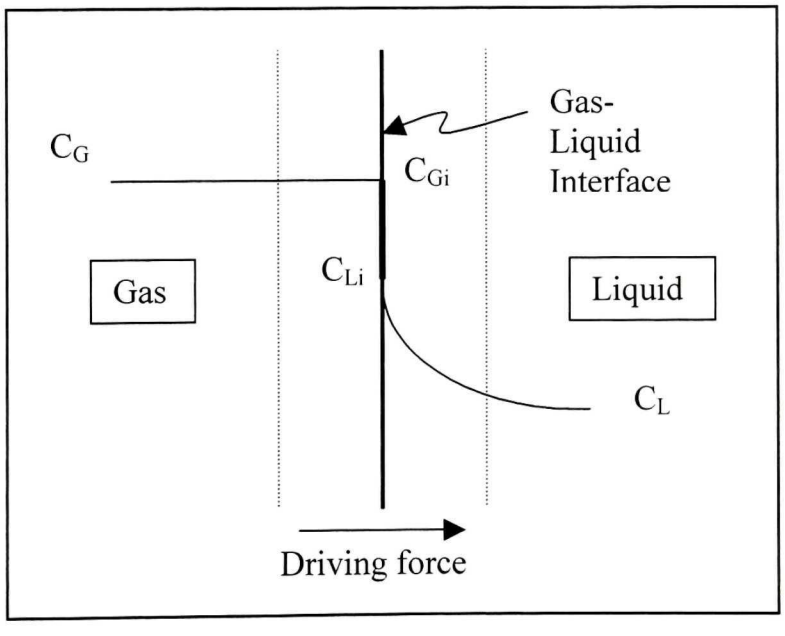

Figure 2.3. Two-film theory with concentration profile shown

To calculate the specific rate of mass transfer into the liquid, the specific interfacial area "a" is required (Equation 2.7), where "a" is transfer surface area per unit volume of liquid (Tatterson, 1991).

$$r = k_L a\left(C_{Li} - C_L\right) \tag{2.7}$$

Film coefficients "k_G" and "k_L" are not normally determined, the volumetric mass transfer coefficient (k_La) being more commonly used (Beenackers and Van Swaaij, 1993). The "k_La" is defined as the difference between the bulk concentration of one phase (C_G or C_L) and the equilibrium concentration (C^*_G or C^*_L) corresponding to the bulk concentration in the other phase. If the controlling resistance is in the liquid phase, the volumetric mass transfer is transformed to the overall mass transfer coefficient for the liquid (K_La). Then Equation 2.7 can be written as:

$$r = k_L a\left(C_{Li} - C_L\right) = k_G a\left(C_G - C_{Gi}\right) = K_L a\left(C_L^* - C_L\right) \tag{2.8}$$

Henry's law is used to describe the equilibrium distribution of a substance between the bulk concentration in the liquid and gas phases. Gottschalk et al. (2000) presents a relationship of the overall and interfacial concentration differences (Figure 2.4) and the following is obtained:

$$H = \frac{C_G - C_{Gi}}{C_L^* - C_{Li}} = \frac{C_{Gi} - C_G^*}{C_{Li} - C_L} \tag{2.9}$$

Passing the function through the origin, it simplifies to:

$$H = \frac{C_{Gi}}{C_{Li}} = \frac{C_G^*}{C_L} = \frac{C_G}{C_L^*} \tag{2.10}$$

Consequently the equilibrium concentration can be calculated from Henry's constant and the bulk concentration.

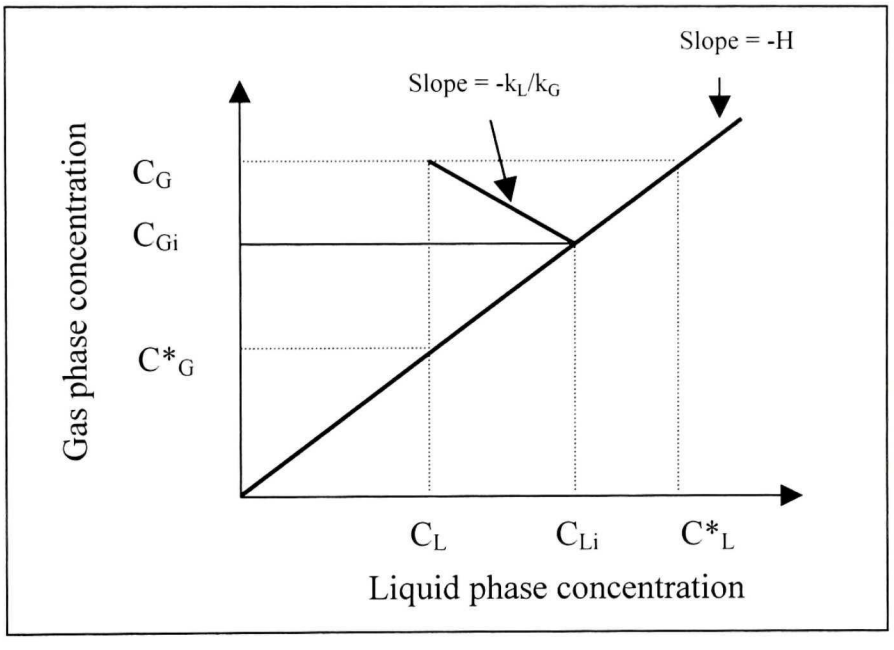

Figure 2.4. Overall and interfacial concentration differences (Gottschalk et al., 2000)

Lewis and Whitman (1924) provided a relationship between overall mass transfer and film mass transfer as a function of film resistance:

$$R_T = R_L + R_G = \frac{1}{K_L a} = \frac{1}{k_L a} + \frac{1}{Hk_G a} \tag{2.11}$$

where:

$$K_L a = k_L a \frac{R_L}{R_T} \qquad (2.12)$$

If the major resistance is in the liquid phase, the ratio R_L / R_T is close to 1, and the overall mass transfer coefficient will be equal to the liquid mass transfer coefficient.

Resistance is affected by several parameters yielding different gradients of concentration. These parameters are classified into two groups: process and physical parameters (Table 2.2).

Table 2.2. Parameters that influence mass transfer

Process parameters	Physical parameters
Power	Kinematic viscosity
Volume	Density
Superficial gas velocity	Surface tension
Gravitational	Bubble coalescence
	Diffusion coefficient

Any chemical reactions also have an influence because they alter the composition of the gas as it passes to the liquid phase.

Methods to determinate mass transfer coefficient depend on the reactor used (Song, 1990). Reactors can be classified in three general types (Levenspiel, 1999): batch, steady state flow and unsteady state flow. The last type of reactor is normally used when there are no chemical reactions. Where a chemical reaction occurs, the steady state reactor is preferred. Experimental determination of the mass transfer coefficient is based on deriving the appropriate mass balance of the process (Roustan et al., 1996).

A general schematic of mass transfer for a continuous element in a liquid-gas process is shown in Figure 2.5.

A material balance expression for any reactant (or product) is the following:

Rate of flow into element	=	Rate of flow out of element	+	Rate of accumulation	+	Rate of reaction

Ozonation is a typical gas-liquid mass transfer process. Different assumptions have been made. Sotelo et al., (1989) assumed that there is no resistance in the gas phase during the absorption step, the only resistance being found in the liquid film near the interface. Kinman (1972) observed that ozone is unstable in the liquid phase and decomposes to oxygen at a rate dependent on temperature. Malleaville (1982) claimed ozone decomposition produces a steady-state aqueous concentration different from the solubility concentration in regions where mass transfer is limiting, this concentration being less than the saturation (equilibrium) concentration.

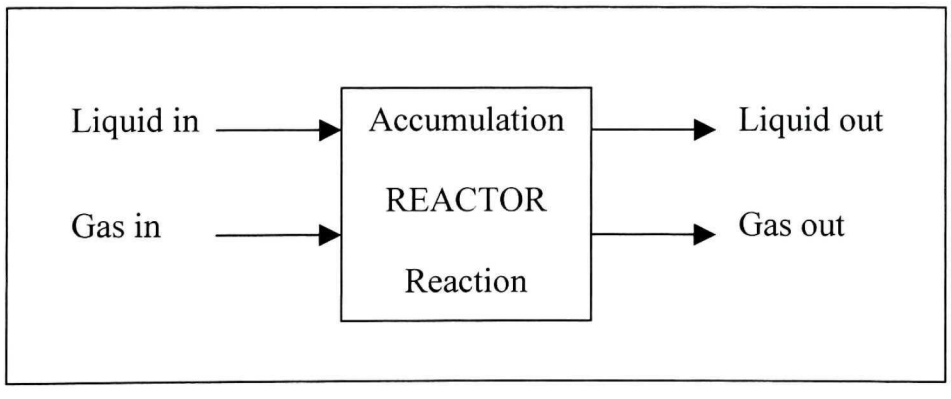

Figure 2.5. Material balance for an element in the liquid-gas process

For dilute non-reacting solutions, Henry's Law describes the equilibrium distribution of a gas between the bulk liquid and gas phases (Roustan and Malleaville,

1982). Henry's Law constant is difficult to measure as the presence of impurities, ozone decomposition and ionic strength changes produce variations (Sotelo et al., 1989).

Several reactor designs have been considered to determine the mass transfer coefficient, each with its own characteristics. Specifically for a multiphase column reactor, Rice (1990) developed differential equations predicting the concentration profile of reactants and products. He assumed that the gas moves in plug flow and the liquid is perfectly mixed only by the gas; the equation for any single component was written as:

$$\frac{\partial c}{\partial t} = D_L \frac{\partial^2 c}{\partial z^2} - U_L \frac{\partial c}{\partial z} + k_L a\ (c^* - c) \tag{2.13}$$

$$\frac{\partial y}{\partial t} = -U_G \frac{\partial y}{\partial z} - k_L a \frac{1-\varepsilon}{\varepsilon}(c^* - c) \tag{2.14}$$

Equation 2.14 makes it possible to calculate the volumetric mass transfer coefficient in a semi-batch reactor based on the mass balance and behavior of the gas when passing through the reactor.

A method to determinate the mass transfer coefficient ($k_L a$) in the ozone – water system called the "dynamic electrode method" is described by Bin et al. (2001). The interpretation from the response of the ozone electrodes is by differential mass balance equations (neglecting dispersion in the gas phase) for gas and liquid using the following:

Gas phase

$$-\frac{\partial (U_G C_G)}{\partial z} - (k_L a)\left(\frac{C_G}{H} - C_L\right) = \varepsilon\left(\frac{\partial C_G}{\partial t}\right) \tag{2.15}$$

Liquid phase

$$D_L \frac{\partial^2 C_L}{\partial z^2} + (k_L a)\left(\frac{C_G}{H} - C_L\right) - (1 - \varepsilon)\left(\frac{\partial C_L}{\partial t} + k_d C_L^m\right) = 0 \qquad (2.16)$$

where "k_d" and "m" are the kinetic constant of ozone decomposition (s^{-1}) and reaction order, respectively.

2.7 Ozone decomposition by hydroxide ions

The decomposition of ozone in aqueous solution has been studied for several decades and various mechanisms have been proposed (Langlais et al., 1991). Decomposition kinetics have also been addressed with no agreement as to the order of the reaction and the magnitude of the reaction rate constants (Peleg, 1976). Various orders and combinations have been proposed (Tomiyasu et al., 1985). Since many of the studies were not under comparable conditions (ozone concentration, pH, with/without buffers, presence of possible scavengers and promoters, etc.) it is difficult to reach conclusions from the literature.

Alder and Hill (1950) measured the decomposition rate by iodometric and spectrophometric methods with differing results. They postulated that the iodometric method gave the total reducible ozone and proposed the following mechanism for O_3 decomposition:

$$O_3 + H_2O \xrightarrow{k_1} HO_3^+ + OH^- \qquad (2.17)$$

$$HO_3^+ + OH^- \xleftrightarrow{k_2, k'_2} 2HO_2 \qquad (2.18)$$

$$O_3 + HO_2 \xrightarrow{k_3} HO + 2O_2 \qquad (2.19)$$

$$HO + HO_2 \xrightarrow{k_4} H_2O + O_2 \qquad (2.20)$$

Steps (2.17) and (2.19) are responsible for O_3 disappearance (consumption) in water and were assumed to be relatively slow and rate controlling. Step (2.18) was assumed to represent equilibrium. The rate equations were solved under the assumption that:

$$\frac{d[HO]}{dt} = 0; \quad \frac{d[HO_2]}{dt} = 0; \quad \frac{d[HO_3^+]}{dt} = 0 \qquad (2.21)$$

These quasi-steady-state approximation lead to the following intermediate equation:

$$\frac{d[O_3]}{dt} = -3k_3 [HO_2][O_3] \qquad (2.22)$$

that is, first order with respect to ozone. When step (2.18) was included, K being the equilibrium constant, Equation (2.22) became:

$$\frac{d[O_3]}{dt} = -3k_3 K^{0.5} [HO_3]^{0.5} [OH^-]^{0.5} [O_3] \qquad (2.23)$$

which indicates a pH dependency for the rate of ozone decomposition.

Results by Stumm (1954) at high pH indicated that the reaction was first order with respect to ozone concentration and varied with $[OH^-]$ as follows:

$$\frac{d[O_3]}{dt} = - k [OH^-]^{0.75} [O_3] \qquad (2.24)$$

where "k" is the reaction rate constant and the total order is 1.75. Rothmund and Burgstaller, referenced in Hewes and Davison (1971), studied the decomposition of ozone in a batch system from pH 2 to 4 at 0 °C and concluded that the total reaction was second order. Sennewald (1933) investigated the rate of ozone decomposition in a batch system from pH 5.3 to 8 at 0 °C. He found the reaction was second order and reported a rate increase with pH. Hewes and Davison's (1971) concluded that the rate and order of decomposition of ozone in water are pH dependent.

Weiss (1935), Staehelin et al. (1982) and Tomiyasu et al. (1985) proposed a chain of reactions, which they grouped into three steps: initiation, propagation, and termination. Various chemical species play a role in the three steps; these substances, reflective of their action, are called initiators, promoters and inhibitors (or scavengers) (Staehelin and Hoigné, 1985). Table 2.3 is a resume of the principal species identified. Following is a description of the steps.

Table 2.3. Typical initiators, promoters and inhibitors for decomposition of ozone in water

Initiator	Promoter	Inhibitor or Scavenger
OH^-	Humic acid	HCO_3^-/CO_3^{2-}
H_2O_2/HO_2^-	Aryl-R	PO_3^{4-}
Fe^{2+}	Primary and secondary alcohols	Humic acid
	Ozone	Alkyl-R

Initiation: The interaction of hydroxide ions and ozone induces formation of the superoxide anion radical O_2^{*-} and the hydroperoxyl radical HO_2^*,

$$O_3 + OH^- \rightarrow O_2^{*-} + HO_2^* \quad (2.25)$$

The hydroperoxyl radical is in acid-base equilibrium,

$$O_2^{*-} + H^+ \leftrightarrow HO_2^* \quad (2.26)$$

Propagation: Reaction between ozone and the superoxide anion radical produces the ozonide radical ion O_3^{*-} which decomposes immediately into the OH^* radical,

$$O_3 + O_2^{*-} \rightarrow O_3^{*-} + O_2 \quad (2.27)$$

$$HO_3^* \leftrightarrow O_3^{*-} + H^+ \quad (2.28)$$

$$HO_3^* \rightarrow OH^* + O_2 \quad (2.29)$$

Although not confirmed yet, Staehelin and Hoigne (1982) proposed the reaction of radical OH^* with ozone and formation of the radical HO_4^*:

$$OH^* + O_3 \rightarrow HO_4^* \quad (2.30)$$

The reaction chain can start anew with the decay of HO_4^* into oxygen and the hydroperoxide radical:

$$HO_4^* \rightarrow O_2 + HO_2^* \quad (2.31)$$

Promoters convert OH^* into O_2^{*-}/ HO_2^* in the reaction chain. Tomiyasu et al. (1985) do not include the radical HO_4^* in their model; however, the final result is the same as that of Staehelin and Hoigné.

Termination: Any reaction that interrupts the reaction chain will slow ozone decomposition. One possibility is a reaction between two radicals such as:

$$OH^* + HO_2^* \rightarrow O_2 + H_2O \quad (2.32)$$

Another possibility is to use inhibitors, compounds that consume OH^* radicals and break the chain at reaction 2.30. Some of the more common inhibitors include borate, phosphate and carbonate ions (Hoigné et al., 1985). In the case of carbonate ions, the inhibiting reactions are as follows:

$$OH^* + CO_3^{--} \rightarrow OH^- + CO_3^{*-} \quad (2.33)$$

$$OH^* + HCO_3^- \rightarrow OH^- + HCO_3^* \quad (2.34)$$

Staehelin and Hoigné (1982) claim that presence of excess radical scavenger generates a pseudo first order decomposition rate,

$$-\left(\frac{d[O_3]}{dt}\right)_{pH} = k'_{OH}\,[O_3]^{1.0} \quad (2.35)$$

where k'_{OH} is the first-order rate constant for a given pH value. The pseudo rate constant is a linear function of [OH^-] (Figure 2.6), and the rate of decomposition of ozone can then be described by:

$$-\frac{d[O_3]}{dt} = k_{O_3/OH}\,[O_3]^{1.0}\,[OH^-]^{1.0} \qquad (2.36)$$

where:

$$k_{O_3/OH^-} = \frac{k'_{OH}}{[OH^-]^{1.0}} \qquad (2.37)$$

The rate constant (k_{O_3/OH^-}) determined had a value of 175 ± 10 $M^{-1}\,s^{-1}$ based on the OH^- analytical concentration.

The first order reaction assumption is not valid unless radical scavengers (such as carbonate) are present. In their absence, for example over the range pH 8-11, a combined first- and second-order rate law comes closer to describing the results, and Tomiyasu et al. (1985) proposed the following:

$$-\frac{d[O_3]}{dt} = k_{O_3OH^-}\,[O_3]^{1.0}\,[OH^-]^{1.0} + k_2\,[O_3]^{2.0}\,[OH^-]^{1.0} \qquad (2.38)$$

where values of $k_{O_3OH^-}$ and k_2 vary with the solution composition.

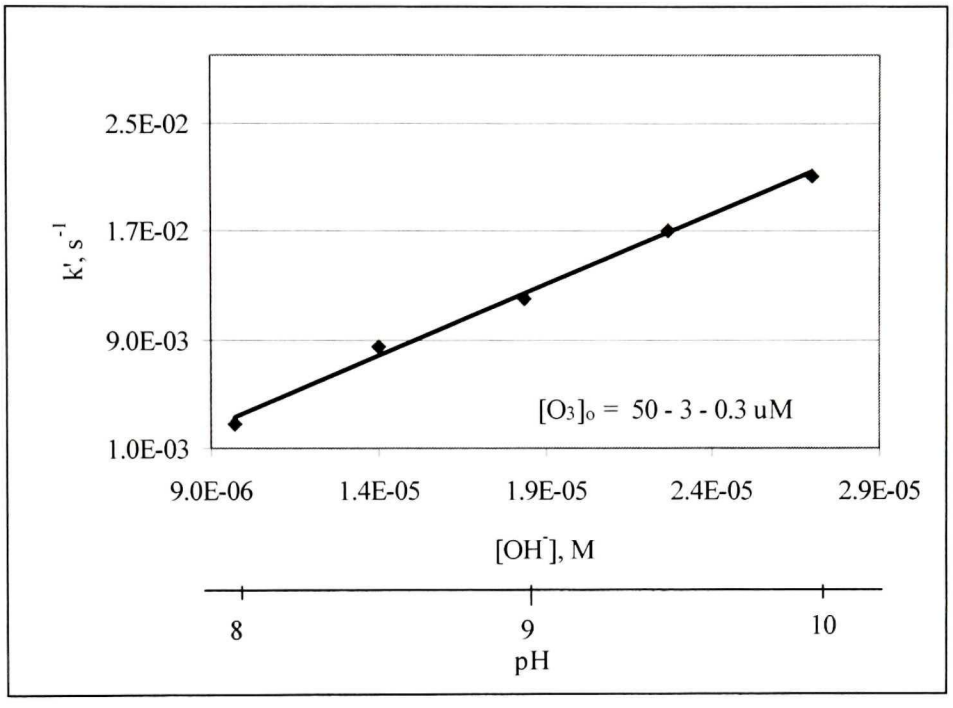

Figure 2.6. Variation of pseudo first-order rate constant k' versus [OH^-] (Staehelin and Hoigné, 1982)

A compendium of total reaction orders (sum of individual orders) and rate equations for decomposition of aqueous ozone taken from the review of Gurol and Singer (1982) are presented in Tables 2.4 and 2.5, respectively. Table 2.6 gives some k-values.

Table 2.4. Reaction order of ozone decomposition in water (Gurol and Singer, 1982)

Referenced by	pH range	Temperature (°C)	Reaction order
Rothmund et al. (1913)	2 – 4	0	2
Sennewald, K. (1933)	5.3 – 8	0	2
Weiss, J. (1935)	Acidic Basic		3/2 1
Alder, G.A. and Hill, G.R. (1950)	1 – 2.8	0 – 27	1
Stumm, W. (1954)	7.6 – 10.4	1.2 – 19.8	1
Kilpatrick et al. (1956)	0 – 6.8	25	3/2
Kilpatrick et al. (1956)	8 – 10	25	2
Rankas et al. (1964)	5.4 – 8.5	5 – 25	3/2
Czapaki et al. (1968)	10 – 13	25	1
Rogozhkiu, G. (1970)	9.6 – 11.9	25	1
Hewes, C.G.and Davidson, R.R. (1971)	6	10 – 50	3/2 – 2
Hewes, C.G.and Davidson, R.R. (1971)	8	10 – 20	1
Hewes, C.G.and Davidson, R.R. (1971)	2.4	30 – 60	2
Merkulova et al. (1971)	0.22 – 1.9	5 – 40	1 or 2
Sharobaugh et al. (1976)	9	20	1
Rizutti et al. (1977)	8.5 – 13.5	18 – 27	1
Sullivan et al. (1979)	0.5 – 10.0	3.5 – 60	1
Li, K. (1977)	2.1 – 10.2	25	3/2
Teramoto et al. (1979)	Acidic basic	25 25	1 – 2 1

Table 2.5. Ozone decomposition rate equations (Gurol and Singer, 1982)

Sennewald, K. (1933)	$k\,[OH^-]^{0.36}\,[O_3]^2$
Weiss, J. (1935)	$k_1\,[OH^-][O_3] + k_2\,[OH]^{0.5}\,[O_3]^{1.5}$
Alder, G.A. and Hill, G.R. (1950)	$k\,[OH^-]^{0.5}\,[O_3]$
Stumm, W. (1954)	$k\,[OH^-]^{0.75}\,[O_3]$
Rizutti et al. (1977)	$k\,[OH^-]\,[O_3]$
Sullivan et al. (1979)	$k\,[OH^-]^{0.12}\,[O_3]$
Li, K. (1977)	$k\,[OH^-]^x\,[O_3]^{3/2}$, x is pH dependent
Teramoto et al. (1979)	$k\,[OH^-]^{0.88}\,[O_3]$

Table 2.6. Rate constant (k) values

Referenced by	**pH**	**Na_2CO_3 mol/L**	**k L mol^{-1} s^{-1}**	**Total Reaction order**
Gurol, M.D. and Singer, P.C. (1982)	>4	0.0	0.27	2
	<4	0.0	$k[OH^-]^{0.55}$ *	2
Staehelin et al. (1982)	>10	0.0	70 ± 7	2
	2	0.0	4.00E-4	2
Tomiyasu et al. (1985)	11.9	5.00E-4	190.0	2
	11.85	0.0	$k_1 = 1.26$ $k_2 = 6.4 \times 10^{-4}$ **	2 and 3

* k depends on hydroxide concentration

** k_1 (s^{-1}) and k_2 (L mol^{-1} s^{-1})

2.8 Ozone use in metal recovery from solution

There are not many publications on the use of ozone in metal recovery from solutions. One example is the use of ozonated air to remove iron and manganese (0.1 to 0.5 mg/L level) and odour from pumped ground water contaminated by polluted water from the Rhine River (Weissenhorn, 1984). Recently ozone has been experimented in recovery/removal of metals from acid mine drainage (Sato et al., 2000). Elements such as Mn, Fe, Ni, Co, Pb and Ag were rapidly and selectively precipitated as a function of pH.

2.9 Nickel and properties of nickel compounds

Nickel is twenty-fourth in order of abundance (Adamec and Kihlgren, 1967) at a concentration (by weight) of 0.008% of the earth's crust (Boldt, 1967). The main nickel ores are garnierite $[(Ni,Mg)_6Si_4O_{10}(OH)_2]$ and pentlandite $[(Ni,Fe)_9S_8]$. World production is ca. 500,000 tonnes/year and reserves are ca. $70x10^6$ tonnes (Emsley, 1991). A secondary source of nickel is sludge from mining and metallurgical sites. This material may carry a significant quantity of nickel (up to 6% on a dry weight basis) (El-Ammouri, 2000), higher than in most natural ores. A potential reserve of 560,000 tons of nickel in the Sudbury area (i.e., about 1 year's supply) has been estimated (Inco Ltd., private communication).

Nickel chemical and physical properties are listed in Appendix 1.

2.9.1 Nickel: Potential – pH equilibrium diagram

A graphical representation of thermodynamic and electrochemical equilibrium for different nickel species in water is shown in Figure 2.7 (Pourbaix, 1974) and 2.7a (FACT, 2002). The position of the domain of stability for $Ni(OH)_2$ shows thermodynamic stability at slightly alkaline pH in oxidizing or reducing conditions. Dissolution in acid solutions produces nickelous ions (Ni^{++}) and in alkaline solution produces nickelite ions

($HNiO_2^-$). Oxidation of nickelous hydroxide in alkaline media can give rise to the formation of Ni_3O_4, Ni_2O_3 and NiO_2 (Pourbaix, 1974). Other stable compounds are $Ni_{(s)}$, $NiO_{(s)}$, $NiOOH_{(s)}$ and $NiO_2(H_2O)_{(s)}$; their formation will depend of pH and oxidation-reduction potential. The usual oxidising agents (hypochlorite, hydrogen peroxide, ozone, etc) can bring about this conversion. Besson (referenced in Pourbaix, 1974) makes the observation that all these oxidising agents convert $Ni(OH)_2$ into NiOOH or Ni_3O_4 or Ni_2O_3 depending on the amount used.

2.9.2 Nickel hydroxides and oxides (higher oxidation states)

There is no evidence for anhydrous oxides of Ni(III) and Ni(IV) but there are a number of hydrous oxides and mixed metal oxides, some of considerable complexity (Durrant, 1970). The best defined hydroxide is β-NiOOH, obtained as a black powder by the oxidation of nickel (II) nitrate solutions for example with bromine in aqueous potassium hydroxide below 25°C (Cotton, 1966). It is readily soluble in acids; on aging, or by oxidation in hot solutions, a Ni(II)-Ni(III) hydroxide of stoichiometry $Ni_3O_2(OH)_4$ is obtained (Cotton, 1966). Ni(IV) formation is mentioned by Emsley (1991) but was not confirmed. An effective way to produce higher oxidation states of nickel is by using ozone to produce NiOOH; Nishimura et al., (1992) proposed the following stoichiometric reaction:

$$O_3 + 2Ni^{++} + 3H_2O \rightarrow 2NiOOH + O_2 + 4H^+ \qquad (2.39)$$

Figure 2.8 shows the free energy versus temperature for reaction (2.39) which is spontaneous at temperatures over 298 K. Figure 2.9 represent a typical β-NiOOH X-ray diffraction pattern.

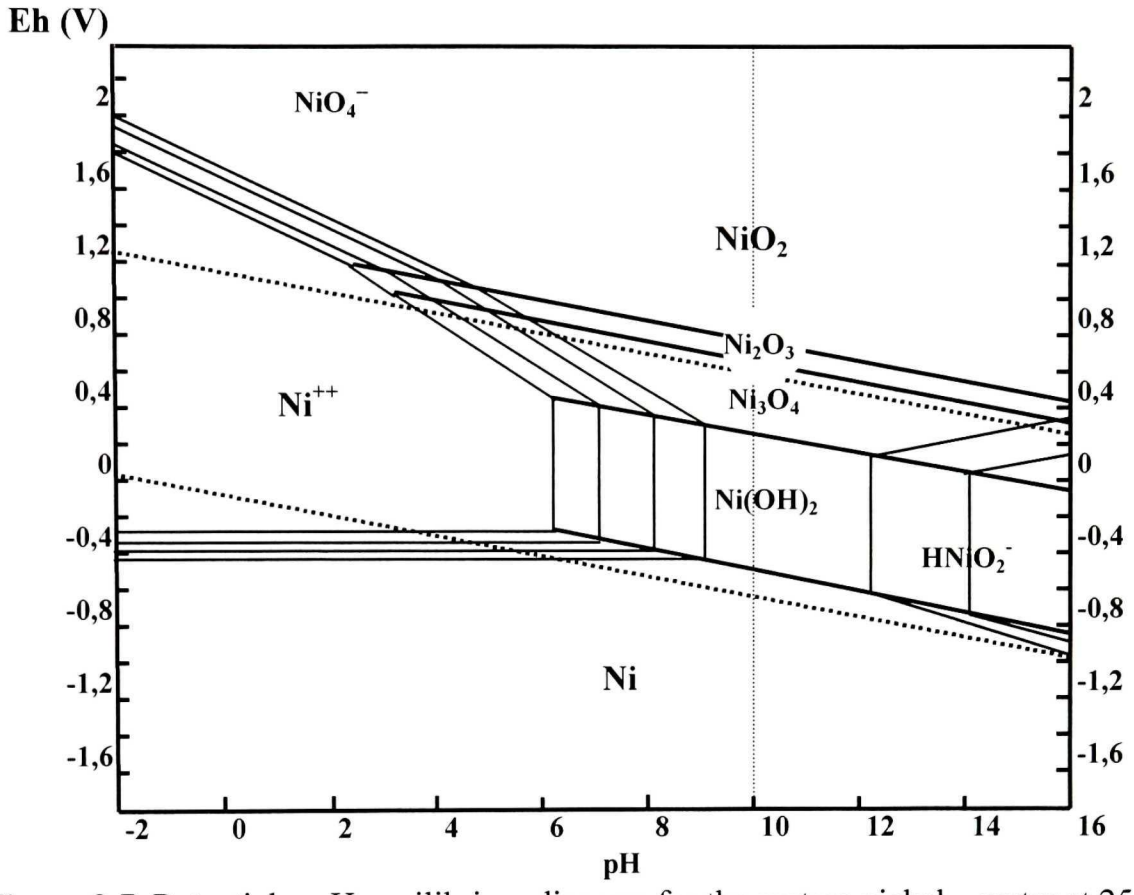

Figure 2.7. Potential – pH equilibrium diagram for the system nickel – water at 25 °C (Pourbaix, 1974)

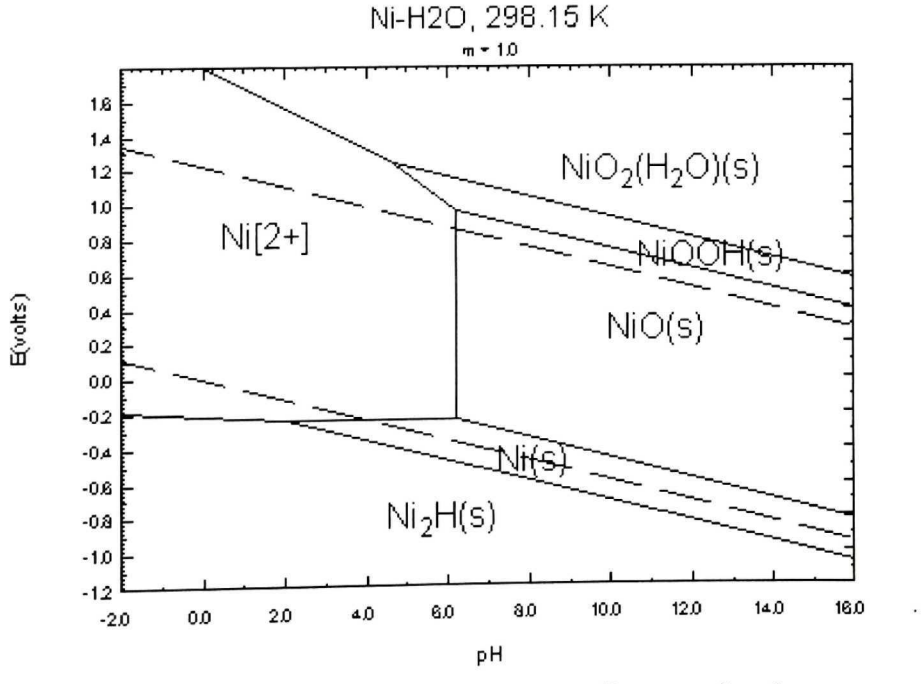

Figure 2.7a. Potential – pH equilibrium diagram for the system nickel – water (FACT, 2002)

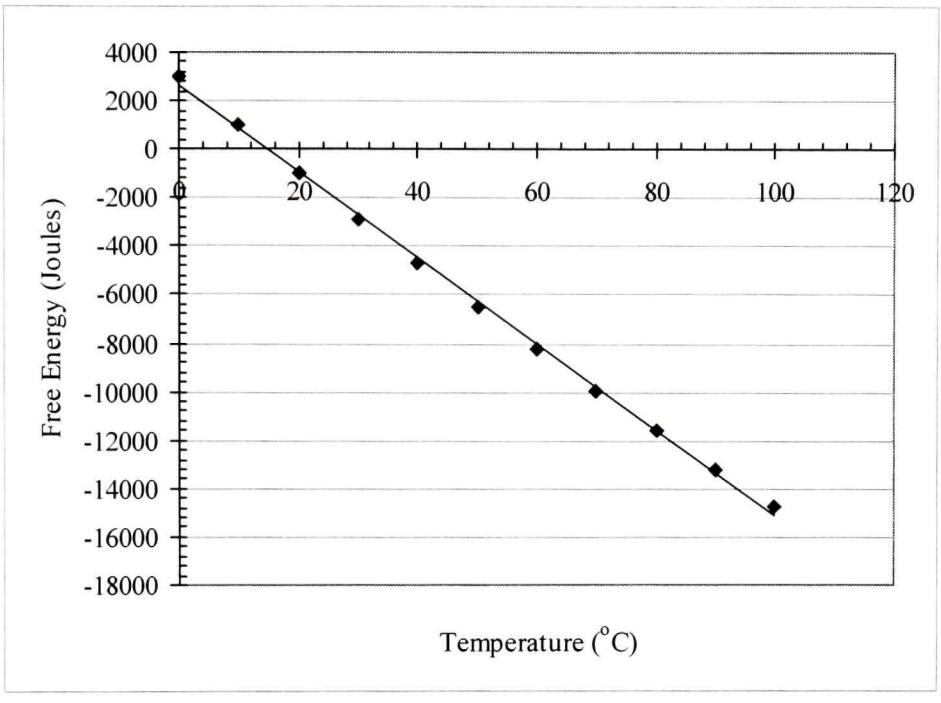

Figure 2.8. Free energy - temperature variation for nickel precipitation as NiOOH (Ref. FACT, 2002)

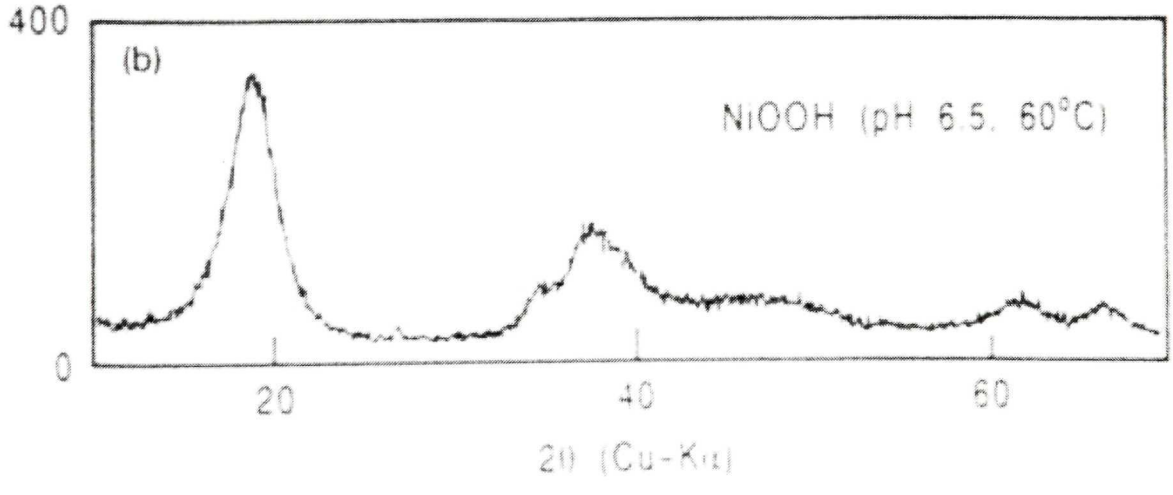

Figure 2.9. X-ray diffraction (2θ (Cu-Kα)) pattern of NiOOH (Nishimura et al. 1992)

2.9.3 Kinetics: reaction order and rate constant

Gottschalk et al. (2000) proposed that reaction order and rate constant of ozone reaction with inorganic compounds can be determined by three methods: half-life, initial reaction rate, and trial and error. The first two methods use directly the ozone concentration variation with time, and the last one finds a rate equation that best fits the experimental points. In general, the method of determining the reaction rate constants is based on knowing the reaction order, and is calculated by linearization of the concentration or rate variation. Reactions in aqueous solutions tend to follow a first order kinetic law with respect to both ozone and the oxidizable compound. The ozone consumption rate is typically expressed by equations of the following form (Langlais et al., 1991):

$$-\frac{d[O_3]}{dt} = k_{O_3}[O_3][M] \qquad (2.40)$$

where [M] is the element being oxidized.

In the case of nickel oxidation-precipitation, taking into account the stoichiometric equation (2.39), the appropriate kinetic equation would be:

$$-\frac{d[O_3]}{dt} = k\,[O_3]^a\,[Ni^{++}]^b\,[OH^-]^c \qquad (2.41)$$

where a, b and c are the reaction order for each compound.

Despite evident potential, the author is only aware of one systematic study involving ozonation of nickel. Nishimura et al. (1992) presented an example in the separation of cobalt from nickel at 60 °C and pH 6.5. They concluded that the Ni ozonation-precipitation reaction follows zero-order kinetics with respect to the nickel concentration and a first-order with respect to the ozone partial pressure of the O_2-O_3 feed gas.

CHAPTER 3

Equipment Set–up and Calibration

3.1 Introduction

In any ozonation process, efficient utilization of ozone is important. To fulfill this fundamental requirement, the appropriate experimental conditions and a well-designed and instrumented set-up are required. Nevertheless, there will be certain limitations, two here being the volume of solution to prepare and dispose of, and the capacity of the ozone generator and diffuser. Every system used in ozonation tests has its own characteristics. In the present Chapter, the author describe the set-up, which is different from that typically used in ozonation studies, and includes the calibration of key components in order to achieve mass balance.

3.2 Bubble column

Figure 3.1 shows the experimental set-up. Oxygen (purity > 99.6%) is fed to an electric discharge ozone generator. The ozone concentration (0 – 3%w/w) is controlled by regulation of the electric current. The ozone-oxygen mixture can either be sent to the reactor or to the gas phase monitor. The reactor is a closed PVC column, 10.16 cm in diameter by 156 cm high. A replaceable porous steel plate gas diffuser is located at the bottom of the column. On the sides of the column are ports to insert pH electrodes, reagent addition lines, the solution sample loop, and connections to the pressure transducers (to determine gas holdup). The sample loop comprises two concentric tubes connected to a pump and housing an ozone liquid phase sensor, temperature sensor and ORP (oxidation-reduction potential) electrode. Continuous readings of these parameters were taken. Tubing at the top of the column transports the gas to the ozone gas phase

monitor and then to the ozone destructor column containing a bed of metallic oxides (Carulite 200) to decompose the O_3. Gas flow and pressure are regulated using valves; gas flow-rate measurement is made using an orifice connected to a differential pressure transducer. All sensors are connected to the analog-to-digital interface to record data continuously during a test using a computer. Figure 3.2 is a photograph of the setup.

3.3 Bubble size measurement

The set-up used to measure the bubble size, first described by Hernandez-Aguilar et al. (2002), is shown in Figure 3.3. Bubbles are collected from the reactor using a sampling tube and transported to the viewing chamber where they encounter and slide up a sloped glass window. The sloped window gives two advantages: spreading the bubbles into a single layer thus minimizing overlap, and providing an unambiguous plane for imaging. To limit bubble distortion, the angle to vertical is only 5^{o}. A digital video camera is used to take pictures of the bubbles. Well-focused and high-contrast images are obtained using backlight illumination. The lighting produces a dark image of bubbles (usually with a bright center) on a bright background. Automatic processing of the pictures is performed using a commercial software (Eclipse). Measurement of bubble size is made by determination of pixel size, assigned a length by calibration with an object of known size in the field of view. This technique allows the measurements for one test to be completed in about two hours, processing approximately 4000 bubbles. For images of non-circular bubbles, the minimum (d_{min}) and maximum diameter (d_{max}) (in the x-y plane) are measured, and the equivalent sphere diameter (diameter of sphere having the same volume as the bubble calculated by rotation around the large diameter) is calculated using:

$$d_b = \sqrt[3]{d_{max}^2 \cdot d_{min}} \qquad (3.1)$$

Figure 3.4 shows the bubble viewer.

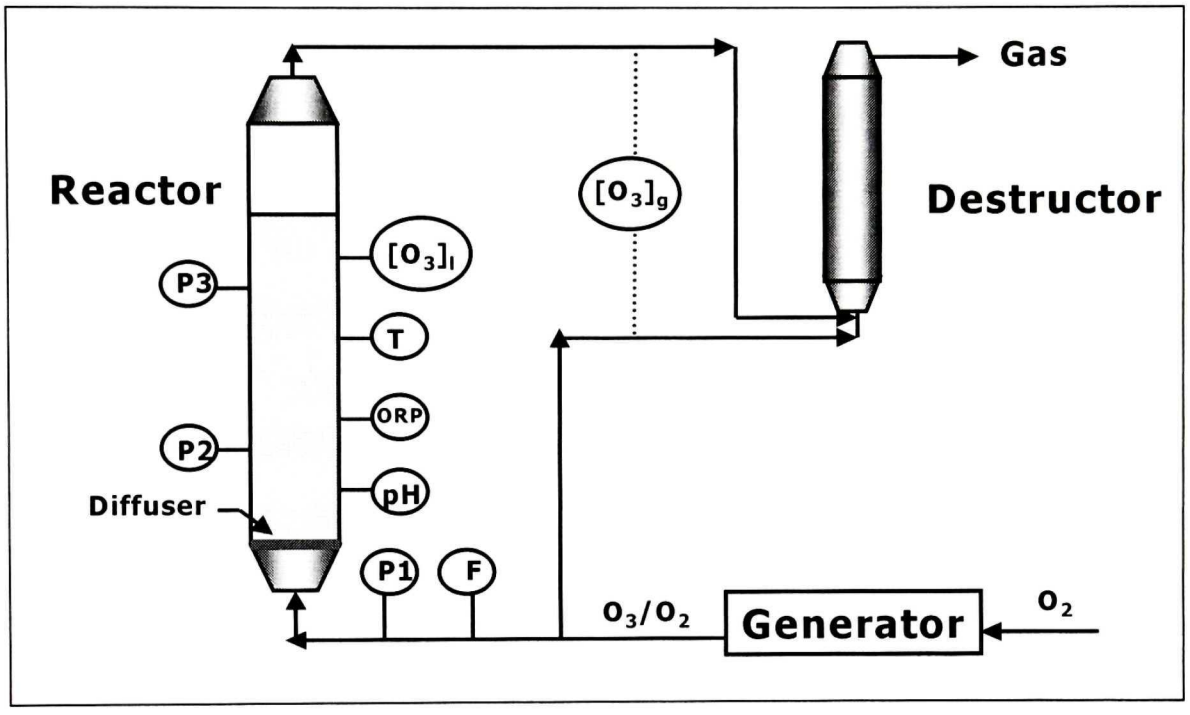

Figure 3.1. Experimental set-up: schematic

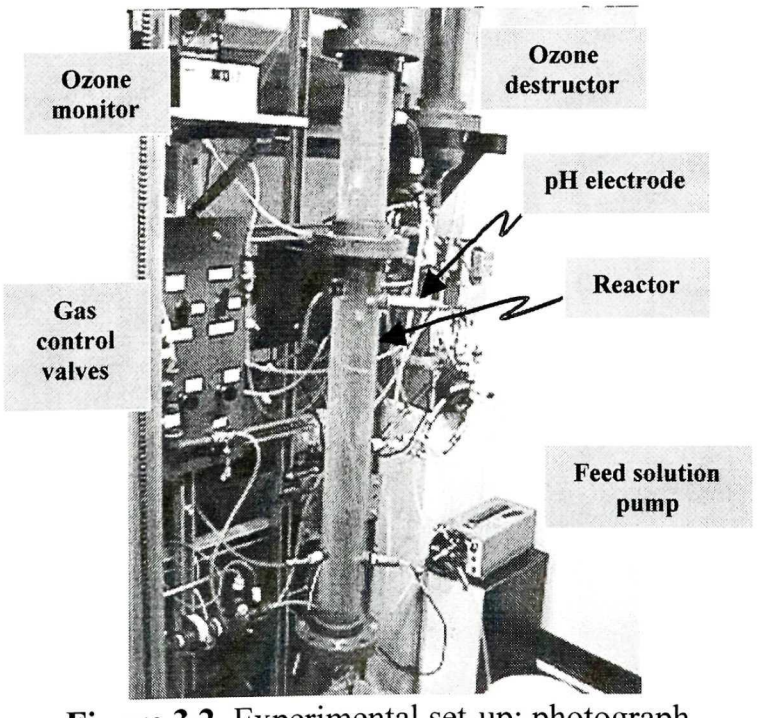

Figure 3.2. Experimental set-up: photograph

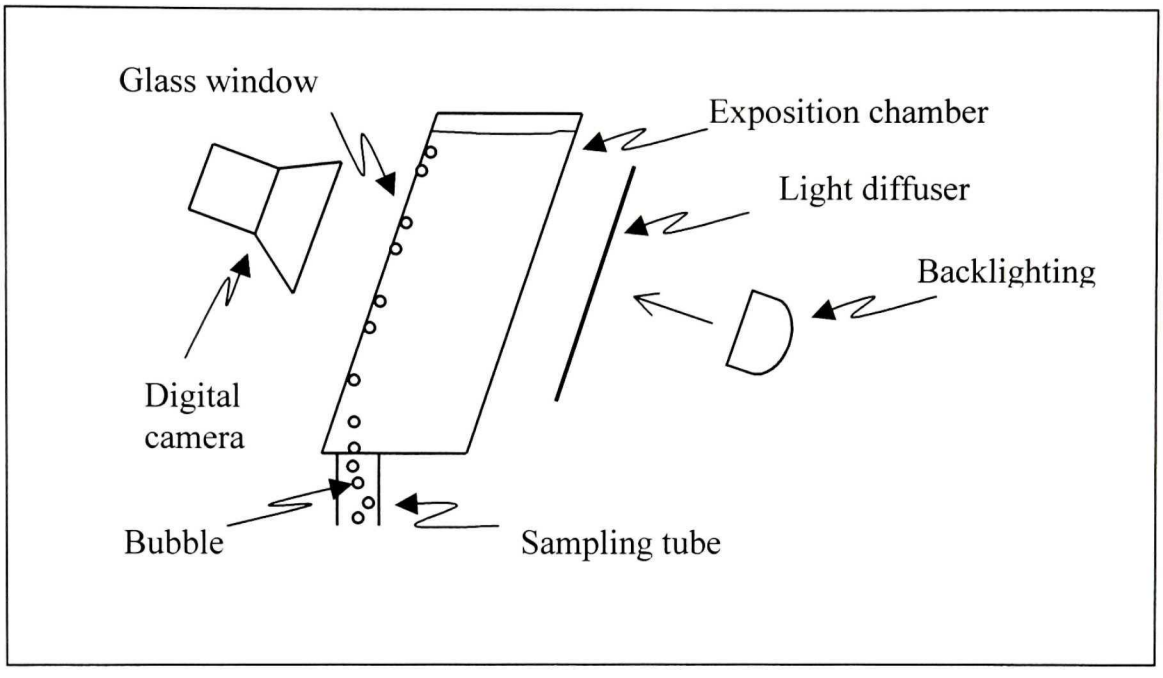

Figure 3.3. Bubble viewer: schematic

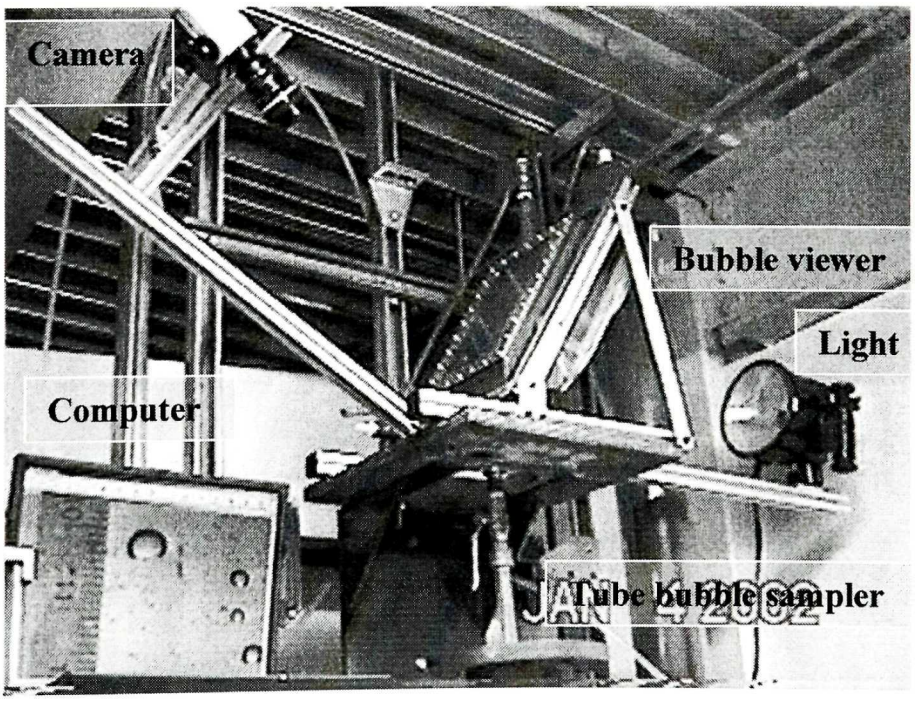

Figure 3.4. Bubble viewer: photograph

3.4 Calibration

3.4.1 Ozone generator and gas phase monitor

The ozone generator was calibrated using the iodometric wet-chemistry method described by Rakness et al. (1996). The generator was regulated at 9.0843×10^4 Pa and the oxygen flowrate was 6.84 L/min. By controlling the current, the concentration of ozone in the gas was manipulated. Temperature was ambient (~ 20 °C). Calibration results are presented in Figure 3.5. The iodometric method was also used to calibrate and adjust the gas phase monitor. Characteristics of the ozone generator and gas phase monitor are presented in Appendix 2.

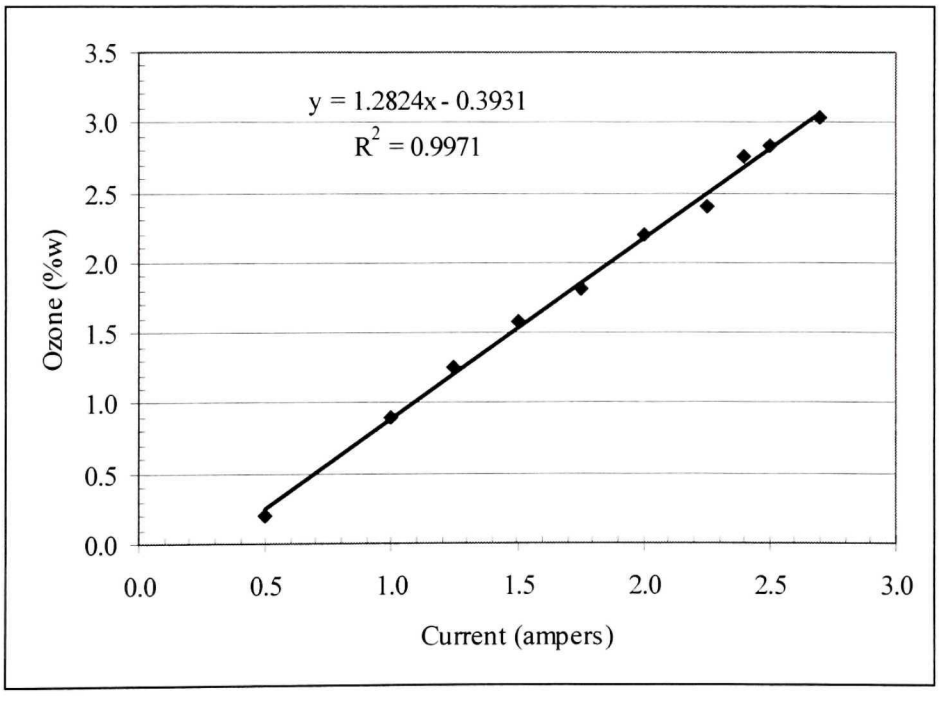

Figure 3.5. Ozone generator calibration using iodometric method

3.4.2 Gas flow-meter (orifice)

In order to produce a continuous measurement of gas-flow rates a differential pressure transducer was connected across a calibrated orifice (1.1 mm diameter). To calibrate, the outlet was connected to cylinder containing water to measure liquid displacement per unit time (i.e., volumetric gas flow rate) as a function of the pressure differential (Figure 3.6).

To calculate the gas flow to the reactor, the following formula proposed by Cohen and Hering (1995) was used.

$$Q_{reactor} = Q_{or}\left(\frac{T_{reactor}}{T_{or}}\frac{P_{or}}{P_{reactor}}\right) \qquad (3.2)$$

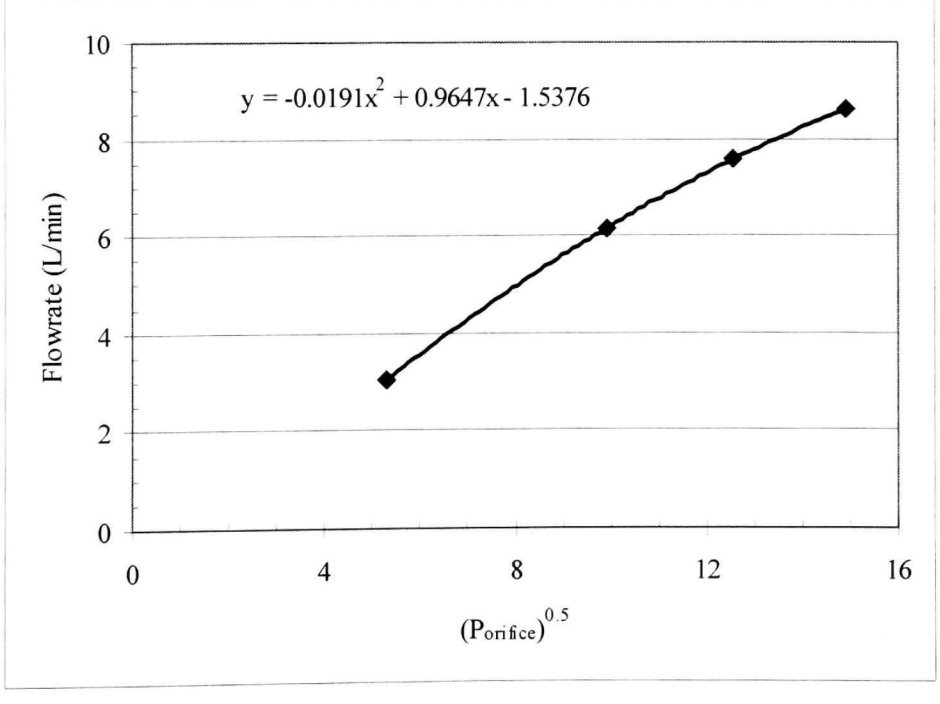

Figure 3.6. Calibration of orifice: gas flow-rate vs differential orifice pressure

3.4.3 Ozone liquid phase monitor

The indigo method recommended by Bader and Hoigné (1982) was used to determinate the aqueous ozone concentration and calibrate the ozone in liquid phase monitor. The method is based on decolorization of indigo trisulfate (measured at a wavelength of 600 nm) where one mole of ozone decolorizes, essentially instantaneously, one mole of indigo.

CHAPTER 4

Characterization of Ozone Mass Transfer

4.1 Introduction

Two important aspects of ozonation are mass transfer of gaseous ozone into the aqueous phase, and the rate of auto-decomposition of absorbed ozone (Roth and Sullivan, 1981). The mass transfer study in this Chapter establishes a methodology to determine the volumetric mass transfer coefficient ("k_La") and to determine the specific interfacial area ("a") from which to derive the mass transfer coefficient ("k_L"). The test work examined the following parameters: diffuser porosity and gas superficial velocity to vary "a" and reactor volume to test the assumption of perfect mixing. Distilled water, previously treated with ozone to destroy impurities that may cause ozone decomposition, was used. Mixtures of ozone-oxygen gas were used and the bubble column instrumentation permitted mass balancing of ozone in gas and liquid, and estimation of gas holdup which, combined with bubble size measurement (using the bubble viewer), gives interfacial area.

4.2 Determination of volumetric ozone mass transfer

A semi-batch bubble column is a reactor where a continuous flow of gas is dispersed in the form of bubbles rising through a stationary volume of liquid. The dispersion induces mixing during which gas is transferred to the liquid.

In the present study, the liquid in the column is considered perfectly mixed while the gas is considered to be under plug flow transport. The consequent ozone concentration profiles in both liquid and gas phases and their behavior over time are illustrated in Figure 4.1. The concentration of ozone in the liquid phase is uniform. In

the gas the ozone concentration decreases from bottom to top as a result of transfer to the liquid. The gas outlet concentration will change until no more ozone is transferred to liquid, at which time gas inlet and outlet ozone concentration will be the same.

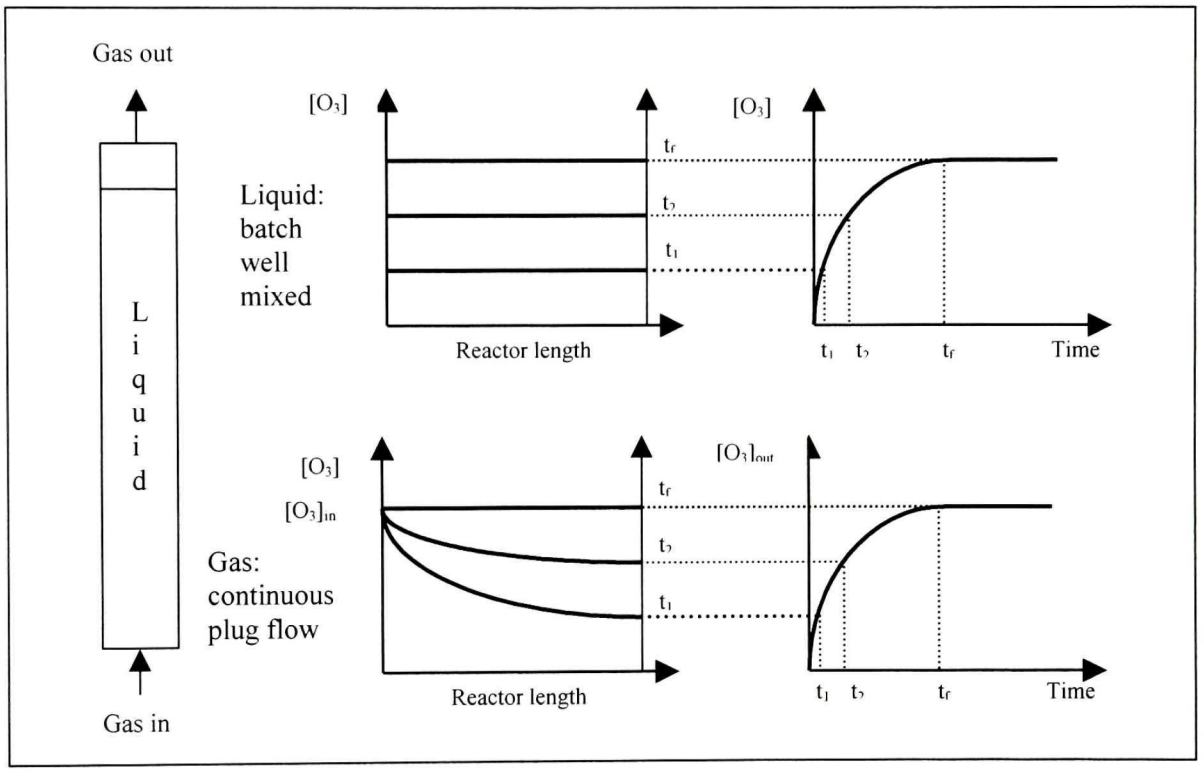

Figure 4.1. Reactor ozone concentration profiles and their variation in the time

4.2.1 Reactor mass balance

The mass balance across the reactor can be expressed using the volumetric flow or the mass flow. When volumetric flow is used, inlet gas flow and outlet gas flow must be measured because their temperature and pressure are not the same; this does not apply when mass flow is used. Figure 4.2 is a representation of these two kinds of measurement.

Mass flow considers the gas is oxygen (maximum ozone content was 3% w/w) and ozone concentration is expressed in ozone mass per oxygen mass to perform the balance.

Under these considerations the mass balance uses the following relationship (no reaction occurs during the process):

O_3 in (gas) = O_3 out (gas) + O_3 accumulated (liquid)

Then:

$$W_{O2} \cdot X_{in} = W_{O2} \cdot X_{out} + \frac{d(V \cdot [O_3]_{liq})}{dt} \quad (4.1)$$

$$W_{O2} \cdot (X_{in} - X_{out}) = \frac{V \cdot d[O_3]_{liq}}{dt} \quad (4.2)$$

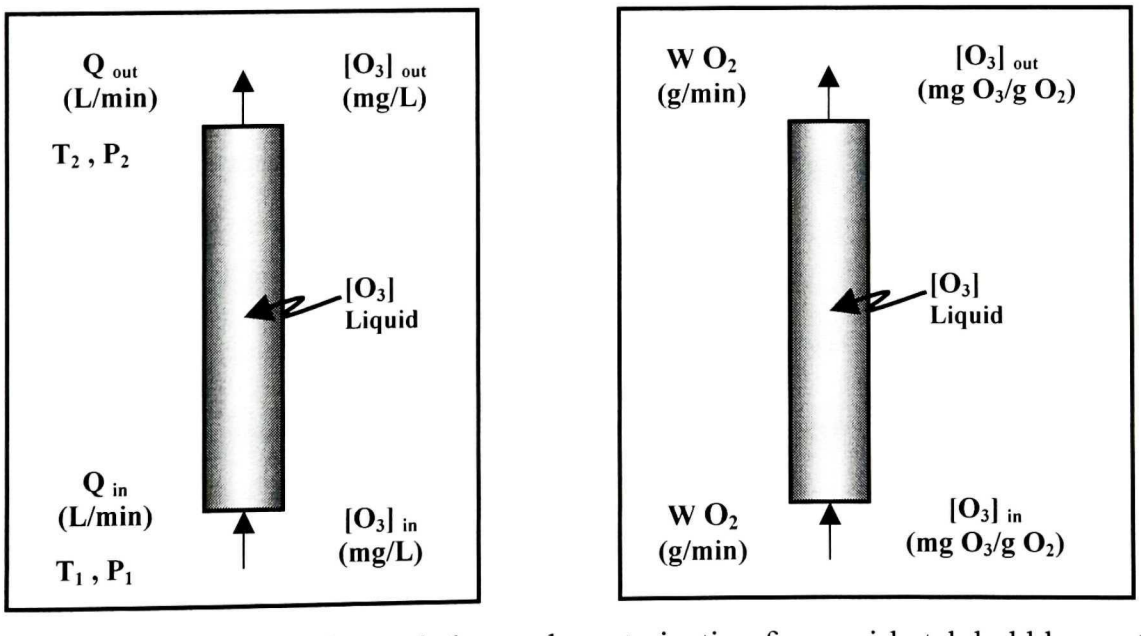

Figure 4.2. Two forms of mass balance characterization for semi-batch bubble reactor

4.2.2 Mass transfer characterization

The flux of species can be defined with respect to the mixture (J_i) or interface (N_i) (Wesselingh and Krishna, 1990). With respect to the mixture flux is proportional to the concentration gradient, $J_i = -D\frac{dC_i}{dz}$; in the second case flux is proportional to the concentration difference times a mass transfer coefficient, i.e., $N_i = k\,(C_{io} - C_i)$. Mass transfer coefficient (k) is defined by the diffusivity (D) and thickness of the film (∂),

$$k = \frac{D}{\partial} \tag{4.3}$$

Flux related to the interface is used to characterize mass transfer from gas to liquid.

Then:

$$N_{O_3} = \left|\frac{O_3 \text{ tranferred}}{\text{area} \cdot \text{time}}\right| = k_L\,([O_3]_{l\,(i)} - [O_3]_l) \tag{4.4}$$

The mass transfer coefficient considers that the resistance to mass transfer is mainly in the liquid phase.

Total ozone transferred in the reactor can be calculated using the following expression:

$$\left|\begin{matrix}\text{Total ozone}\\ \text{transferred}\\ \text{in the reactor}\end{matrix}\right| = \left|\frac{O_3 \text{ transferred}}{\text{area} \cdot \text{time}}\right| \cdot a \cdot V \tag{4.5}$$

The representative equation for this relationship is:

$$W_{O_2} \cdot (X_{in} - X_{out}) = k_L ([O_3]_{l(i)} - [O_3]_l) \cdot a \cdot V \quad (4.6)$$

The ozone concentration at the interface is calculated from Henry's law and the following is derived:

$$[O_3]_{l(i)} = \frac{[O_3]_{g(i)}}{H} = \frac{[O_3]_g}{H} \quad (4.7)$$

substituting (4.7) in (4.6)

$$W_{O_2} \cdot (X_{in} - X_{out}) = k_L \left(\frac{[O_3]_g}{H} - [O_3]_l \right) \cdot a \cdot V \quad (4.8)$$

The calculation of "k_La" from Equation (4.8) for a particular time requires specifying an ozone concentration in the gas phase which, however, is not the same along the reactor (it varies between the inlet and outlet concentrations in a non-linear manner). If the calculation is made on the whole reactor and an average value is used, for example, then the estimated mass transfer coefficient will have an error whose magnitude will change with time. A schematic representation is shown in Figure 4.3. The "k_La" under these circumstances will be equal to:

$$k_L \cdot a = \frac{W_{O_2} (X_{in} - X_{out})}{V \left(\frac{[O_3]_g}{H} - [O_3]_l \right)} \quad (4.9)$$

where,

$$[O_3]_g = \frac{[O_3]_{g\,in} + [O_3]_{g\,out}}{2} \qquad (4.10)$$

A better approach to calculate the volumetric mass transfer is to divide the reactor into a series of elements of equal volume and sequentially apply the mass balance to each of them. The calculation proceeds iteratively by assuming a value of "k_La", calculating the outlet ozone concentration for every element which becomes the inlet ozone concentration for the next one, and comparing the outlet concentration of the final element to that measured exiting the reactor. The "k_La" is varied until the cumulative difference between predicted and measured outlet concentrations, for all the times, is minimum. Figure 4.4 is a schematic representation of this methodology, referred as the "differential method".

The expression to calculate 'k_La" is similar to that in the whole reactor method (Equation 4.8), the variation being in gas ozone concentration.

Small differences in the solution temperature could not be avoided. To compare mass transfer coefficient values, they were brought to a common temperature (20 °C was selected) using the correction factor proposed by Stenstron and Gilbert (1981):

$$k_L a_{20} = k_L a_T \theta^{(20-T)} \qquad (4.11)$$

4.3 Measurement of interfacial area "a"

Interfacial area "a" expressed as surface area per unit volume of bed can be calculated from the gas holdup "ε" (the dimensionless volume fraction of gas phase in the dispersion) and bubble diameter "d_b" (Tatterson, 1991):

$$a = \frac{6 \cdot \varepsilon}{d_b} \qquad (4.12)$$

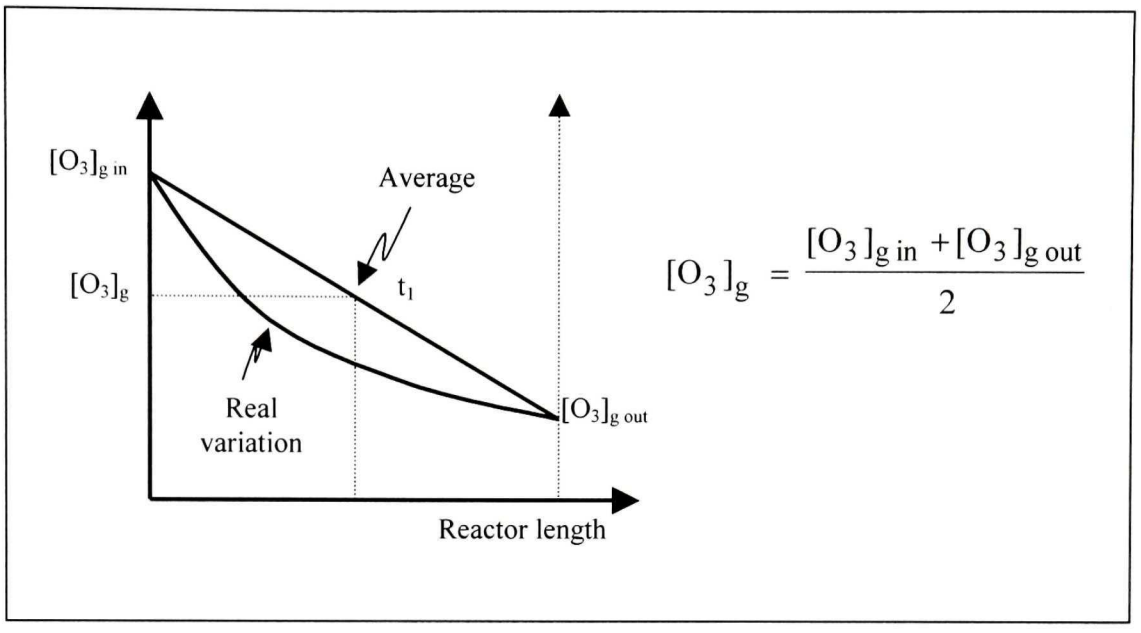

Figure 4.3. Ozone gas concentration calculation using the whole reactor method

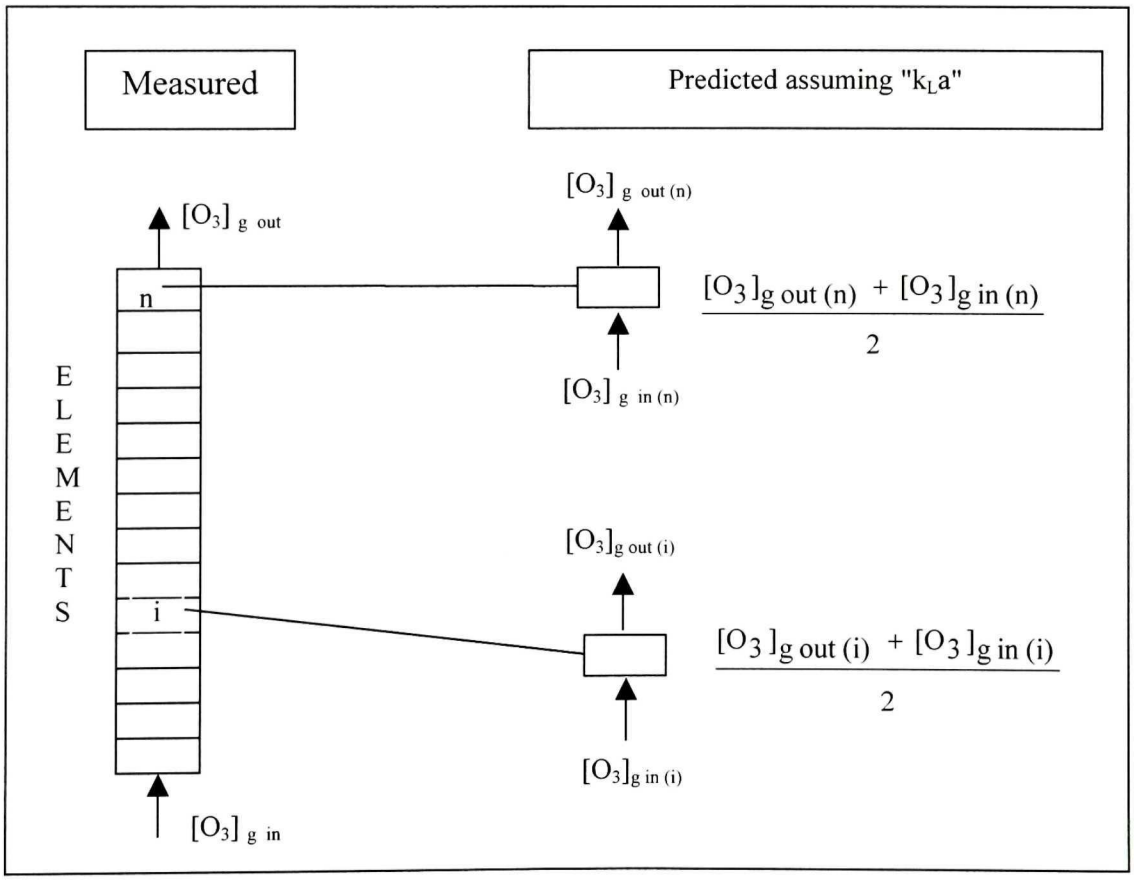

Figure 4.4. Schematic representation of proposed methodology ("differential method") to calculate "k_La"

To measure gas holdup a differential pressure method was employed. For a bubble column a pressure difference ΔP measured over a distance "L" gives "ε" as

$$\varepsilon = \left(1 - \frac{\Delta P}{L}\right) \cdot 100 \tag{4.13}$$

The technique of bubble size measurement to be used, that described by Hernandez-Aguilar et al. (2002), not can be used directly in a pressured reactor without modifications to install the sampling tube. As a compromise the reactor was left "open" and only oxygen used at the same selected conditions as in the ozonation tests. This change should have negligible effect on the bubble size produced because the ozone concentration was never more than 3%w. Images generated were processed to yield a frequency distribution from which d_b was estimated by the Sauter mean diameter ($d_{3,2}$) (Equation 4.14), which is the appropriate metric to calculate the volume to surface ratio of the bubble population (Orsat et al., 1993):

$$d_{3,2} = \frac{\sum_{i=1}^{n} d_i^{\,3}}{\sum_{i=1}^{n} d_i^{\,2}} \tag{4.14}$$

4.4 Experimental program and procedure

The variables, gas diffuser porosity, gas flow-rate and solution volume, were tested over the ranges given in Table 4.1. The input ozone concentration in the gas was set at 5×10^{-4} mol/L, the actual value being recorded. Until the concentration stabilized at the set point the gas stream was diverted to the ozone destructor. When concentration was achieved, the stream was switched to the reactor and the test initiated.

Ozone concentration in liquid phase and gas phase was measured continuously. The delay times for gas and liquid samples to arrive at the sensors and for ozone concentration to reach steady state after gas stream was directed to the reactor were determined for every test. Other delays (monitors and analog-digital conversion) were negligible. Gas holdup and bubble size were determined for each condition. Each run was repeated at least once and the average and standard deviation was calculated.

Table 4.1. Tests conditions

Run[1] #	Conditions			
	Diffuser[2] (μm)	Sup. Gas Vel. (cm/s)	Sol. Vol (L)	Temperature (°C)
Diffuser				
1	10	0.658	8	18.0
2	20	0.658	8	18.0
3	40	0.658	8	18.0
Superficial gas Velocity				
4	20	0.352	8	17.5
5	20	0.658	8	18.0
6	20	1.302	8	18.0
Solution Volume				
7	20	0.658	4	18.0
8	20	0.658	8	18.0
9	20	0.658	12	18.0

[1] Tests 1, 2, 3 represent "one set" of tests, etc

[2] Nominal pore size quoted by manufacturer (Mott Industries)

4.5 Results and discussion

4.5.1 Consistency of mass balance

Typical concentration results obtained in one run are presented in Figure 4.5. Measurement of ozone concentration in the liquid and gas leaving the reactor were collected once every 15 seconds. The ozone concentration in the gas entering the reactor was measured once at the start of the test. The test was stopped when the ozone concentration in both liquid and gas phase did not change (for at least 10 minutes) and it was assumed saturation concentration was reached.

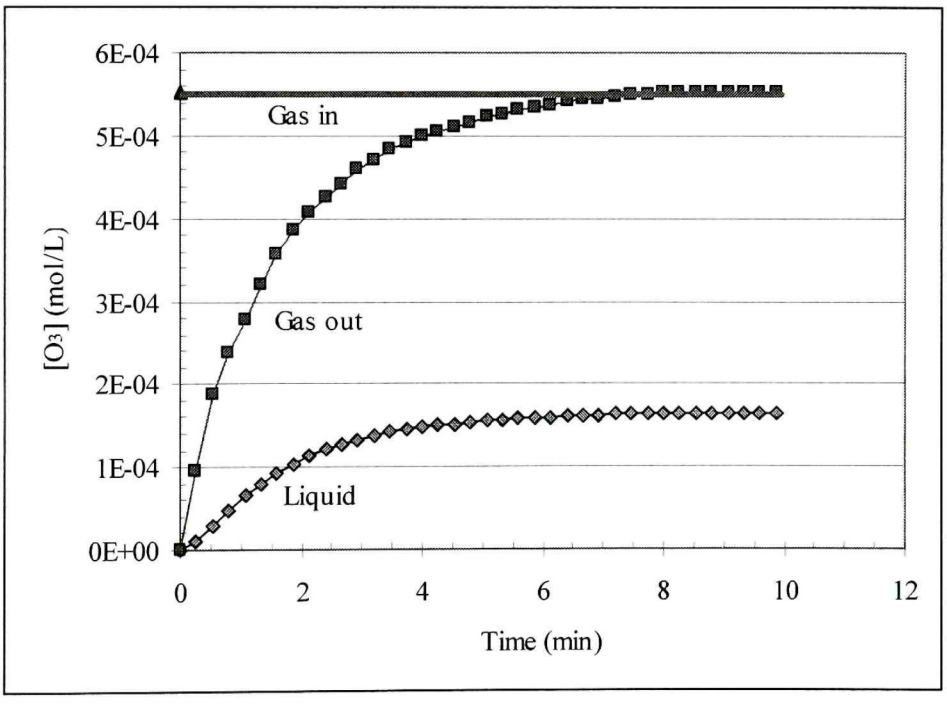

Figure 4.5 Typical concentration variation in the gas and liquid phase

The mass balance was checked by comparing the ozone transferred from the gas phase to that accumulated in the liquid phase, for every time. To calculate the ozone accumulated in the liquid phase the instantaneous liquid phase ozone concentration versus time is required. This was determined from the derivative of a polynomial fitted to the data (Figure 4.6).

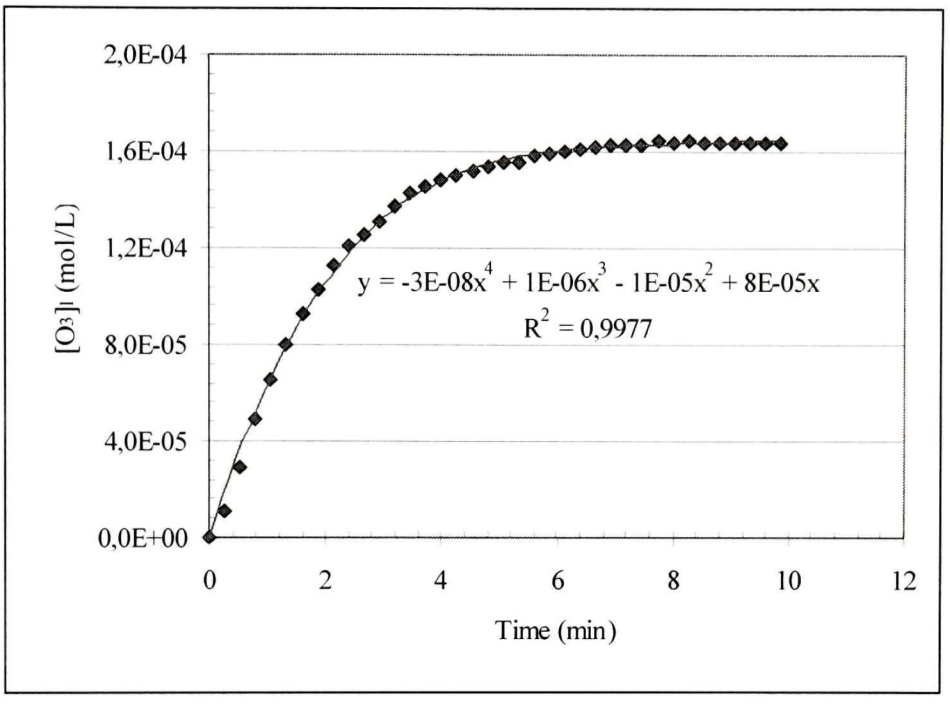

Figure 4.6. Example polynomial fit of ozone concentration variation in liquid phase

There was excellent agreement between the calculated values of ozone transferred from the gas phase and the ozone accumulated in the liquid phase (Figure 4.7). This indicates that measurement of the gas flow rate and ozone concentration in the gas and liquid phase are adequate, and the assumptions proposed, perfectly mixed liquid phase, no resistance to mass transfer in the gas phase and no side reactions consuming ozone, are valid. The negligible ozone decomposition found means the model proposed by Roth and Sullivan (1981) to calculate the "true" ozone concentration in water is not required here.

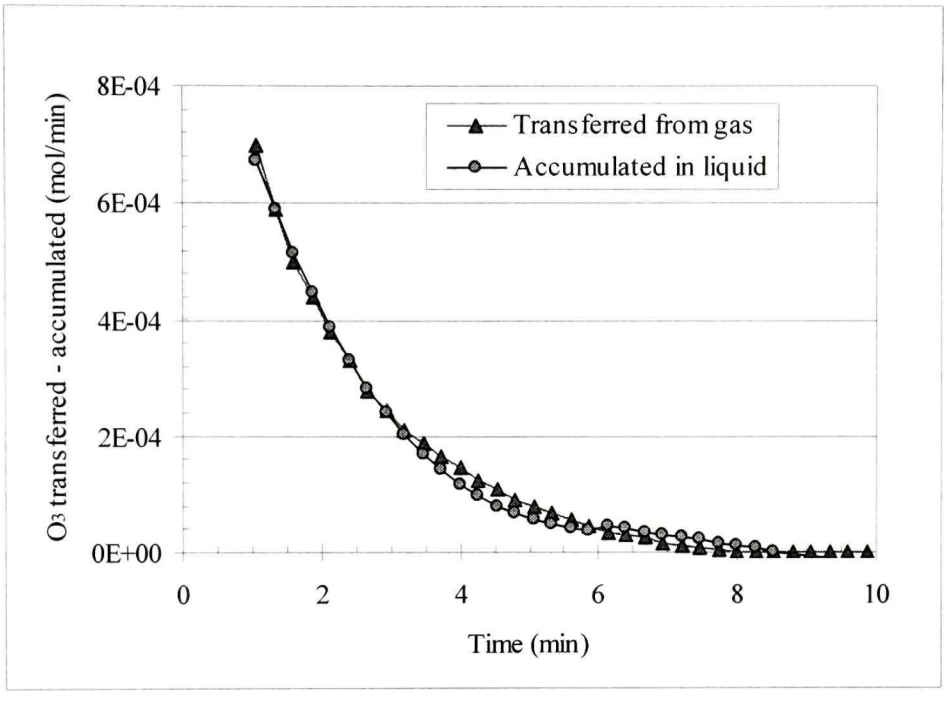

Figure 4.7. Consistency of ozone mass balance

4.5.2 Volumetric mass transfer coefficient

The differential method of determining "k_La" was the preferred option. The reactor volume was divided into "n" elements to solve Equation 4.8. Assuming a starting "k_La" value the reactor output ozone gas concentration was predicted. By searching on "k_La" a value was found which best fitted the measured output, determined by identifying the minimum in the "sum of squares" function SS = (fit. – meas.)^2. The value of "k_La" became independent of "n" for n > 20; n = 40 was selected for the determination. An illustration of the search is shown in Figure 4.8; the sum of squares "SS" is plotted against "k_La" to find the minimum. Figure 4.9 illustrates the subsequent fit to the measured output.

The estimation by the differential method is compared to the estimation using the whole reactor method in Figure 4.10.

To verify the assumption of perfect mixing, tests were performed with the liquid sampler at two positions, 4 cm and 48 cm above the bottom of the reactor. The "k_La" values determined were 0.0259 and 0.0255 s^{-1}, respectively; thus it is concluded that the well-mixed assumption is justified. The sampler was left at the 48 cm position for the tests.

The "k_La" estimated from the differential method are given in Table 4.2. The values are the average of at least two runs and range from a low of 0.0165 s^{-1} to 0.0447 s^{-1}, corresponding with the low to high gas rate. The pooled standard deviation is 0.0008 s^{-1}, indicating good reproducibility.

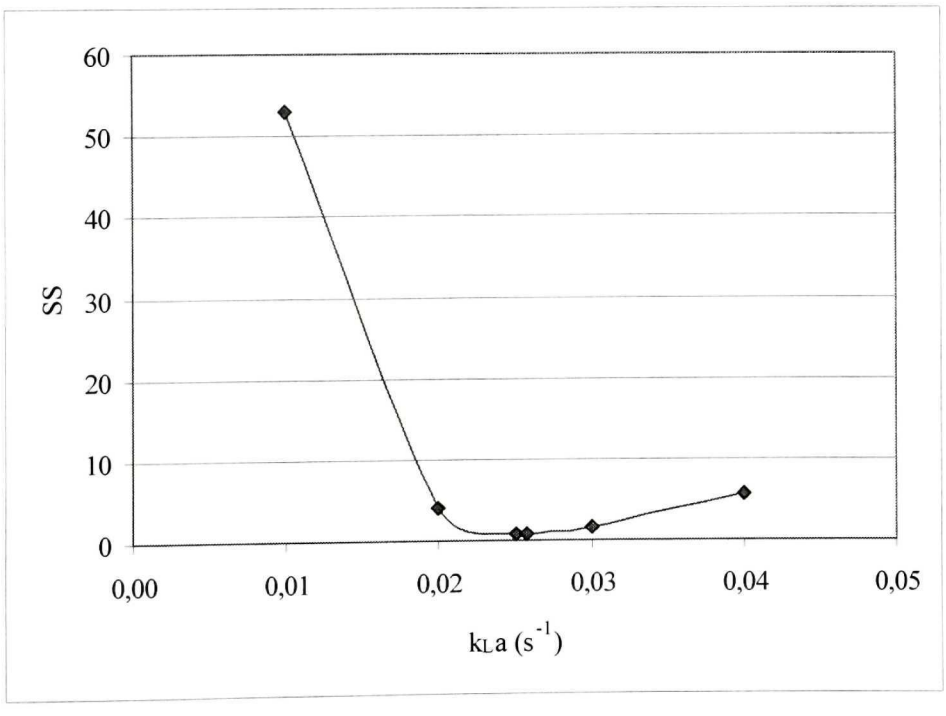

Figure 4.8. Sum of squares (SS) variation with volumetric mass transfer coefficient

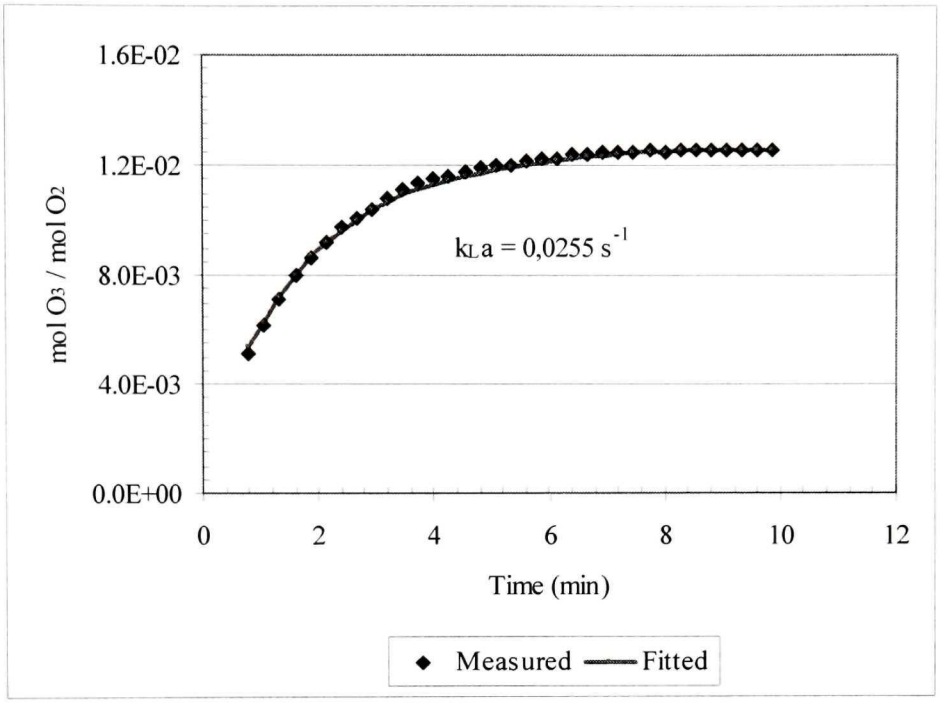

Figure 4.9. Fitted (line) and measured ozone outlet concentrations using differential method to estimate "k_La"

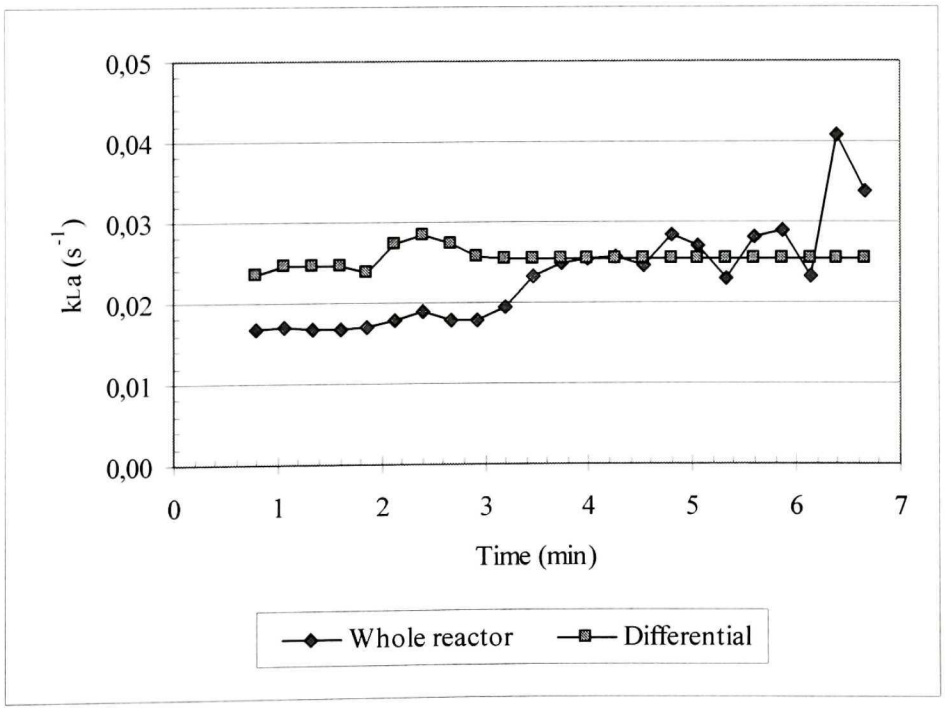

Figure 4.10. Comparison of "k_La" values yielded by "differential" and "whole reactor" methods

Table 4.2. Volumetric mass transfer determination (note: ORP ranged from 1135 to 1150 mV)

Run #	Results			
	$[O_3]_g$ inlet (mol/L)	$[O_3]_l$ (mol/L)	k_La (s^{-1})	k_La_{20} (s^{-1})
Diffuser				
1	4.979E-04	1.656E-04	0.0266	0.0272
2	5.004E-04	1.542E-04	0.0258	0.0264
3	4.781E-04	1.519E-04	0.0250	0.0256
Superficial Gas Velocity				
4	4.704E-04	1.475E-04	0.0161	0.0165
5	5.004E-04	1.542E-04	0.0258	0.0264
6	5.023E-04	1.733E-04	0.0436	0.0447
Solution Volume				
7	4.875E-04	1.523E-04	0.0321	0.0331
8	5.004E-04	1.542E-04	0.0258	0.0264
9	5.000E-04	1.623E-04	0.0256	0.0262

The values and variation in "k_La", notably with gas rate, were similar to published data. Table 4.3a gives a summary of values obtained in the gas rate range 1 - 1.3 cm/s compared with the present result at 1.3 cm/s. The present result, similar to that of Beltran et al. (1997), is on the high side, but the scatter is quite large as the data from Bin et al. (2001) indicate. Table 4.3b compares the trend with gas rate noted here (admittedly based on limited data) with the correlations quoted by Bin et al. (2001); again this shows the present "k_La" data are to the high end of the group.

The methodology to estimate "k_La" applied to a semi-batch reactor proved tractable, and avoided the need to develop an analytical solution (Bin et al., 2001).

Table 4.3. Comparison of volumetric mass transfer coefficients

a). at J_g = 1 - 1.3 cm/s

Ridway[1]	Le Sauze et al. (1993)	Beltran et al. (1997)	Present work
0.0096	0.0220	0.0400	0.0447

[1] Referred to by Roustan et al. (1996)

b) correlations with J_g (in m/s)

Bin & Roustan[1] (2000)	Bin & Roustan[1] (2000)	Watanabe et al.[1] (1991)	Present work
$0.867\ J_g$	$1.89\ J_g^{0.932}$	$0.67\ J_g^{1.15}$	$\sim 4\ J_g$

[1] Referred to by Bin et al. (2001)

4.5.3 Interfacial area: bubble size and gas holdup

Figure 4.11 is an example image of the bubbles produced and Figure 4.12 gives the number frequency distribution for run #5 (superficial gas rate test 0.658 cm s^{-1}). Around 4,000 bubbles were counted to estimate the Sauter mean diameter, which is given in Table 4.4 along with the gas holdup data. The largest change in both parameters occurred when the gas rate was varied. The approximate dependence is ε (%) ~ 3.7 J_g (cm/s) which compares with $\varepsilon \sim 5.5\ J_g$ found by Bin et al. (2001). Changing the porosity of the diffuser did not give the variation in bubble size anticipated. The increase in gas holdup with decreasing liquid volume was not expected but was consistent. The specific interfacial area varied from 2.58 mm^{-1} to 6.87 mm^{-1}.

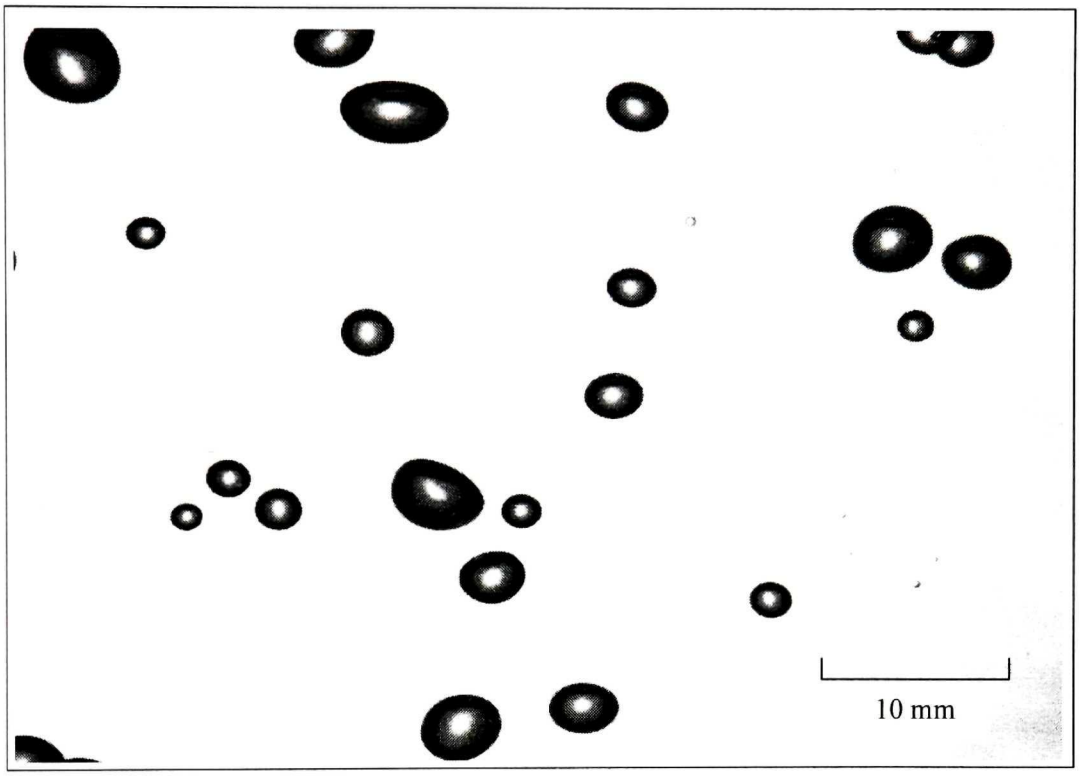

Figure 4.11. Typical image of bubbles produced: solution volume 8 liters, gas superficial velocity 0.352 cm/s, temperature 18 ^{o}C and sparger porosity 20 μm

4.5.4 Mass transfer coefficient

Table 4.4 summarizes the data required to calculate the interfacial area (bubble size and gas holdup) and the mass transfer coefficient (the "k_L" was calculated from the "k_La_{20}"). The values are practically constant with an average $6.7x10^{-4}$ m s^{-1} and a standard deviation of $0.1x10^{-4}$ m s^{-1}. The author is not aware of any previous estimates of "k_L" (measuring bubble size to determine the interfacial area) against which to compare this value.

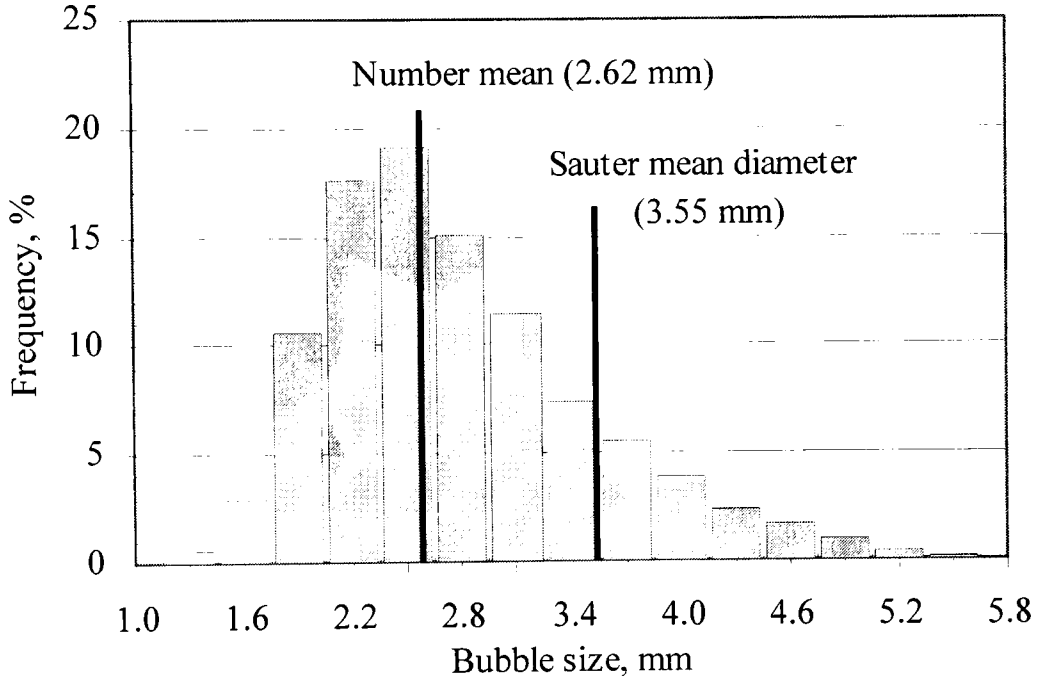

Figure 4.12. Bubble number frequency distribution for the gas rate 0.658 cm s^{-1} (note:

$$\text{number mean} = \sum_{i=1}^{n} \frac{d_i}{n})$$

Table 4.4. Mass transfer coefficient determination (note: ORP ranged from 1135 to 1150 mV vs Ag/AgCl and pH between 5.0 to 5.7)

Run #	Results			
	Bubble $d_{3,2}$ (mm)	**Holdup (%)**	**Interfacial Area (10^3 m^{-1})**	**k_L (10^{-4} m s^{-1})**
Diffuser				
1	3.91	2.56	3.93	6.93
2	3.91	2.56	3.93	6.72
3	3.89	2.56	3.93	6.51
Superficial gas velocity				
4	3.05	1.31	2.58	6.39
5	3.91	2.56	3.93	6.72
6	3.95	4.52	6.87	6.50
Solution volume				
7	3.55	2.85	4.82	6.86
8	3.91	2.56	3.93	6.72
9	3.52	2.29	3.90	6.72

CHAPTER 5

Ozone Decomposition Characterization

5.1 Introduction

Ozone reactions with water have been studied since ozone was first suggested for water treatment. The rate equations, including the direct and indirect reaction mechanisms, form the basis of models to describe these processes. The main problem is to describe the ozone decomposition produced by the hydroxide radical, OH^*. In the proposed process here for nickel oxidation/precipitation the presence of this radical is unavoidable due to alkali addition to conserve the pH. Thus the kinetics of ozone decomposition produced by hydroxide is important. This chapter presents results of tests performed to characterize ozone decomposition in the semi-batch reactor. Two pH ranges were evaluated, above and below 7.2. For interest, the inhibitor effect of carbonate was also tested. At the end a general kinetic equation (for the case of pH > 7.2 in the absence of inhibitor, i.e., conditions relevant to the present study) is proposed. Decomposition rate below pH 7.2 is low and considered negligible.

5.2 Methodology

Holding pH constant by addition of buffer solution or hydroxide ion and monitoring ozone concentration with time is typically how the ozone decomposition rate is measured and reaction order determined. Because of limitations in mixing in a bubble column reactor of the dimensions used in this work, the pH was left to drift but was continuously monitored. The ozone decomposition rate is determined by means of a material mass balance, which the column instrumentation allows to be performed continuously, namely:

Rate of ozone flowing into the reactor	=	Rate of ozone flowing out of the reactor	+	Rate of ozone accumulation in the reactor	+	Rate of ozone decomposition in the reactor

In the present case, the rate of ozone flowing in and out and the rate of ozone accumulation in the reactor were measured. In more mathematical form this can be written

$$W_{O_2} X_{in} = W_{O_2} X_{out} + \frac{d(V[O_3]_l)}{dt} + \text{Rate of ozone decomposition} \qquad (5.1)$$

Thus the measured rate is given by:

$$\text{Rate of ozone decomposition} = W_{O_2} X_{in} - W_{O_2} X_{out} - V\frac{d[O_3]_l}{dt} \qquad (5.2)$$

To estimate the reaction rate the measured rate can be compared, in general form when scavengers are added (Staehelin and Hoigné, 1982), to

$$-\frac{d[O_3]}{dt} = k[OH^-]^a [O_3]^b \qquad (5.3)$$

(cf Equation 2.36)

or with no scavengers (Tomiyasu et al., 1985), to

$$-\frac{d[O_3]}{dt} = k[OH^-]^a [O_3]^b + k_2 [OH^-]^c [O_3]^d \qquad (5.4)$$

(cf Equation 2.38)

The approach used to determine the reaction rate is based on this comparison. For any selected time, ozone (in gas and liquid phases) and hydroxide concentration are measured and Equation (5.2) is solved to give the ozone decomposition rate as shown in Figure 5.1. The rate constant and order of reaction are determined by trial-and-error combination of values for k, a, b, c and d to test the fit of Equations (5.2) or (5.3). The decomposition rates measured and calculated are compared and the best fit (i.e., best estimate of the fitted parameters) identified by the highest correlation coefficient (R^2).

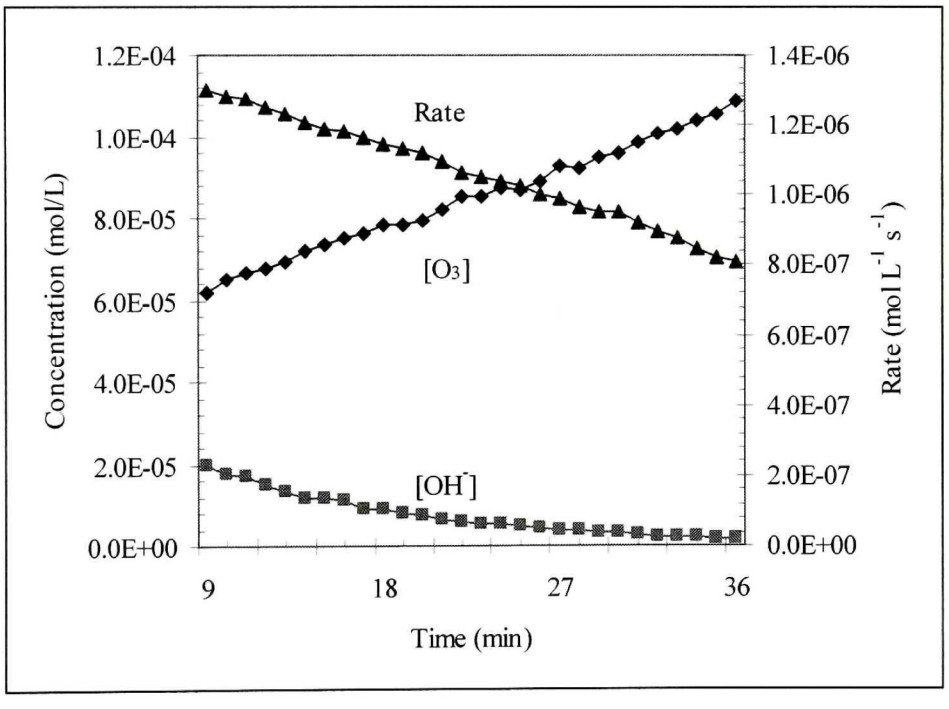

Figure 5.1. Typical results to determine the ozone decomposition rate

5.3 Test procedure

To begin, the water was "treated" with ozone to eliminate impurities: ozone (in oxygen) was dispersed in the water sample till the aqueous and gas outlet concentrations increased to constant values and was then continued for a further 30 minutes. At this point just oxygen was fed to eliminate the aqueous ozone. When the ozone aqueous

concentration reached zero the gas inlet was closed finishing the treatment step. Then the solution pH was set using 0.1M sodium hydroxide.

The ozone generator was adjusted to produce a set gas feed rate and ozone concentration. During the run, parameters such as pH, gas outlet ozone concentration, liquid ozone concentration, redox potential, temperature, superficial gas velocity and gas holdup were continuously monitored and registered. A program with 8 runs was completed using a diffuser porosity of 20 μm, liquid volume of 10 liters and superficial gas velocity of 0.658 cm/s. Other test conditions are given in Table 5.1.

Table 5.1. Test conditions

Run #	Conditions			
	Na_2CO_3 (mol/L) x 10^{-4}	$[O_3]_{gas}$ Feed (mol/L) x 10^{-4}	pH range	Temperature (°C)
Inhibitor Tests				
1	0	5.48	9.86 –7.53	19.1
2	7.077	5.48	9.75 – 7.52	20.3
3	14.340	5.48	9.72 – 7.42	18.7
Feed $[O_3]_{gas}$ Tests				
4	0	3.14	9.74 –7.58	19.4
5	0	5.48	9.86 – 7.53	19.1
6	0	9.17	10.17 – 7.59	17.9
PH Range Tests				
7	0	5.48	7.20 – 6.40	18.9
8	0	5.48	9.86 – 7.53	19.1

5.4 Results and discussion

5.4.1 Use of inhibitor: sodium carbonate

It has been claimed that the first order assumption requires the presence of inhibitor, to consume hydroxide radicals without regenerating the superoxide anion O_2^-. In this regard, sodium carbonate was tested.

Two carbonate levels were used (7.077×10^{-4} and 14.340×10^{-4} M) representing double and triple of the stoichiometric (Equation 2.33). Figures 5.2 and 5.3 show ozone molar concentration in liquid and gas phases versus time; Figure 5.4 shows pH variation.

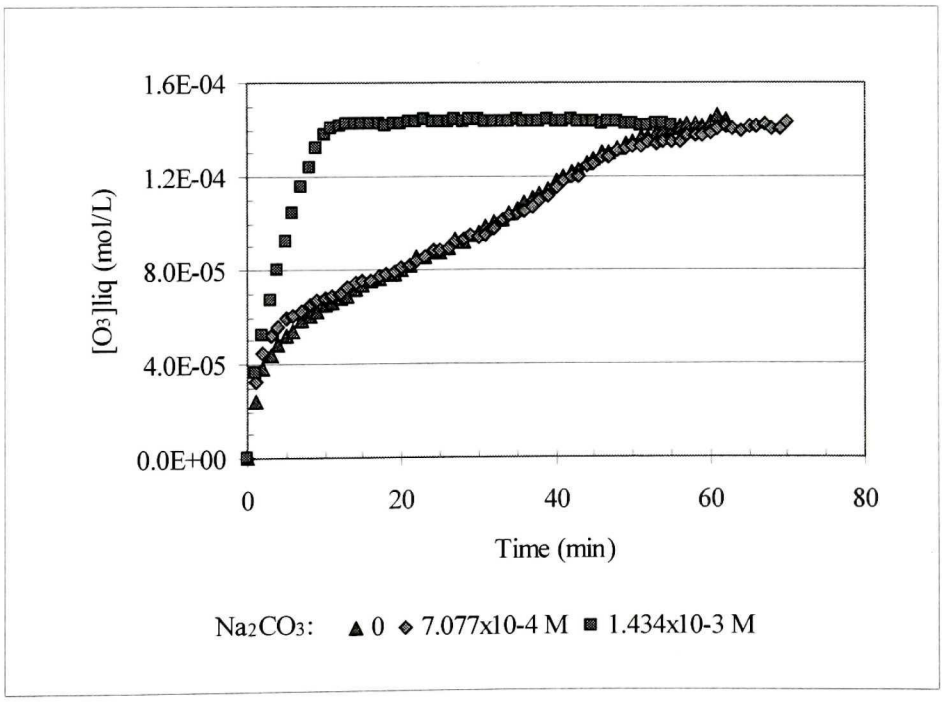

Figure 5.2. Variation of ozone concentration in liquid phase for different carbonate initial concentration

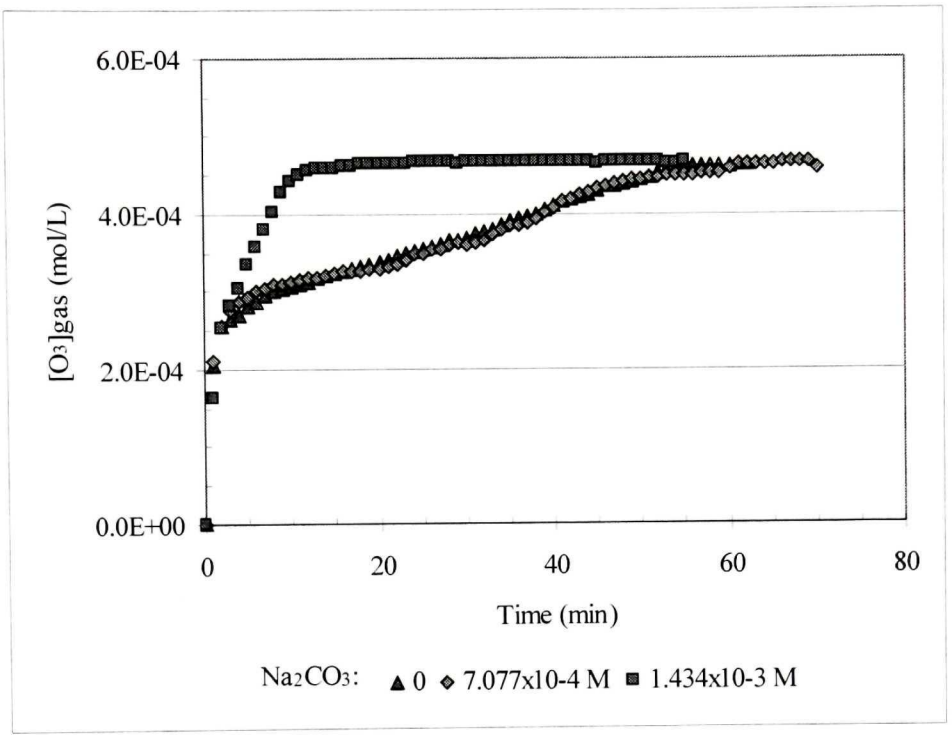

Figure 5.3. Variation of ozone concentration in gas phase for different carbonate initial concentration

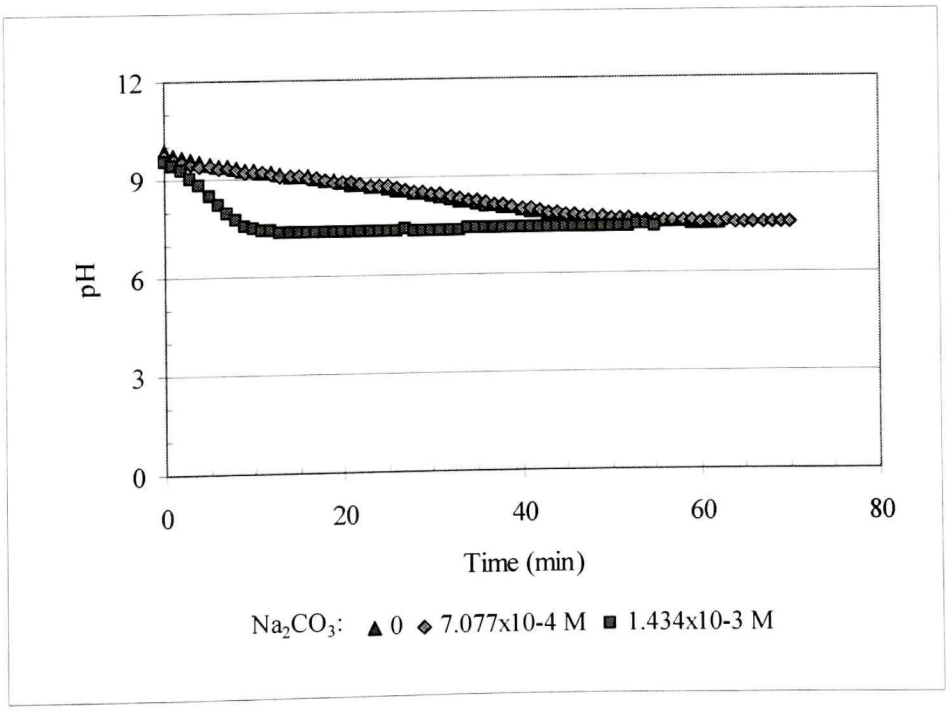

Figure 5.4. pH versus time with/without carbonate

An effect of inhibitor at high concentration ($1.434x10^{-3}$ mol/L CO_3^{2-}) is observed. The ozone liquid and gas phase concentrations reach equilibrium rapidly and pH decrease rapidly. This effect is because reaction (2.30) ceases and OH^- is consumed only by reaction (2.25), as proposed by Tomiyasu et al. (1985).

Ozone decomposition rate is compared for every time in Figure 5.5 and shows a difference. However, on comparing the measured rates with Equation (5.3) and (5.4) it was found that the former fitted both cases, with and without carbonate. Figures 5.6 and 5.7 show ozone decomposition rate measured and calculated using Equation (5.2). This is at odds with the claims of Staehelin and Hoigné (1982) and Tomiyasu et al. (1985) that an equation of the form of Equation (5.4) is required in the absence of inhibitor but in fact agrees with much published data where Equation (5.3) is used without reference to the inhibitor effect.

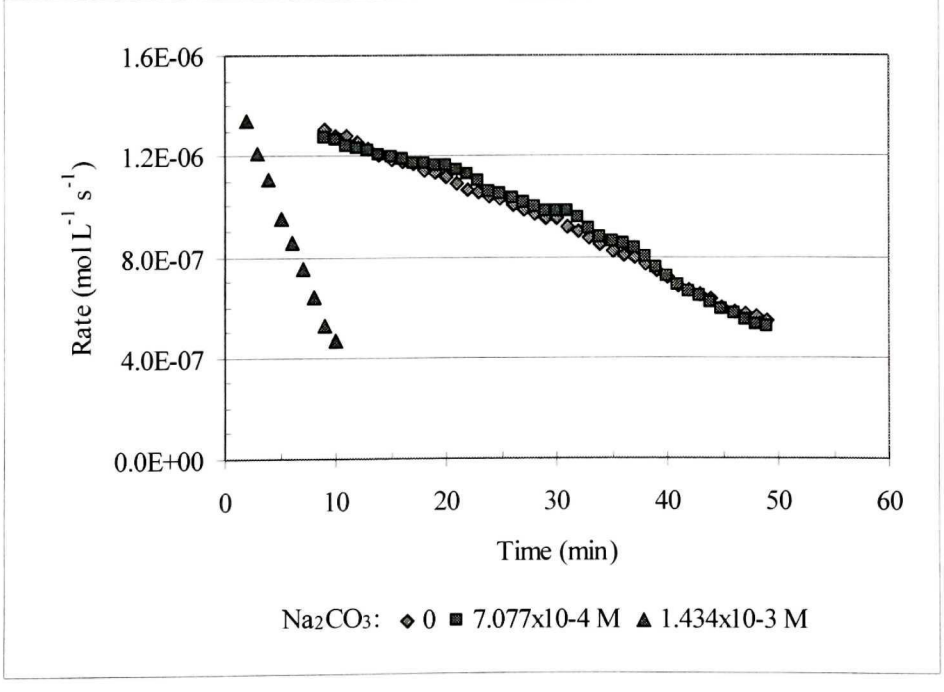

Figure 5.5. Ozone decomposition rate with/without carbonate

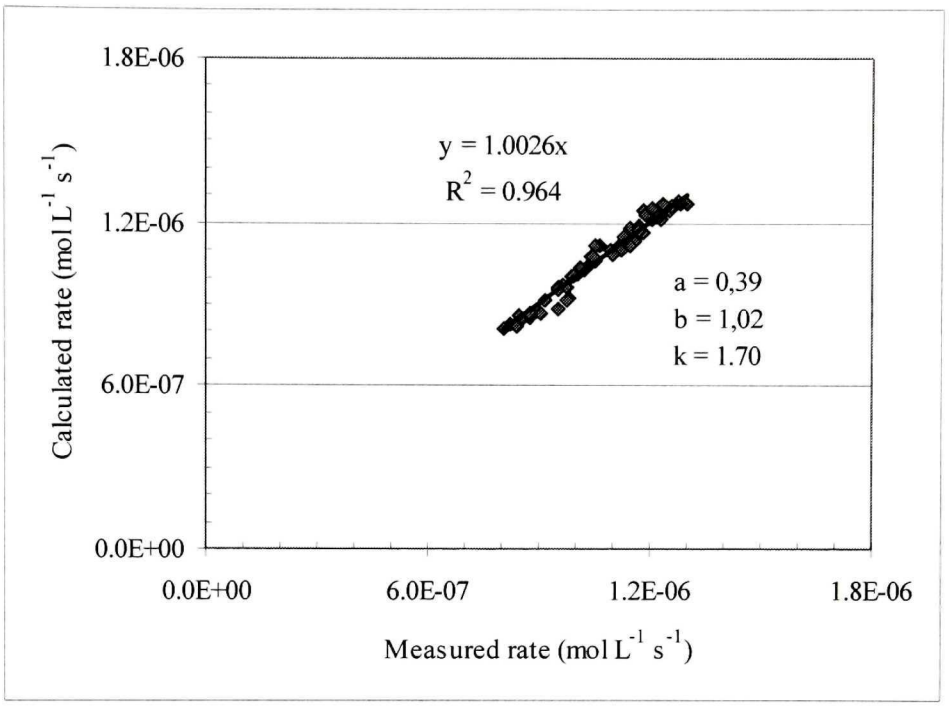

Figure 5.6. Comparison between measured and calculated (Eq (5.3)) decomposition rate at 0 and 7.077×10^{-4} mol/L Na_2CO_3

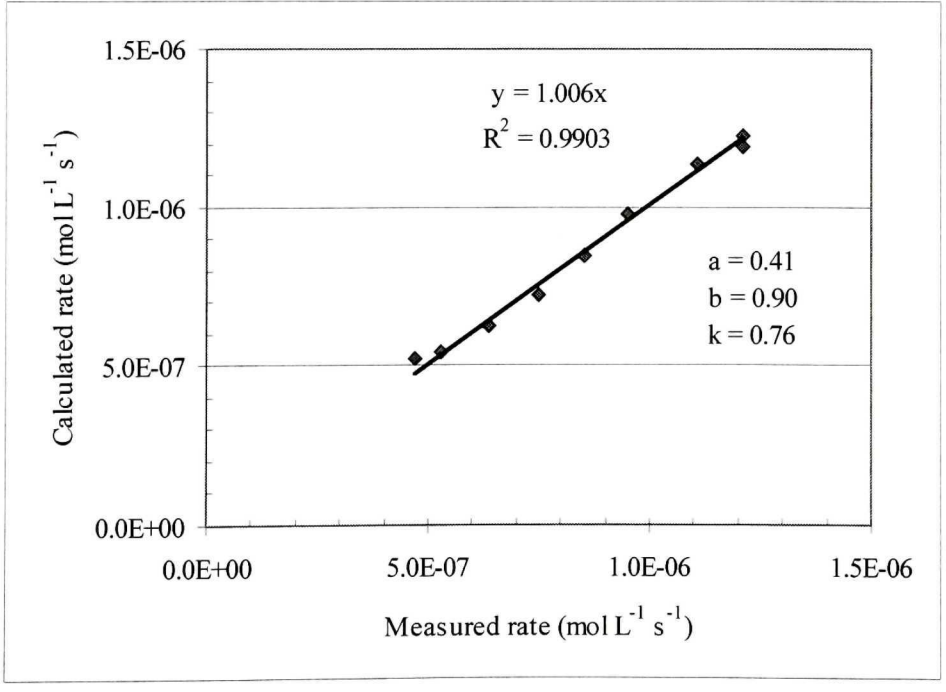

Figure 5.7. Comparison between measured and calculated (Eq (5.3)) decomposition rate with 1.434×10^{-3} mol/L Na_2CO_3

The kinetic rate constant "k" is lower with carbonate (0.76 L mol^{-1} s^{-1} vs. 1.70 L mol^{-1} s^{-1}) but the orders do not change significantly; the total order remains ~ 1.5. The estimate of "k" with carbonate, 0.76 L mol^{-1} s^{-1}, is lower than that found by Tomiyasu et al (190 L mol^{-1} s^{-1}). They did use ~3.8 times as much carbonate and an increase in "k" with inhibitor concentration follows from the present results comparing to the result at 0 carbonate. Another cause of the lower "k" could be the high pH used by Tomiyasu (~11.9 constant) which is outside the range evaluated here.

5.4.2 Ozone concentration effect

The decomposition rate was evaluated at three ozone concentrations in the gas feed (Table 5.1). Figures 5.8 and 5.9 present results of the ozone concentration (gas and liquid phase) and Figure 5.10 the pH variation.

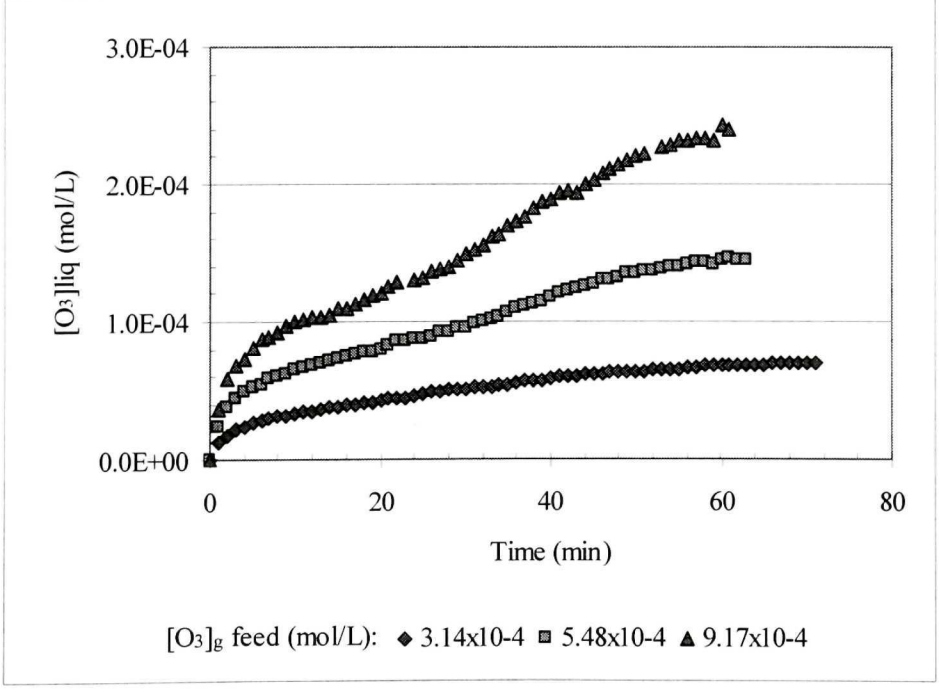

Figure 5.8. Ozone concentration liquid phase as a function of time and ozone concentration

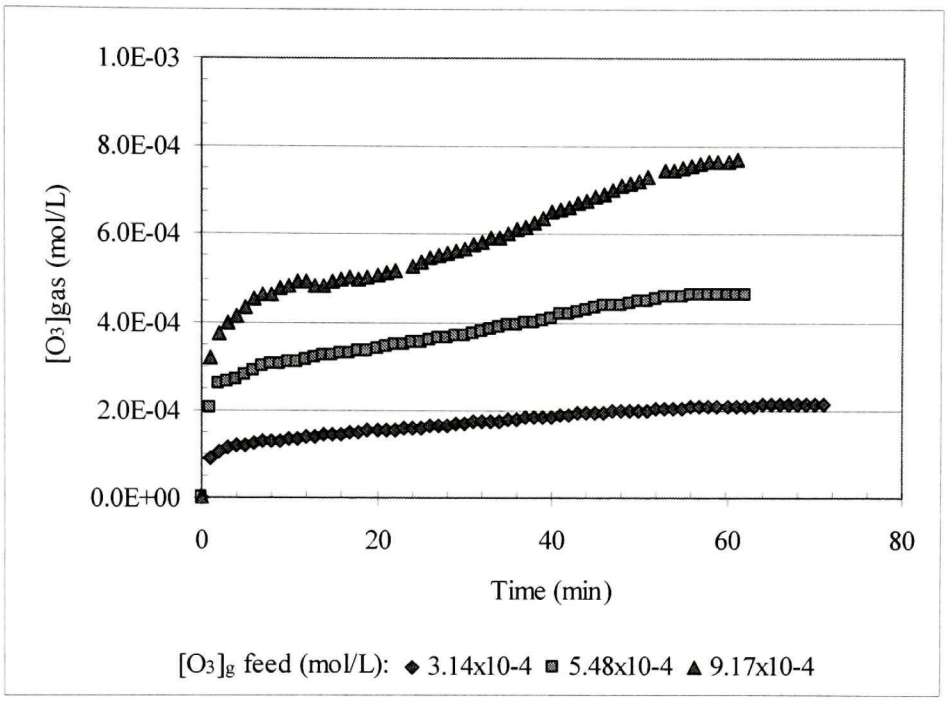

Figure 5.9. Ozone concentration in gas phase as a function of time and initial ozone concentration

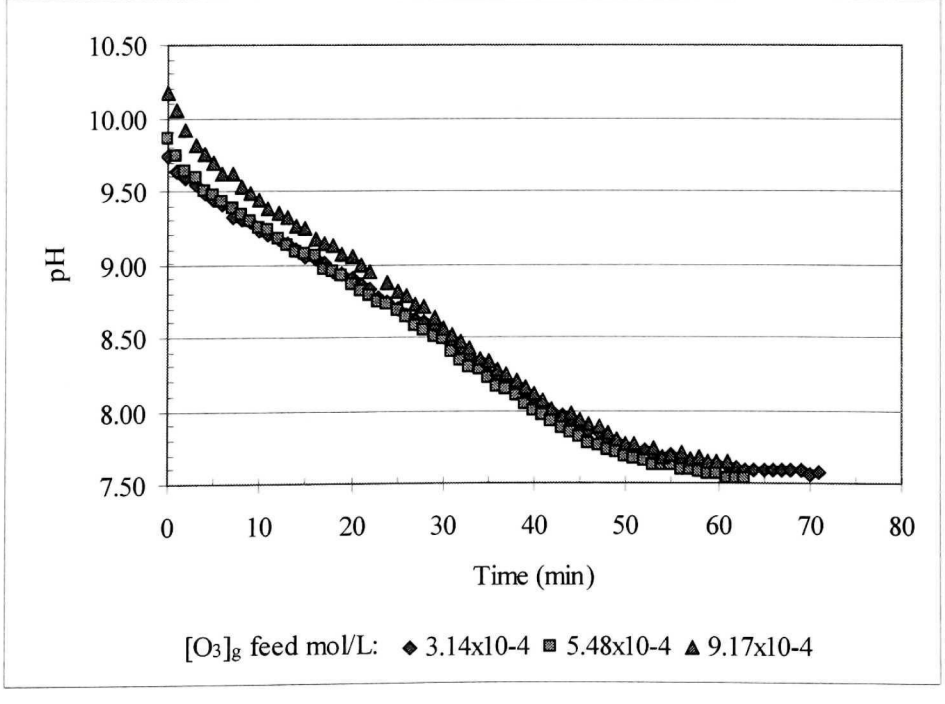

Figure 5.10. pH as a function of time and initial ozone concentration

Ozone solubility is a function of ozone concentration in the gas, as reflected in Figures 5.8 and 5.9. Unfortunately, the initial pHs were not the same but the tendency to decrease attributable to reaction between OH* and O_3 such is mentioned by Staehelin and Hoigne (1982) and Tomiyasu et al. (1985) is evident and the small differences in Figure 5.10 are not material.

Figure 5.11 shows the ozone transferred from gas to liquid for every time; and, Figure 5.12 shows ozone decomposition rate measured and calculated using Equation (5.3); Equation (5.4) offered no improvement.

The estimate of "k" and reaction order "a" and "b" are of the same magnitude when no carbonate was used. It means the variation of ozone concentration in the feed gas has not produced any variation in the kinetics.

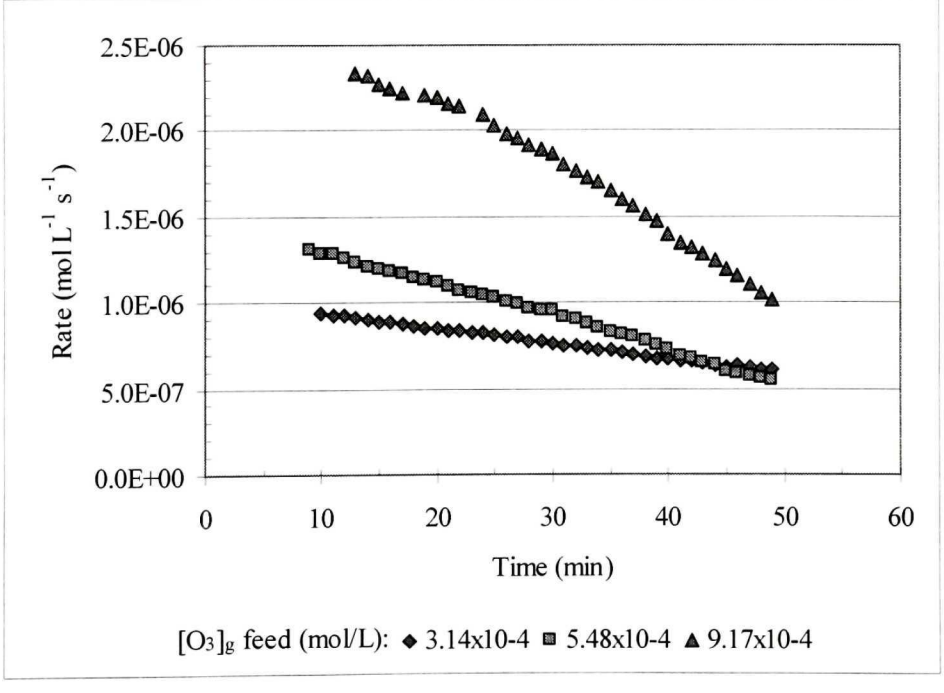

Figure 5.11. Ozone decomposition rate as a function of time and ozone concentration

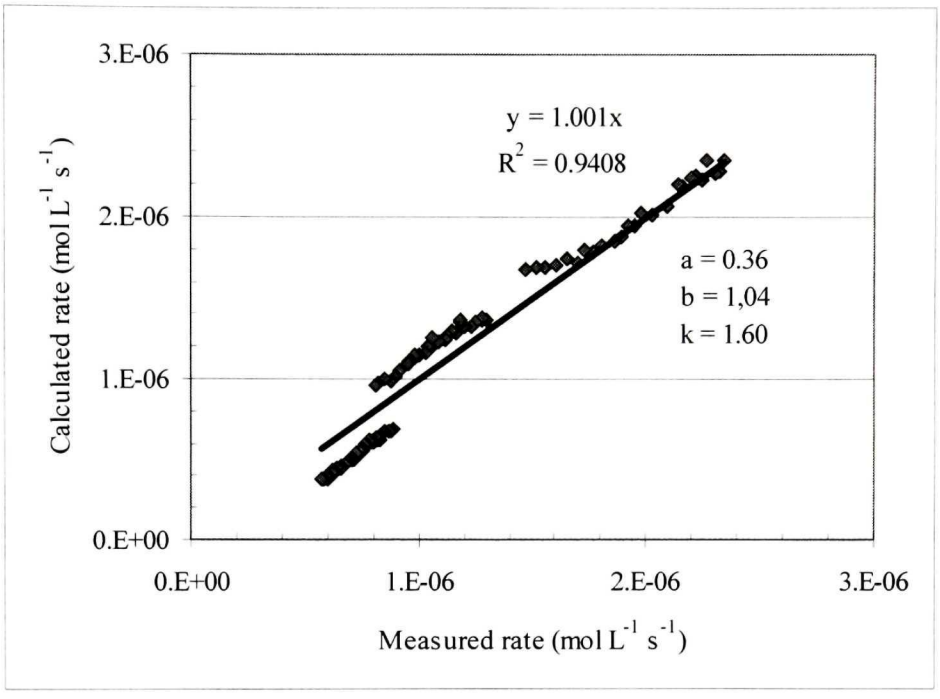

Figure 5.12. Comparison between measured and calculated (Eq (5.3)) decomposition rate. Ozone concentration test effect

5.4.3 pH range effect

Reaction order and kinetic rate constant were determined for two pH ranges, greater and less than pH 7.2. The ozone feed concentration in both cases was the same and remained constant. Figures 5.13 and 5.14 show the variation in ozone concentration (liquid and gas phase), and Figure 5.15 the pH variation.

Ozone concentration in gas and liquid phase reach steady state after 10 minutes when pH was lower than 7.2. In this period of time, pH decreased to 6.6 and remained essentially constant. This indicates that no more ozone decomposition occurred.

Figures 5.16 and 5.17 show the decomposition rate for the two pH ranges; Figure 5.18 shows values of ozone decomposition rate measured and calculated using Equation (5.3).

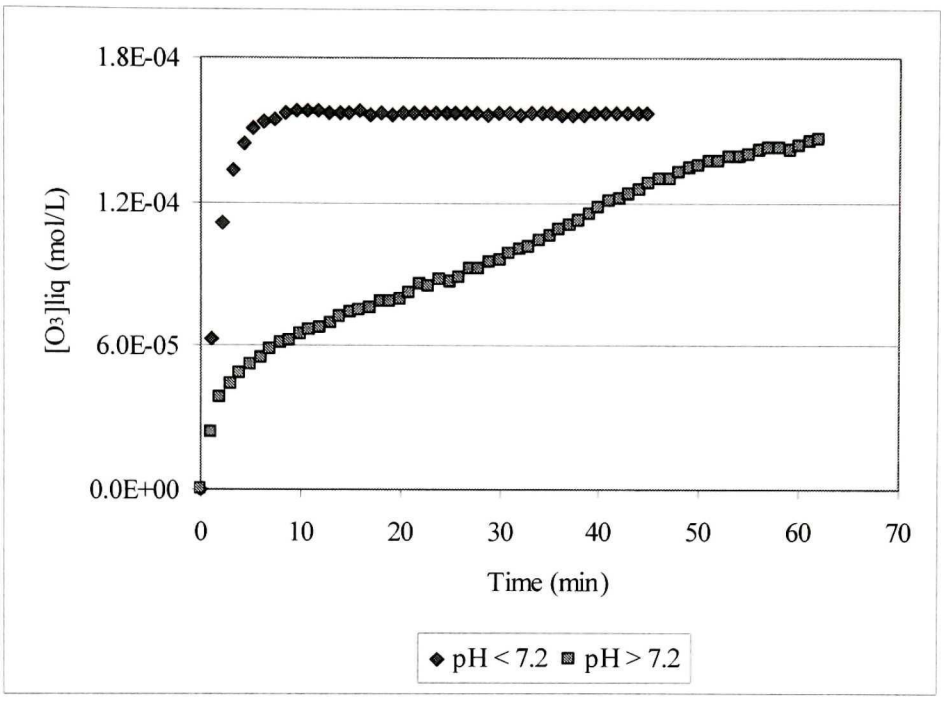

Figure 5.13. Ozone concentration in liquid phase as a function of time at the two pH ranges

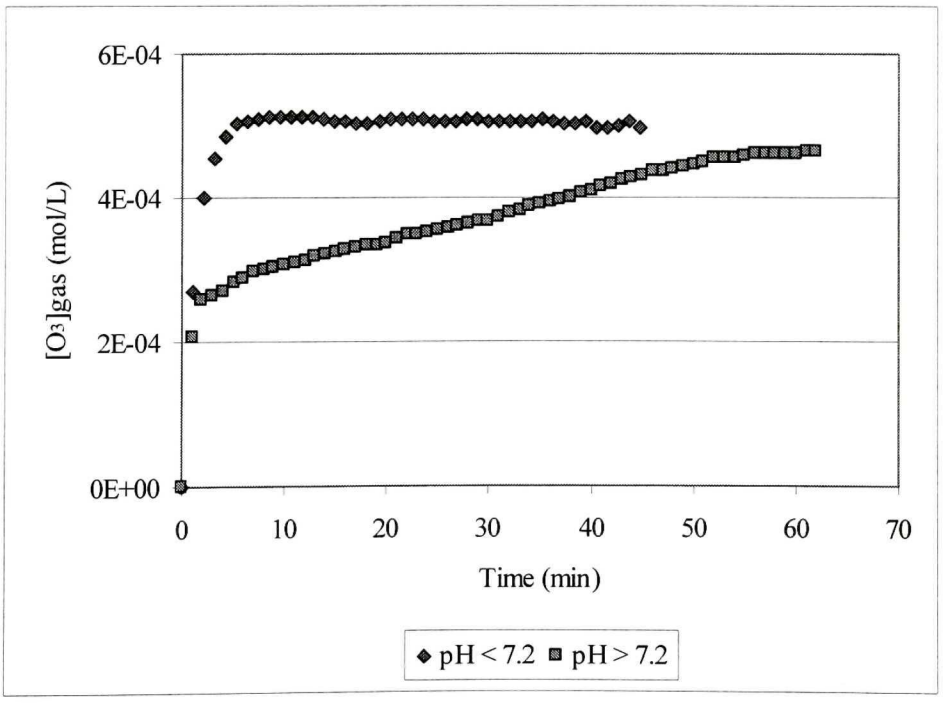

Figure 5.14. Ozone concentration in gas phase as a function of time at the two pH ranges

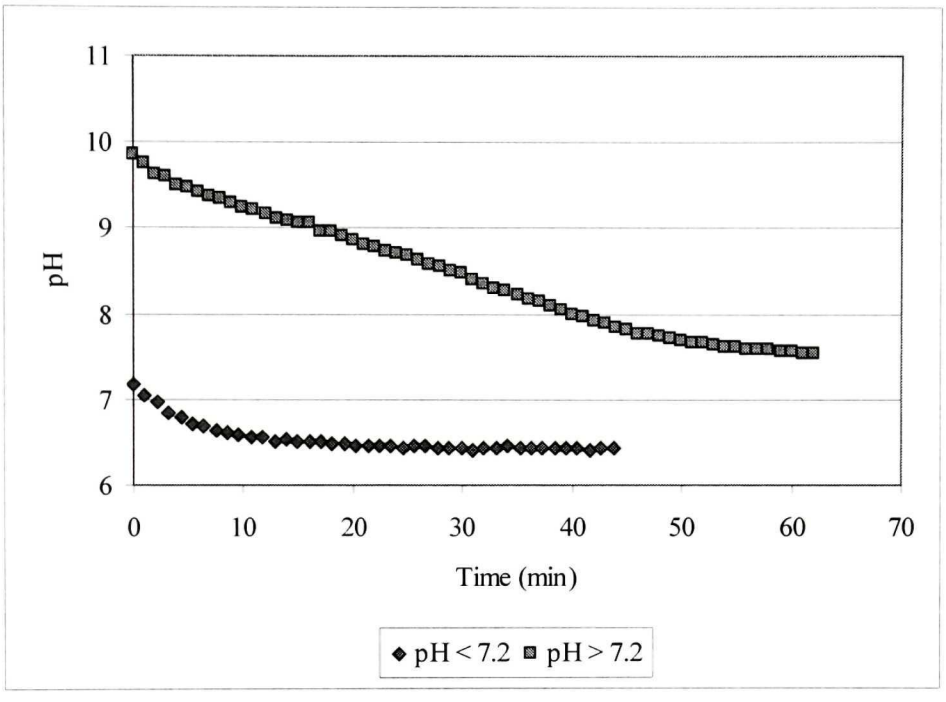

Figure 5.15. pH as a function of time at the two ranges

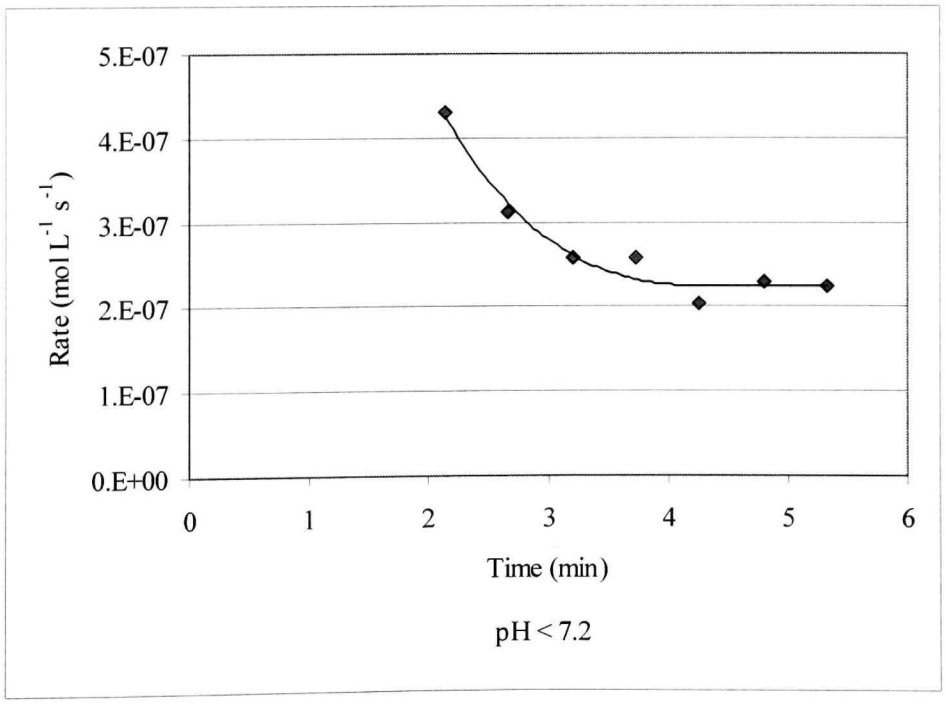

Figure 5.16. Ozone decomposition rate as a function of time at pH < 7.2

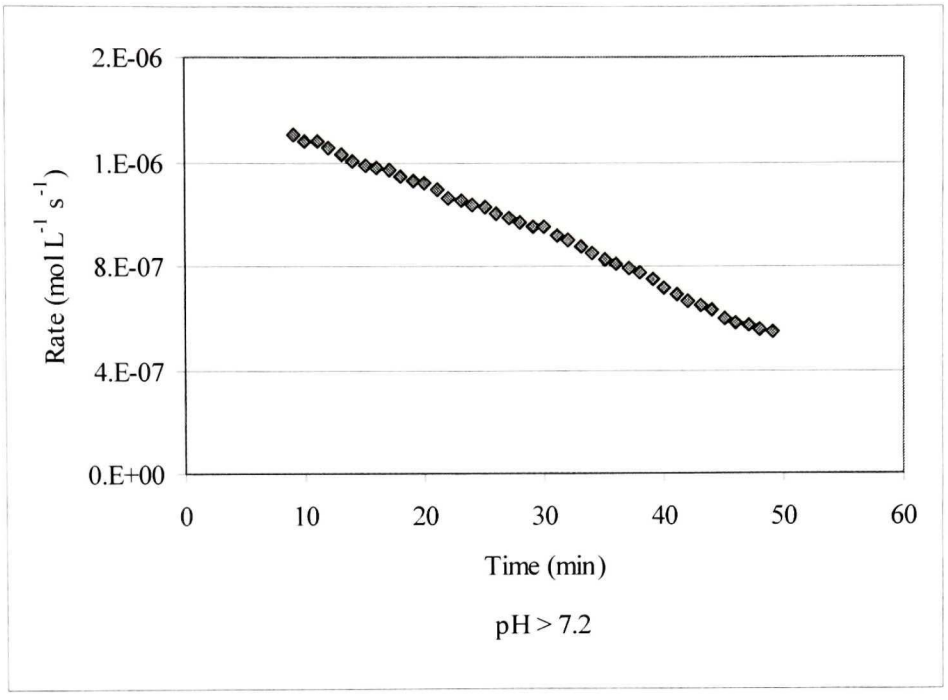

Figure 5.17. Variation of ozone decomposition rate at pH > 7.2

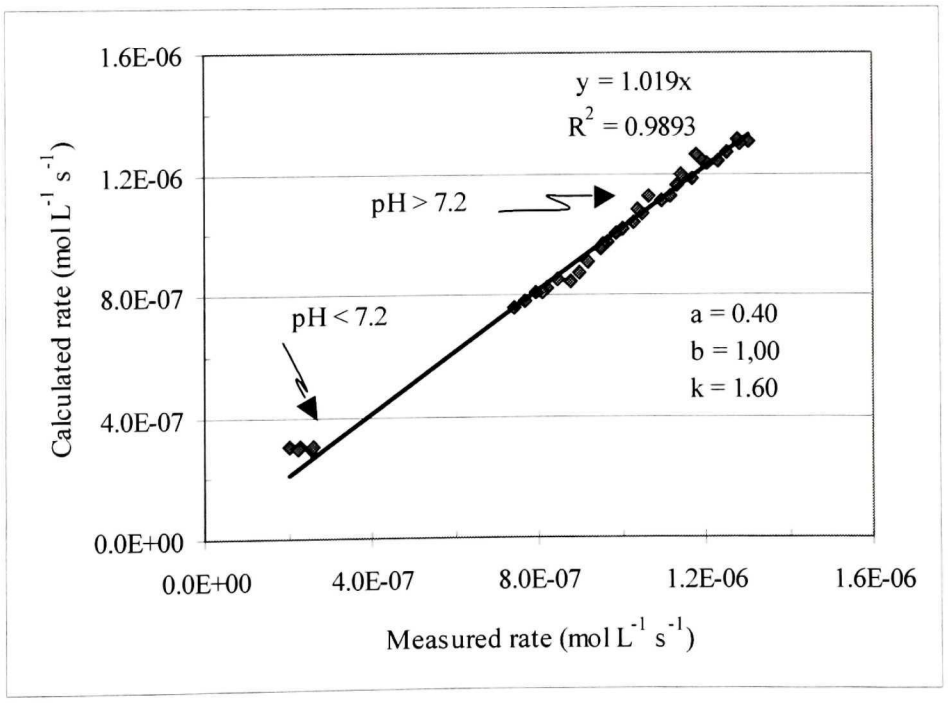

Figure 5.18. Comparison between measured and calculated (Eq (5.3)) decomposition rate. pH range effect

Rate constant "k" and reaction order "a" and "b" found for pH > 7.2 were:

$k = 1.60$ L mol^{-1} s^{-1}

$a = 0.40$

$b = 1.00$

At pH < 7.2 the decomposition rate was low and almost constant (2.34×10^{-7} mol L^{-1} s^{-1} with a 95% confidence interval of $\pm 2.31 \times 10^{-8}$).

5.4.4 General reaction order and rate constant (pH>7.2, without carbonate)

To determine the overall reaction order and rate constant at pH >7.2, Figures 5.6, 5.12 and 5.18 were combined and the best fit between measured and calculated rate found. This relationship is shown in Figure 5.19 where values of "a" and "b" are 0.36 and 1.05, respectively. These values are similar to them founded by Alder et al. (1950) and signaled in Table 2.5. The sum of orders is close to 1.5, which is taken to be the true total order. The corresponding rate constant "k" is 1.67 L mol^{-1} s^{-1}.

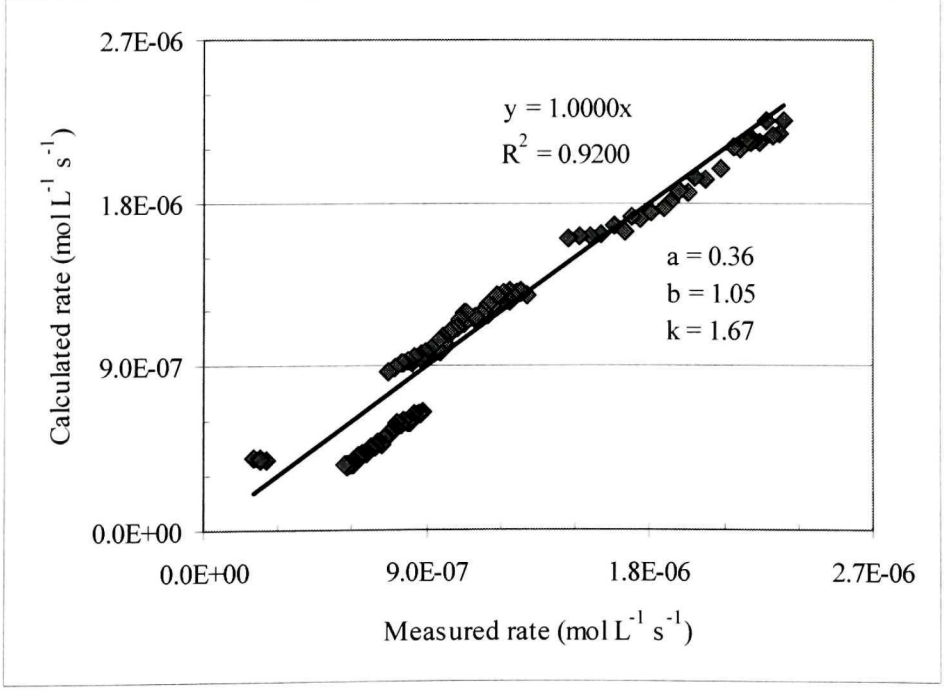

Figure 5.19. Comparison between measured and calculated (Eq (5.3)); general result

CHAPTER 6

Nickel Precipitation by Ozone Oxidation

6.1 Introduction

Some prior investigations into removal and/or separation of metallic ions (Fe, Mn, Co, etc.) from aqueous solutions by ozone have been conducted. In the case of manganese, ozone was found to be capable of producing manganese dioxide precipitate even at a sulfuric acid concentrations as high as 5 molar (Nishimura et al., 1992). Separation of cobalt from nickel is an important step in hydrometallurgy, and strong oxidants such as persulfate, Caro's acid and ozone have been tested (Nikolic et al., 1978). To develop nickel processing using ozone, data on the oxidation rates are required. In this chapter ozone oxidation of nickel (II) ion in aqueous sulfate solution has been determined under various conditions. The effects of pH, ozone gas content and nickel concentration in solution are presented. X-ray diffraction analysis determined that the products comprised $Ni(OH)_2$, NiOOH, $Ni_3O_2(OH)_4$ and $Ni_2O_2(OH)_4$.

6.2 Methodology

Nickel oxidation-precipitation tests were performed holding the reaction conditions constant and monitoring ozone and nickel concentration with time. The present work keeps the pH constant and alters the ozone and nickel concentration while measuring the rate of ozone consumption as a function of time. The methodology is based on the mass balance, characterized by the following equation:

Rate of ozone flowing into the reactor	=	Rate of ozone flowing out of the reactor	+	Rate of ozone accumulation in the reactor	+	Rate of ozone decomposition in the reactor	+	Rate of ozone/nickel reaction in the reactor

Measuring continuously the gas flow in and of the reactor, and the nickel and hydroxide concentration permits the reacted ozone rate at every interval of time to be computed. The mathematical expression of the mass balance is:

$$\text{Rate of } O_3/\text{Ni reaction} = W_{O_2} X_{in} - W_{O_2} X_{out} - V\frac{d[O_3]_l}{dt} - V\frac{d[O_3]_{OH}}{dt} \quad (6.1)$$

The measured rate can be compared with Equation 2.41 to estimate the "kinetic" parameters.

6.3 Procedure

Solutions were prepared using crystals of nickelous sulfate hexahydrate ($NiSO_4 \cdot 6H_2O$ > 98% purity) dissolved in distilled water. The pH of the solution varied according to the nickel concentration (but remained < pH 6). The solution pH was adjusted to ~ 7 using 0.1M sodium hydroxide. It was necessary to add alkali carefully to avoid nickel hydroxide ($Ni(OH)_2$) formation that starts at pH 6.8 when nickel concentration is > 1.70×10^{-2} M (Dyer and Scrivner, 1998).

The ozone generator was adjusted to produce a set feed rate and ozone concentration. During the run, nickel concentration, pH, gas outlet ozone concentration, liquid ozone concentration, redox potential, temperature, superficial gas velocity and gas holdup were measured continuously. A program with 10 tests was completed using a

diffuser porosity of 20 μm and liquid volume of 10 liters. Other test conditions are given in Table 6.1.

Table 6.1 Test conditions

Run #	Conditions				
	pH	$[O_3]_{gas}$ Feed (mol/L)	[Ni] Feed (mol/L)	Jg (cm/s)	Temperature (^oC)
pH Effect Tests					
1	6.80	5.48E-4	2.08E-02	0.592	18.9
2	7.00	5.48E-4	1.84E-02	0.559	18.4
3	7.50	5.48E-4	1.69E-02	0.563	17.8
[Ni] Oxidation Tests					
4	5.80	5.48E-4	0.00	0.659	19.5
6	6.50	5.48E-4	1.70E-03	0.659	18.8
7	6.19	5.48E-4	8.52E-03	0.659	19.0
Feed $[O_3]_{gas}$ Tests					
5	7.00	5.48E-4	8.86E-03	0.668	18.1
6	7.00	7.50E-4	8.74E03	0.669	18.0
7	7.14	9.17E-4	9.06E-03	0.663	18.0
Feed [Ni] Tests					
8	7.23	7.84E-4	1.67E-03	0.658	18.3
9	7.18	7.84E-4	8.87E-03	0.658	18.9
10	7.06	7.84E-4	1.88E-02	0.658	19.1

6.4 Results and discussion

6.4.1 pH effect

According to Figure 2.2 the domain of relative predominance of ozone is > 1 volt over the pH range 0 to 14. Using this value in Figure 2.7 it is noted that this potential is adequate to precipitate nickel as Ni(III) or Ni(IV). Over pH 7.5, however, it is necessary to take into account the possibility of excess $Ni(OH)_2$ being generated.

To determine an appropriate pH to precipitate nickel, primarily as Ni(III), the effect of pH was tested. During ozonation the pH decreased and alkali addition was necessary to conserve it. Variation of the nickel concentration remaining in solution (expressed as %) is shown in Figure 6.1. Nickel concentration in solution decreased faster when pH was higher. Compounds formed during the process were determined using X-ray diffraction analysis of the precipitates: NiOOH and $Ni_3O_2(OH)_4$, (a mixture of NiOOH and $Ni(OH)_2$) were mainly found.

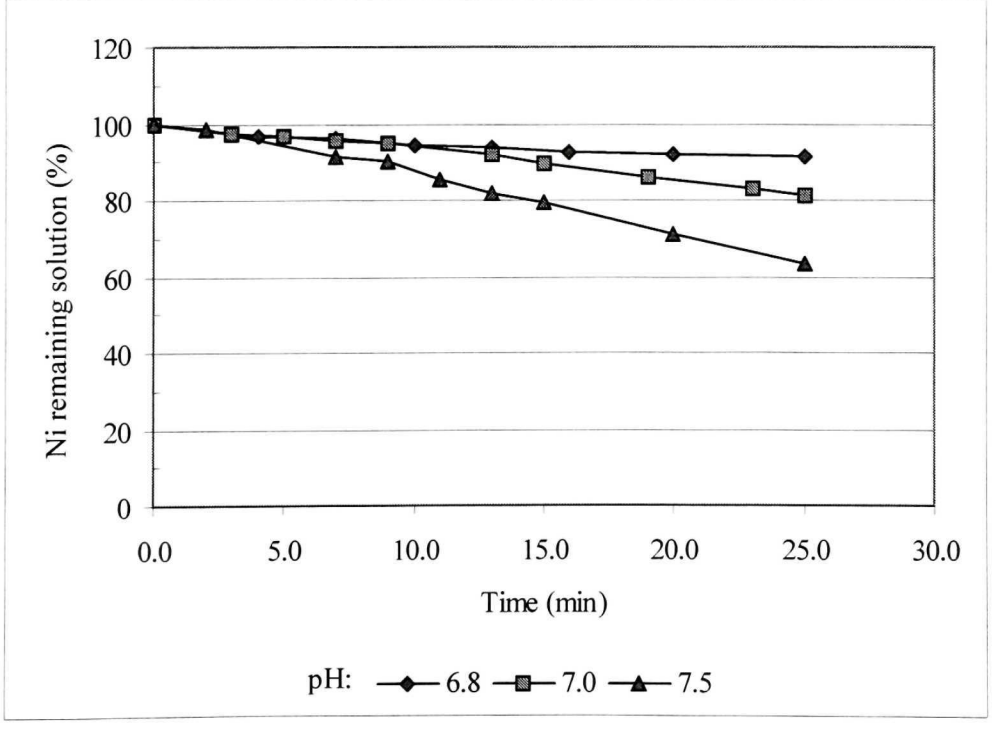

Figure 6.1. Nickel remaining in solution versus time at different pH

6.4.2 Nickel oxidation

A qualitative determination of nickel oxidation (Ni(II) to Ni(III)) in solution was performed. Solutions with different nickel concentration were prepared and exposed to ozone ($5.48x10^{-4}$ mol/L). To avoid hydrolysis of Ni(II) the solution pH was kept below 6.5. Ozone concentration in liquid and gas phase was measured continuously. Figures 6.2 and 6.3 show there was essentially no consumption of ozone, i.e., little oxidation of Ni(II) to Ni(III) in solution. Figure 6.4 shows the oxidation-reduction potential of solutions containing nickel which also suggest there were little reaction.

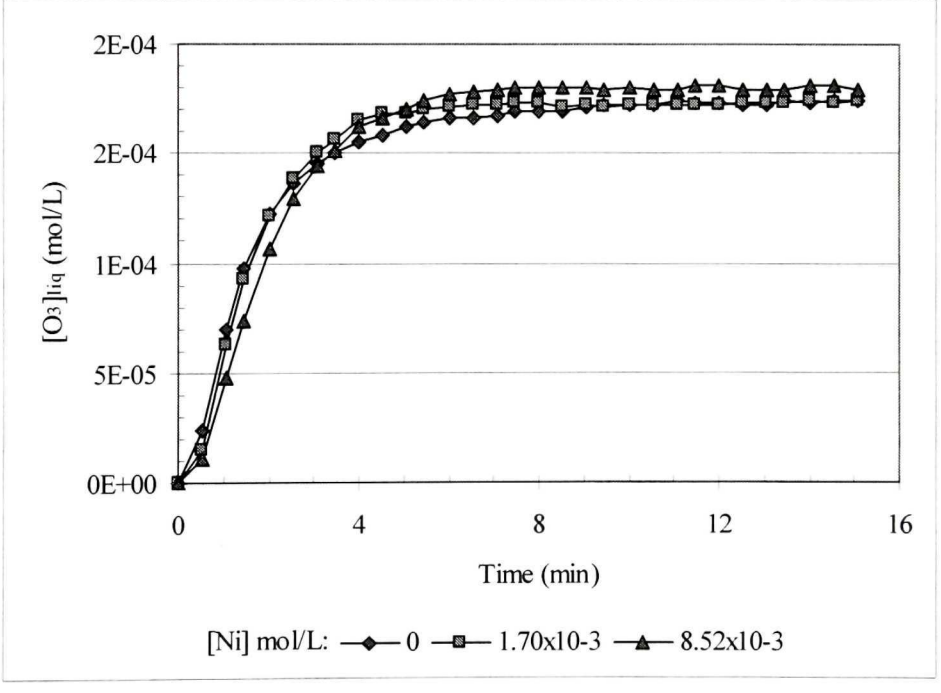

Figure 6.2. Ozone concentration in liquid phase for different nickel concentrations (pH < 6.5)

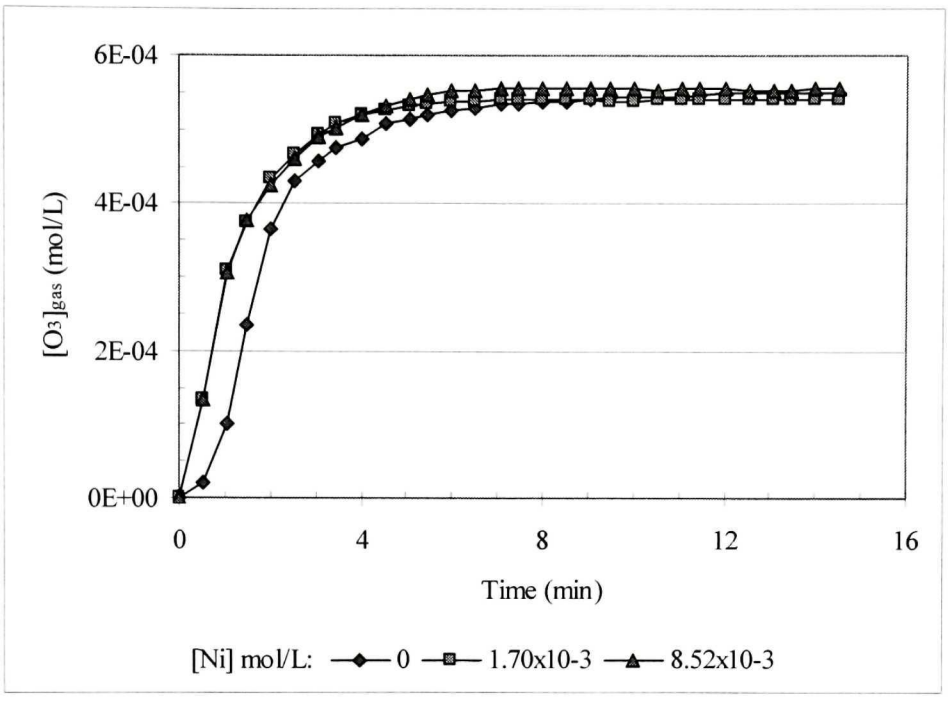

Figure 6.3. Ozone concentration in gas phase for different nickel concentrations

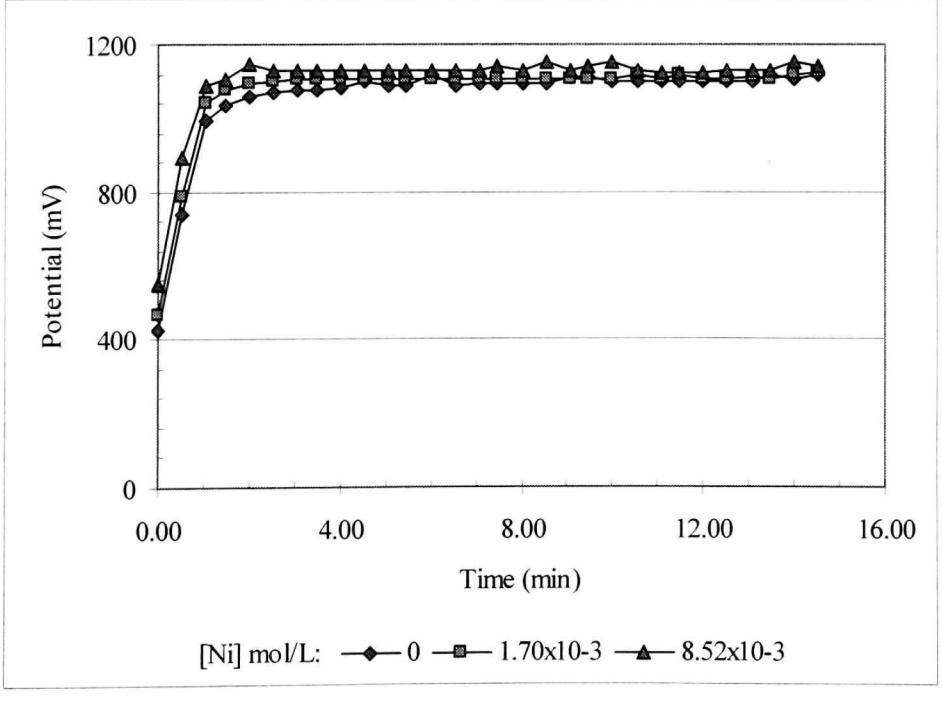

Figure 6.4. Oxidation-reduction potential variation during test of Ni (II) oxidation in solution

The explanation for the lack of oxidation is because reaction (2.39) in acidic medium, proposed by Nishimura et al. (1992), is not spontaneous at room temperature (~293 K). The more likely reaction is the following:

$$O_3 + 2Ni^{++} + 4OH^- \rightarrow 2NiOOH + O_2 + H_2O \qquad (6.2)$$

which requires OH^- to produce NiOOH. The free energy of this reaction is different from that of reaction (2.39) and is spontaneous above 270 K.

6.4.3 Ozone concentration effect

Ozone solubility depends on its concentration in the gas feed. To examine the effect of this variable on nickel oxidation-precipitation, tests were performed according to the conditions shown in Table 6.1. The ozone concentration in liquid and gas phase is shown in Figures 6.5 and 6.6, respectively. In both phases during the first 5 minutes ozone concentration reaches a maximum then decreases with time. In the case of the liquid the ozone concentration arrives near to zero while in the case of gas phase it approaches ca. 40% of the initial concentration.

Oxidation-reduction potential (ORP) versus time is shown in Figure 6.7. For all ozone concentrations the potential is over 900 mV. More time is necessary to reach the maximum potential when the ozone concentration is low.

Figure 6.8 shows nickel remaining in solution as a function of time. At the lowest ozone concentration nickel precipitation required some time (ca. 10 minutes) to initiate. Nickel concentration decreased more rapidly when ozone concentration was increased. The trend in nickel concentration was the same for all conditions.

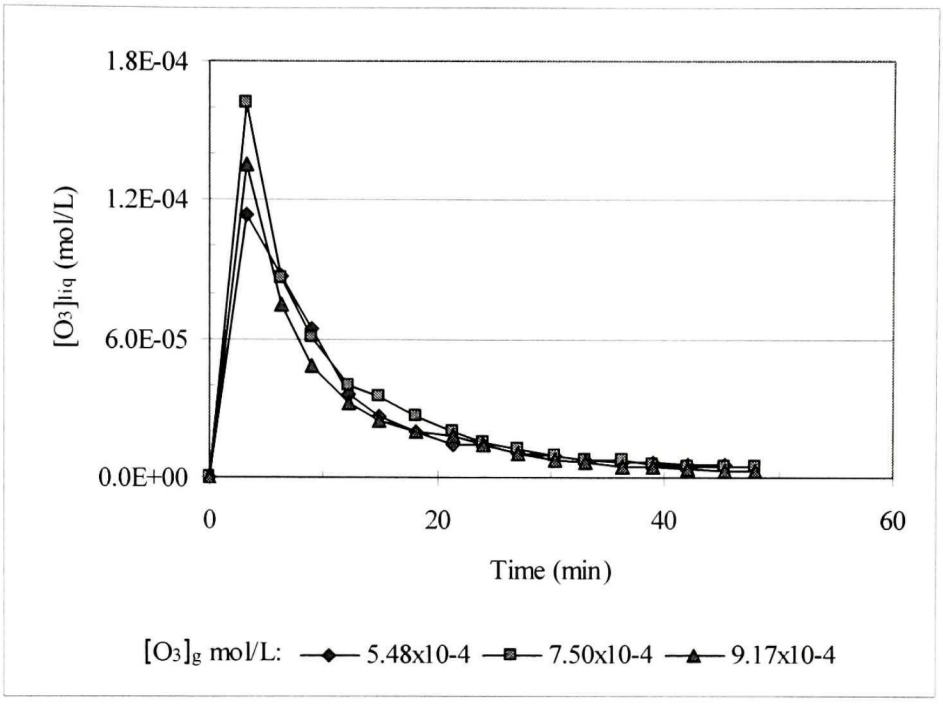

Figure 6.5.Ozone concentration in aqueous phase versus time during nickel precipitation

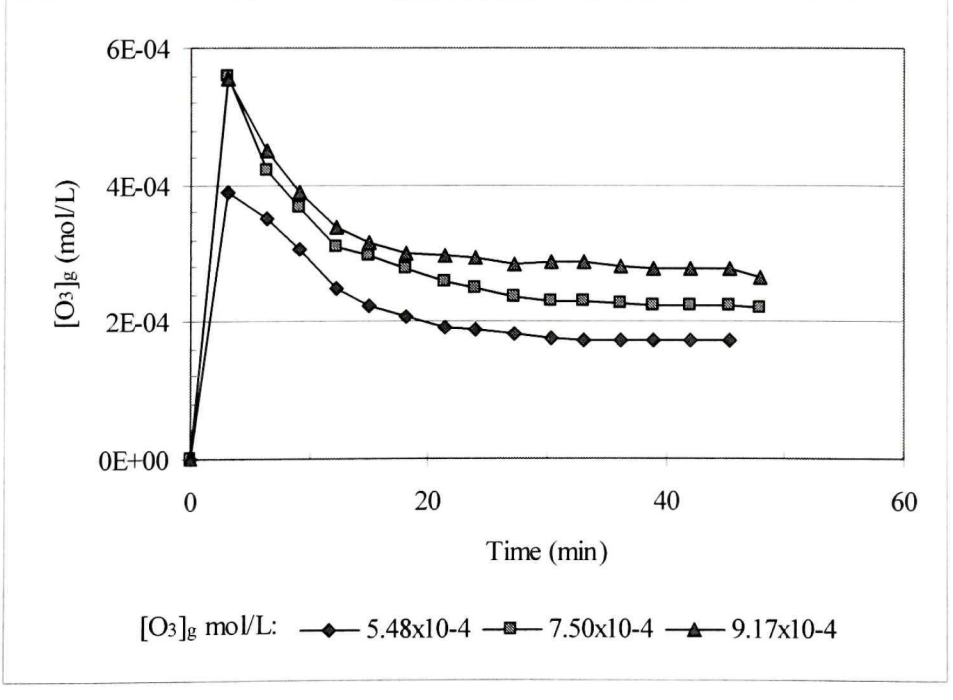

Figure 6.6.Ozone concentration in gas phase versus time during nickel precipitation

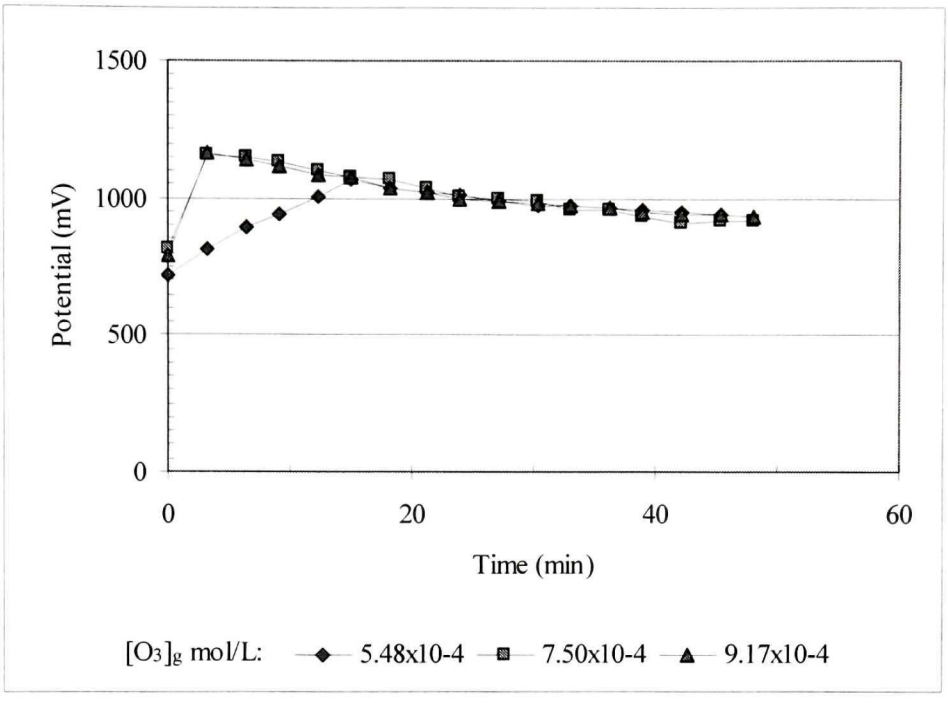

Figure 6.7. Oxidation-reduction potential versus time during nickel precipitation for different $[O_3]$ in gas (reference electrode platinum)

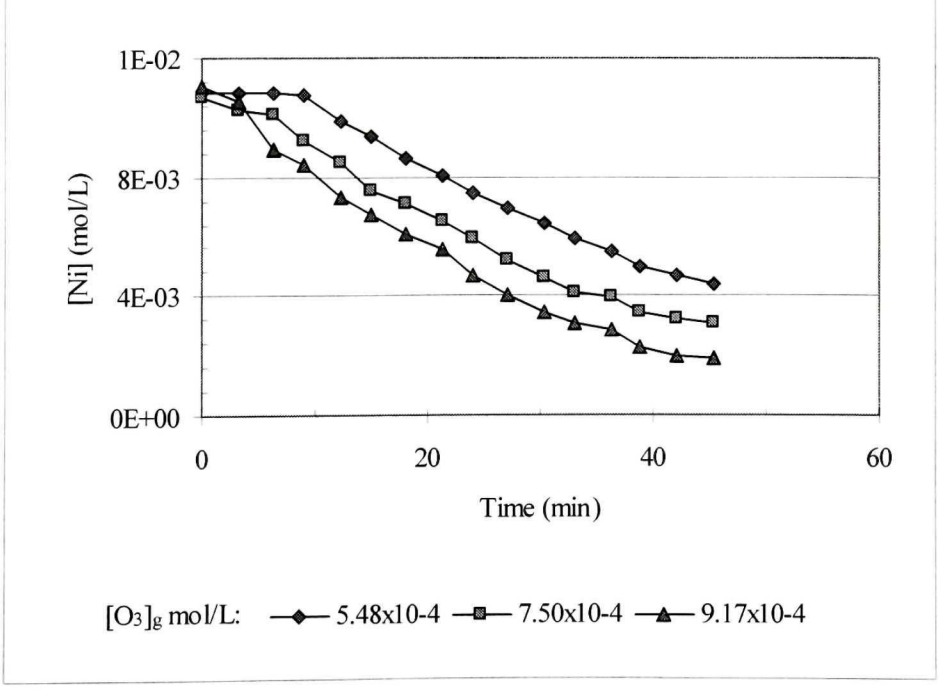

Figure 6.8. Nickel in solution versus time during nickel precipitation for different $[O_3]$ in gas (pH ~ 7)

Figure 6.9 shows the ozone consumption rate (calculated using Equation 6.1) at different times. The rate increases becoming constant after ca. 20 minutes. The rate is high when ozone concentration is high.

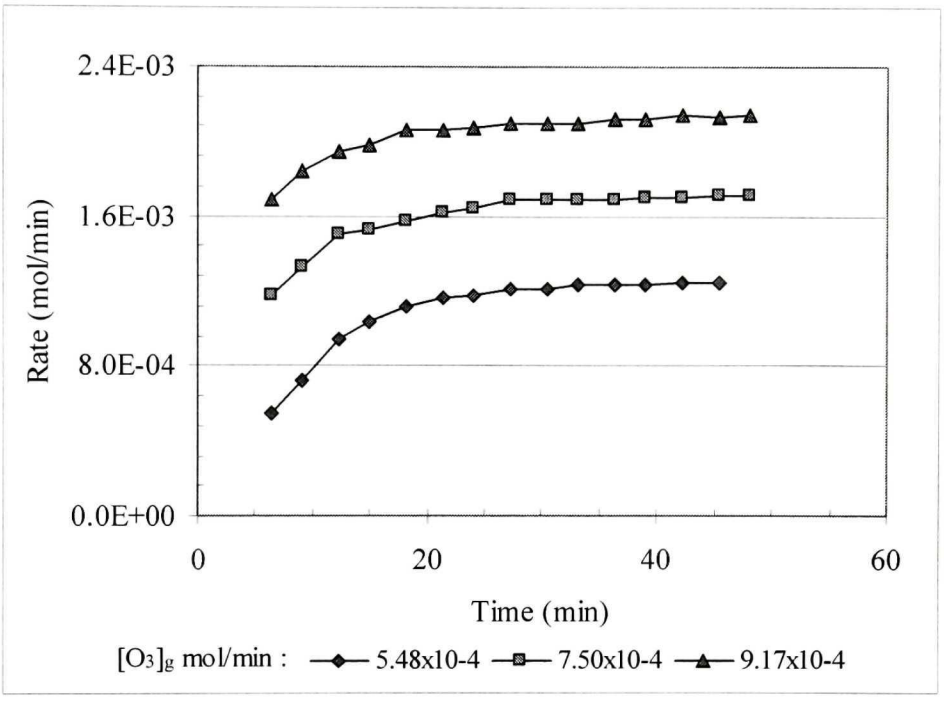

Figure 6.9.Ozone consumption rate for different $[O_3]$ in gas

Reaching a constant rate of consumption was not expected and suggested that a reaction other than Ni(II) to Ni(III) was consuming ozone; this is addressed later. The unexpected result meant it was not possible to calculate directly the ozone consumption just for nickel precipitation. During the test, solution samples were taken and the remaining nickel was determined, permitting the rate of nickel precipitate production to be estimated. Using Equation (6.2), where one mole of ozone reacts with 2 moles of Ni(II), the stoichiometric quantity of ozone required to oxidize and precipitate nickel was determined. The difference between total ozone consumed and ozone used to oxidize nickel gave the excess ozone consumed. Figure 6.10 shows the molar stoichiometric

ozone consumption at different ozone feed gas concentrations. Figure 6.11 shows the excess ozone consumption; it continues to increase with time despite the nickel concentration in solution decrease confirming that another ozone-consuming reaction was occurring.

Data on ozone consumption during nickel precipitation was used to determine the kinetics equation. The methodology of mass balance and trial and error was used to fit to the following equation:

$$-\frac{d[Ni^{++}]}{dt} = k_{Ni}[O_3]^a [Ni^{++}]^b [OH^-]^c \qquad (6.3)$$

Figure 6.12 shows the comparison between the measured and calculated rate of nickel oxidation.

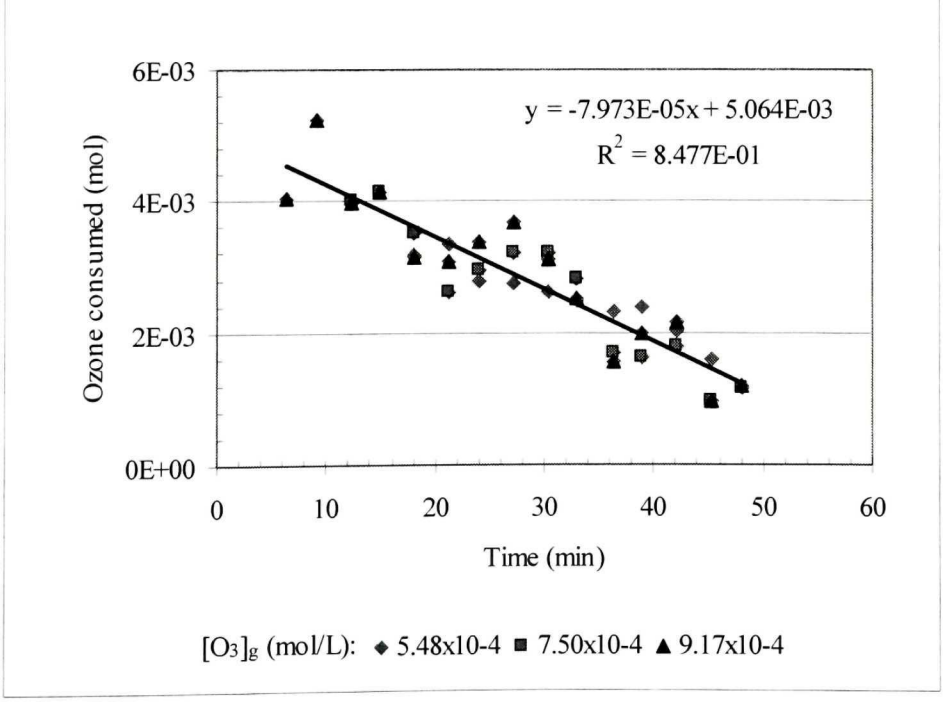

Figure 6.10. Ozone consumption at different $[O_3]$ in gas

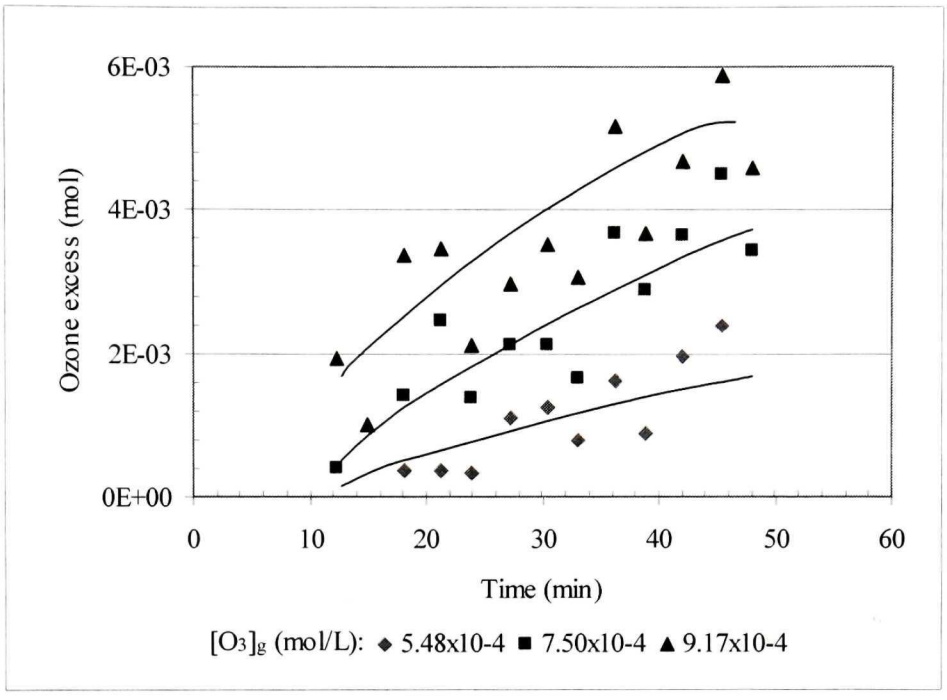

Figure 6.11. Ozone consumption excess at different $[O_3]$ in gas

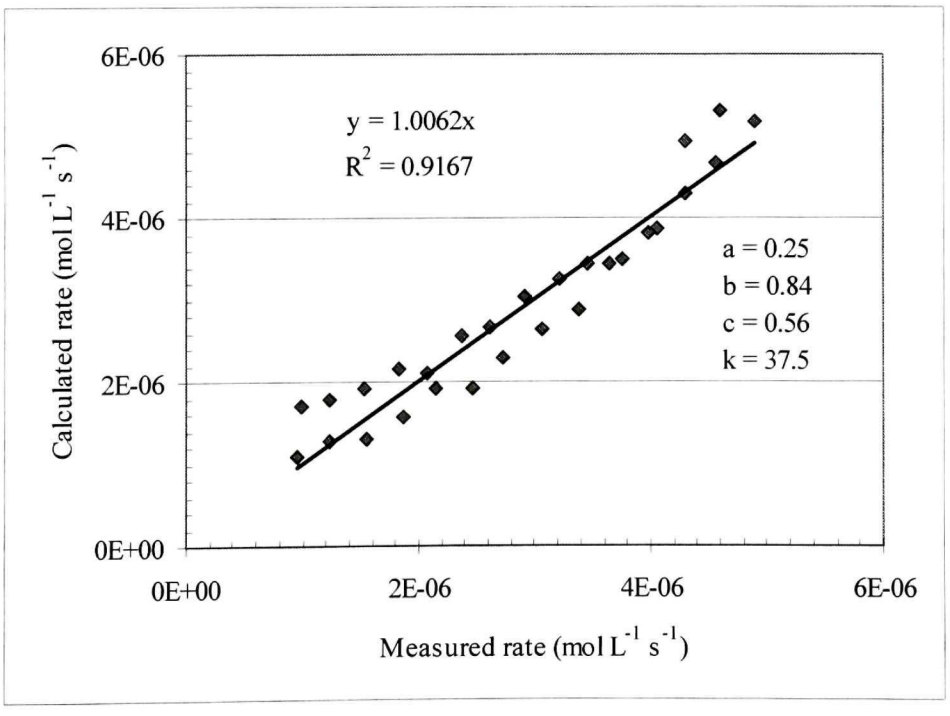

Figure 6.12. Comparison between measured and calculated nickel oxidation rate (Equation (6.3)) at different $[O_3]$ gas

The reaction order with respect to [Ni] is 0.84, which is close to 1.0 as found by Nishimura et al. (1992). There is a difference in the ozone order, however; Nishimura et al. determined it to be 1 while here is 0.25. Nishimura et al. did not give the order of hydroxide nor the value of the rate constant; as determined here they are 0.56 and 37.5 L^2 mol^{-2} s^{-1}, respectively. No indication of ozone mass balance is given by Nishimura et al. so it was not possible determine if they had "excess" consumption.

6.4.4 Nickel concentration effect

Nickel concentration was varied to determine the effect on the precipitation rate. Conditions are shown in Table 6.1. In the same manner as in the other tests pH was held around 7 using sodium hydroxide (0.1 N) as needed. Temperature remained within ± 1°C and the oxidation-reduction potential was over 1000 mV. Figures 6.13 and 6.14 show ozone concentration versus time in gas and liquid phases, respectively. Similar to the previous tests the ozone concentration approached zero in liquid phase and ca. 40% of the initial concentration in gas phase.

Figure 6.15 shows residual nickel concentration; the trend is similar for all three initial [Ni]. Figure 6.16 shows rate of ozone consumption versus time. As before, the ozone rate of consumption increased to become constant.

Ozone consumption was calculated using the stoichiometric reaction of nickel oxidation. The initial concentration of Ni was considered to establish the molar relationship. Figure 6.17 shows the stoichiometric variation of ozone.

Initially ozone consumption increased in a manner dependent on the initial nickel concentration. After 10 minutes when $[Ni]_o = 1.936 \times 10^{-3}$ and after 24 minutes when concentration was greater than 8.87×10^{-3}, ozone consumption reached a maximum then decreased. Excess ozone is always found (Figure 6.18) and there is a tendency for it to increase with time.

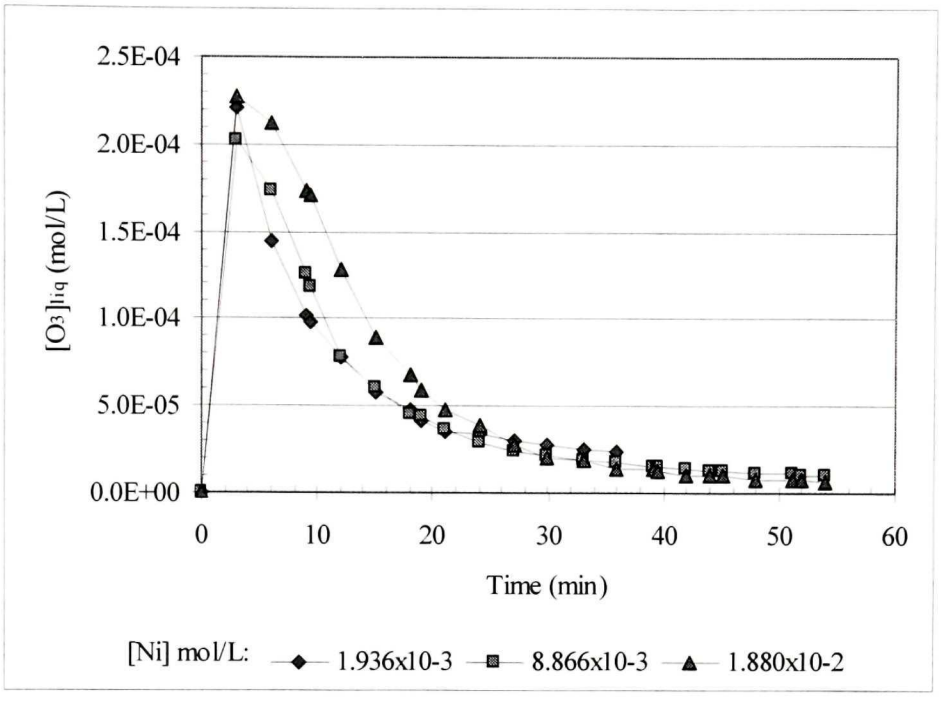

Figure 6.13. Aqueous ozone concentration as a function of time (nickel feed concentration tests)

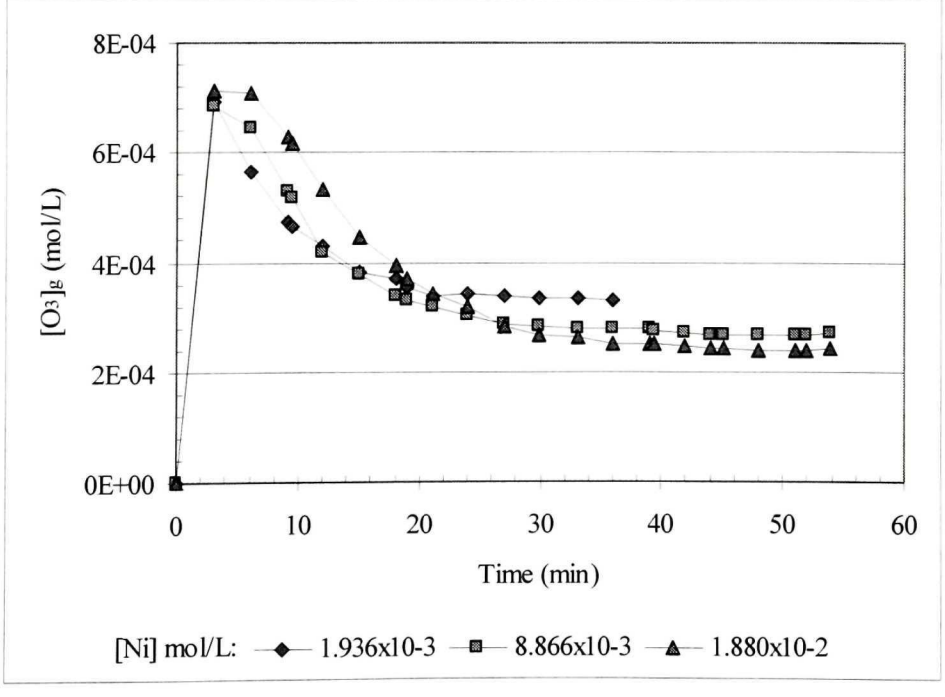

Figure 6.14. Gaseous ozone concentration as a function of time (nickel feed concentration tests)

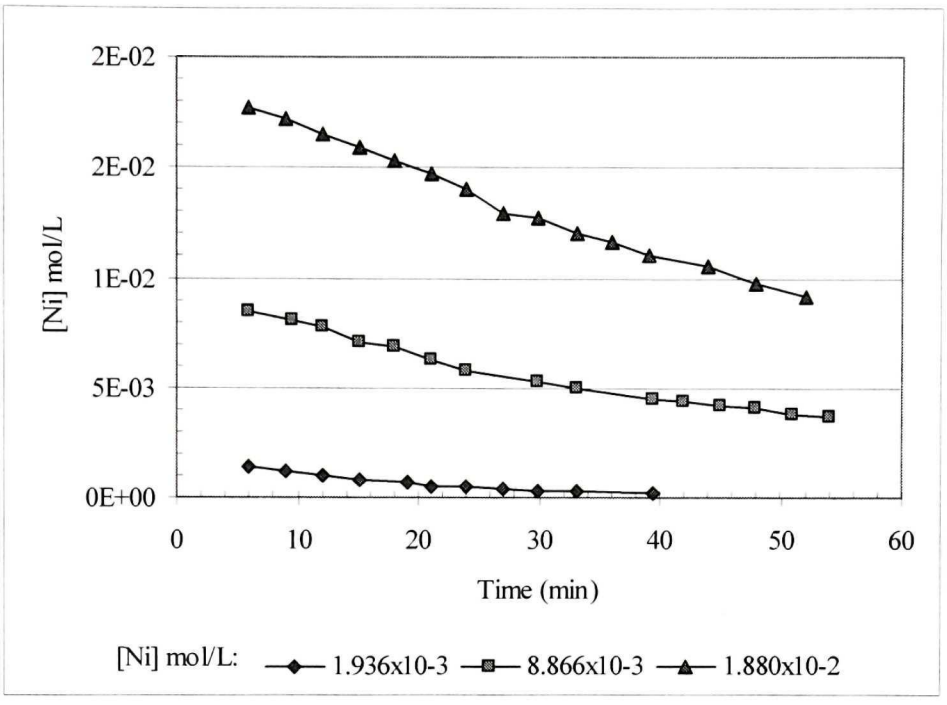

Figure 6.15. Nickel concentration in solution as a function of time (nickel feed concentration tests at pHs 7.23, 7.18 and 7.06)

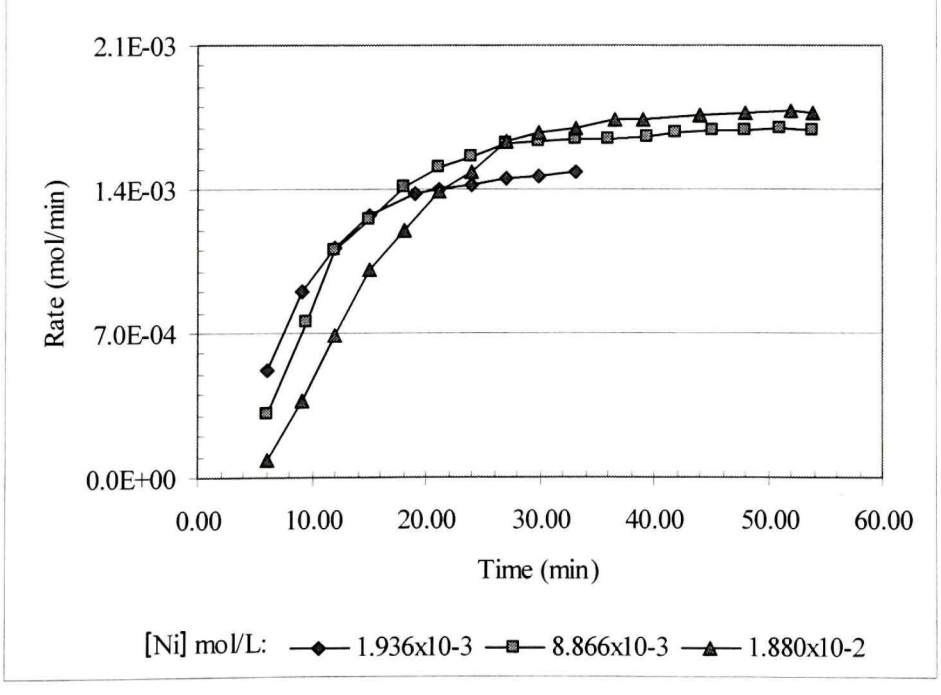

Figure 6.16. Ozone consumption rate for different initial nickel concentration

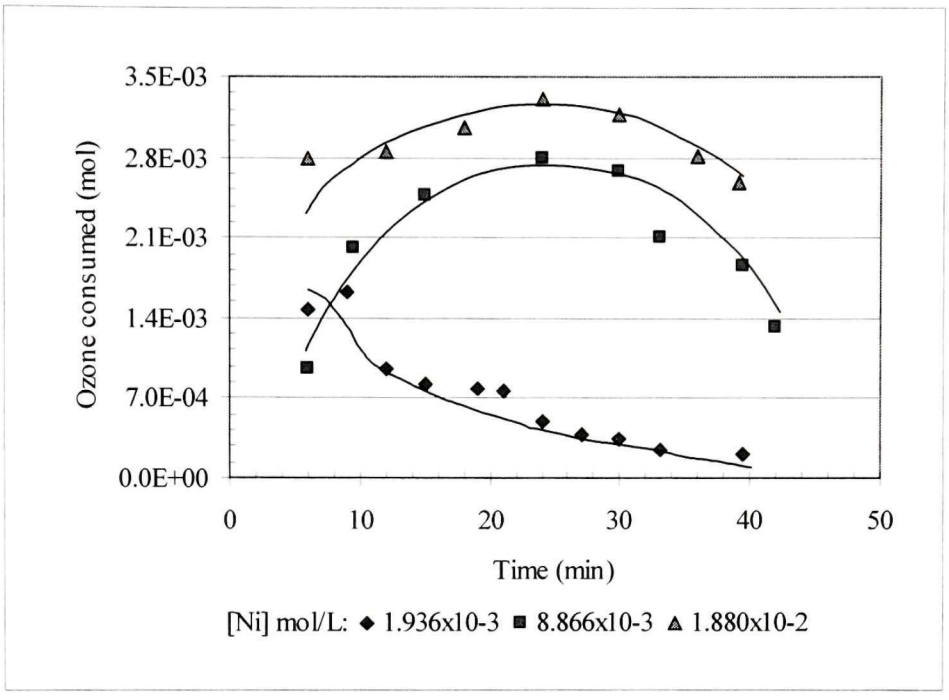

Figure 6.17. Ozone consumption versus time during nickel oxidation at different [Ni]

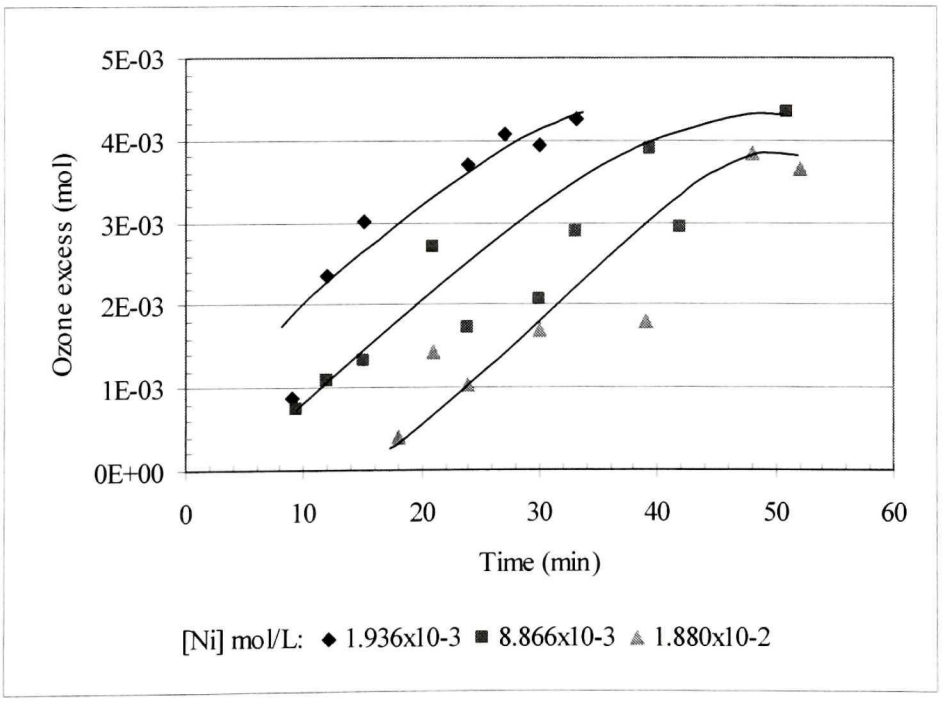

Figure 6.18. Excess ozone consumption during nickel oxidation at different [Ni] feed

6.4.5 Explanation of additional ozone consumption

There was no relationship between the moles of nickel precipitated and moles of ozone consumed (or predicted by reaction 6.2) in any of the tests. Ozone concentration (in liquid and gas phase) continued to decrease even though the nickel concentration was decreasing. This suggested that another ozone-consuming reaction was occurring. One possibility was the alkali used in the process to conserve pH ~7; another was the precipitate itself. The first possibility was discarded because ozone decomposition at the test pH was negligible (Chapter 6), leaving the second. To determine the effect of the precipitate, two tests were performed.

In the first, a solution containing $2.4x10^{-4}$ mol/L Ni(II) was oxidized and precipitated for 50 minutes using ozone and a constant addition of sodium hydroxide to maintain pH ~ 7. After this period alkali addition was stopped and for a further 30 minutes ozone was fed to the reactor. To determine if there was any release of nickel, solution samples were taken (every 5 minutes). Figure 6.19 shows the ozone concentration in gas and liquid phase remained constant after the 50-minute period, i.e., ozone was still being consumed and there was no change in [Ni].

The second test was performed by introducing precipitate previously produced. Before adding the precipitate was washed with distilled water to eliminate remaining Ni solution and other possible ozone consumers. A pulp was prepared using 2 liters of distilled water. The gas rate was fixed in 0.617 cm/s and the test duration was 25 minutes. Figure 6.20 shows that after 5 minutes the ozone concentration in the gas outlet was almost constant and about 40% of the inlet value while the ozone concentration in the liquid phase was too low to record on the figure, remaining below $1.7x10^{-7}$ mol/L. The pH of the slurry decreased during the test. These indicators all point to the ozone continuing to react with the precipitate.

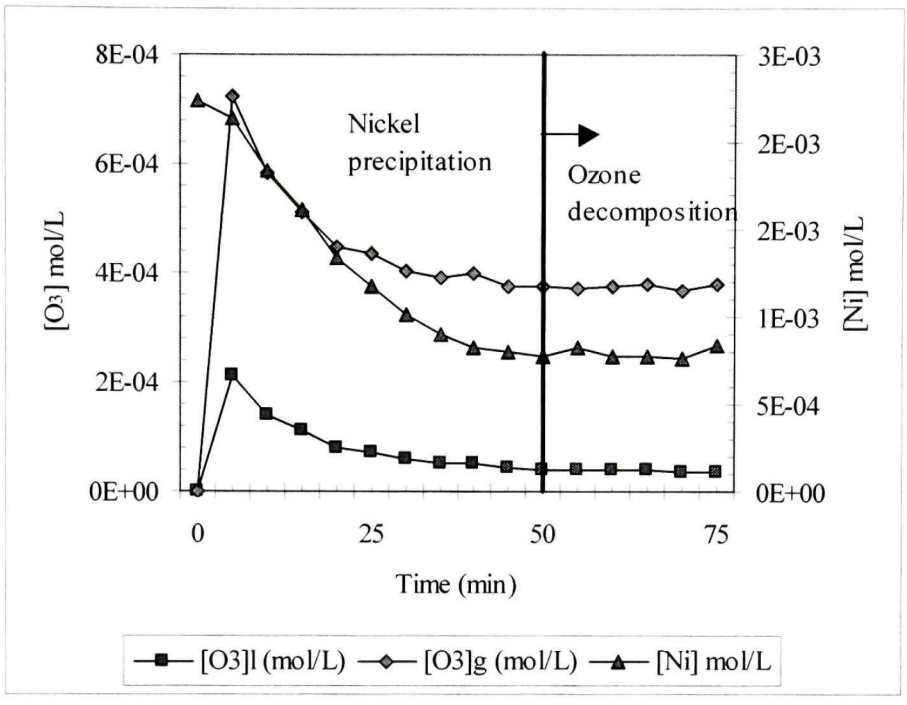

Figure 6.19. Ozone consumption produced by precipitate

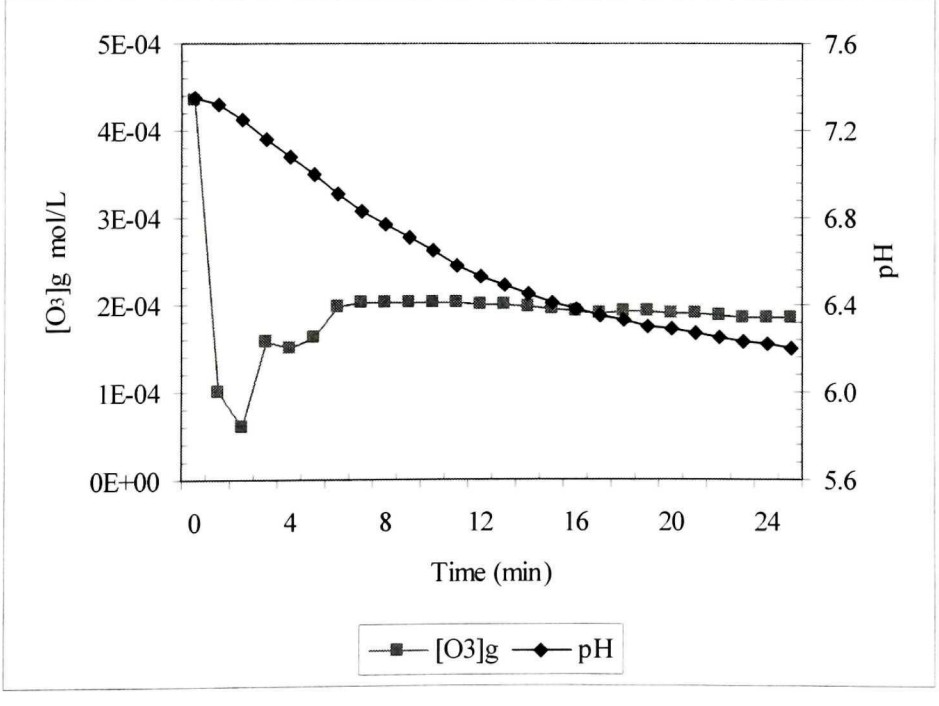

Figure 6.20. Ozone consumption produced by previously prepared precipitate

6.4.6 X-ray diffraction of solid products

To determinate the nickel compounds produced, the precipitates were analyzed by X-ray diffraction. The spectra for samples produced under different conditions were similar. Figures 6.21 to 6.25 shows that $Ni(OH)_2$, NiOOH, $Ni_3O_2(OH)_4$ and $Ni_2O_2(OH)_4$ were present.

According to Dyer and Scrivner (1998) nickel hydroxide ($Ni(OH)_2$) precipitation starts at pH 6.8 when nickel concentration is > 1.70×10^{-2} M. Although the concentration used here was lower some precipitate was produced. This initial product could be the initiator of nickel oxidation to produce the NiOOH when tests are performed at room temperature (ca. 20 °C). With these considerations two mechanisms of nickel oxy hydroxide precipitation can be proposed: oxidation – hydrolysis – precipitation or hydrolysis – precipitation - oxidation. A critique of both is presented.

Oxidation – hydrolysis – precipitation

This mechanism proposes two steps: oxidation of Ni(II) to Ni(III) and hydrolysis/precipitation of N(III). The final product is nickel oxide-hydroxide, NiOOH. The following reaction sequence is suggested:

Oxidation

$$2Ni^{++} \rightarrow 2Ni^{+++} + 2e^{-} \qquad (6.4)$$

$$O_3 + 2H^{+} + 2e^{-} \rightarrow O_2 + H_2O \qquad (6.5)$$

combining,

$$O_3 + 2Ni^{++} + 2H^{+} \rightarrow 2Ni^{+++} + H_2O + O_2 \qquad (6.6)$$

Hydrolysis

$$2Ni^{+++} + 6OH^{-} \rightarrow 2NiOOH + 2H_2O \quad (6.7)$$

combining with reaction (6.6),

$$O_3 + 2Ni^{++} + 3H_2O \rightarrow 2NiOOH + O_2 + 4H^{+} \quad (6.8)$$

Hydrolysis – precipitation - oxidation

Hydrolysis

Hydrolysis produces nickelous hydroxide

$$2Ni^{++} + 4OH^{-} \rightarrow 2Ni(OH)_2 \quad (6.9)$$

Oxidation

Nickelous hydroxide is oxidized by ozone

$$2Ni(OH)_2 + O_3 \rightarrow 2NiOOH + H_2O + O_2 \quad (6.10)$$

and combining with (6.9) produces

$$O_3 + 2Ni^{++} + 4OH^{-} \rightarrow 2NiOOH + H_2O + O_2 \quad (6.11)$$

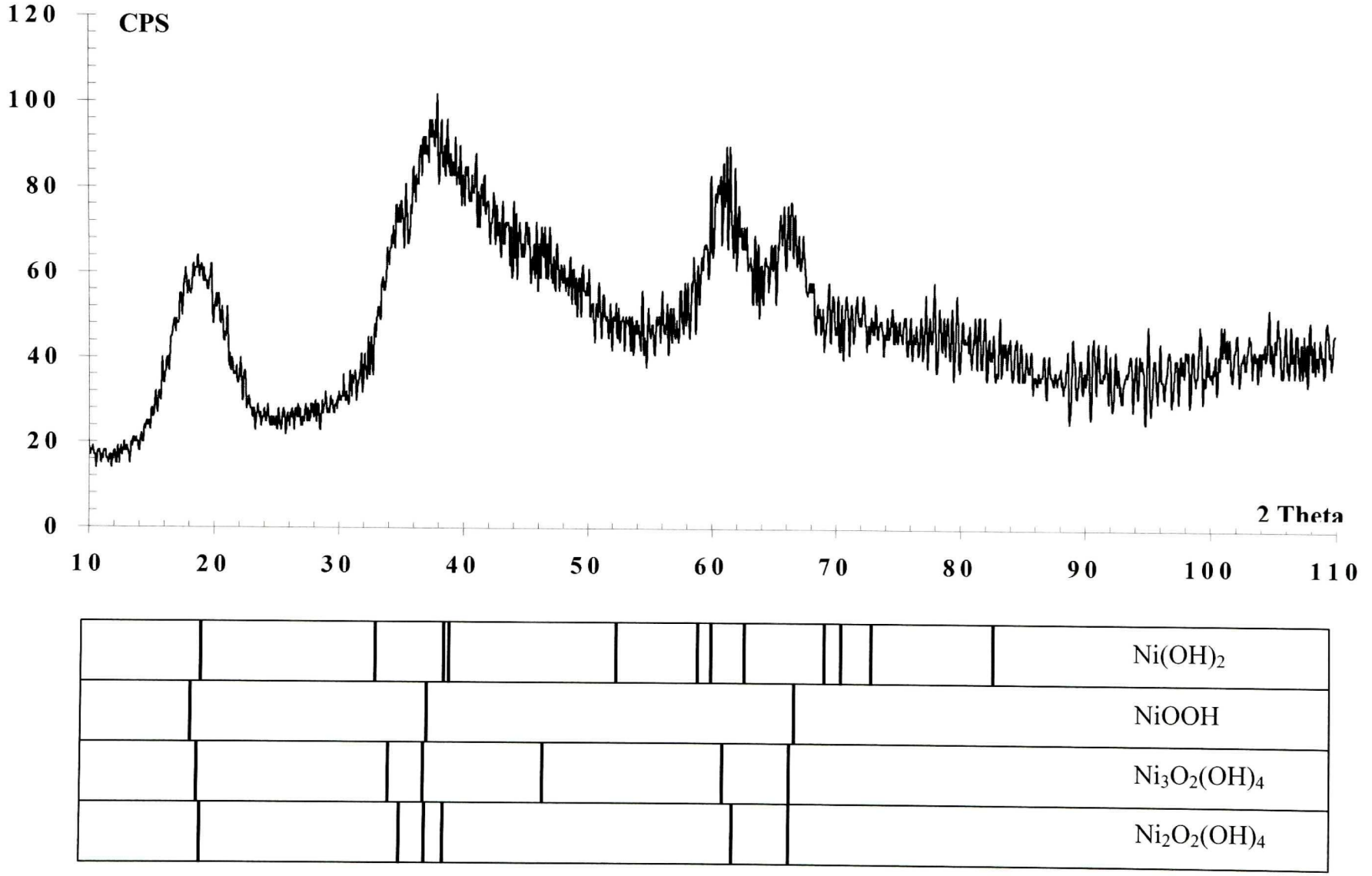

Figure 6.21. Nickel precipitate X-ray diffraction (test at $[O_3]_g = 7.50x10^{-4}$ mol/L), pH = 7.00

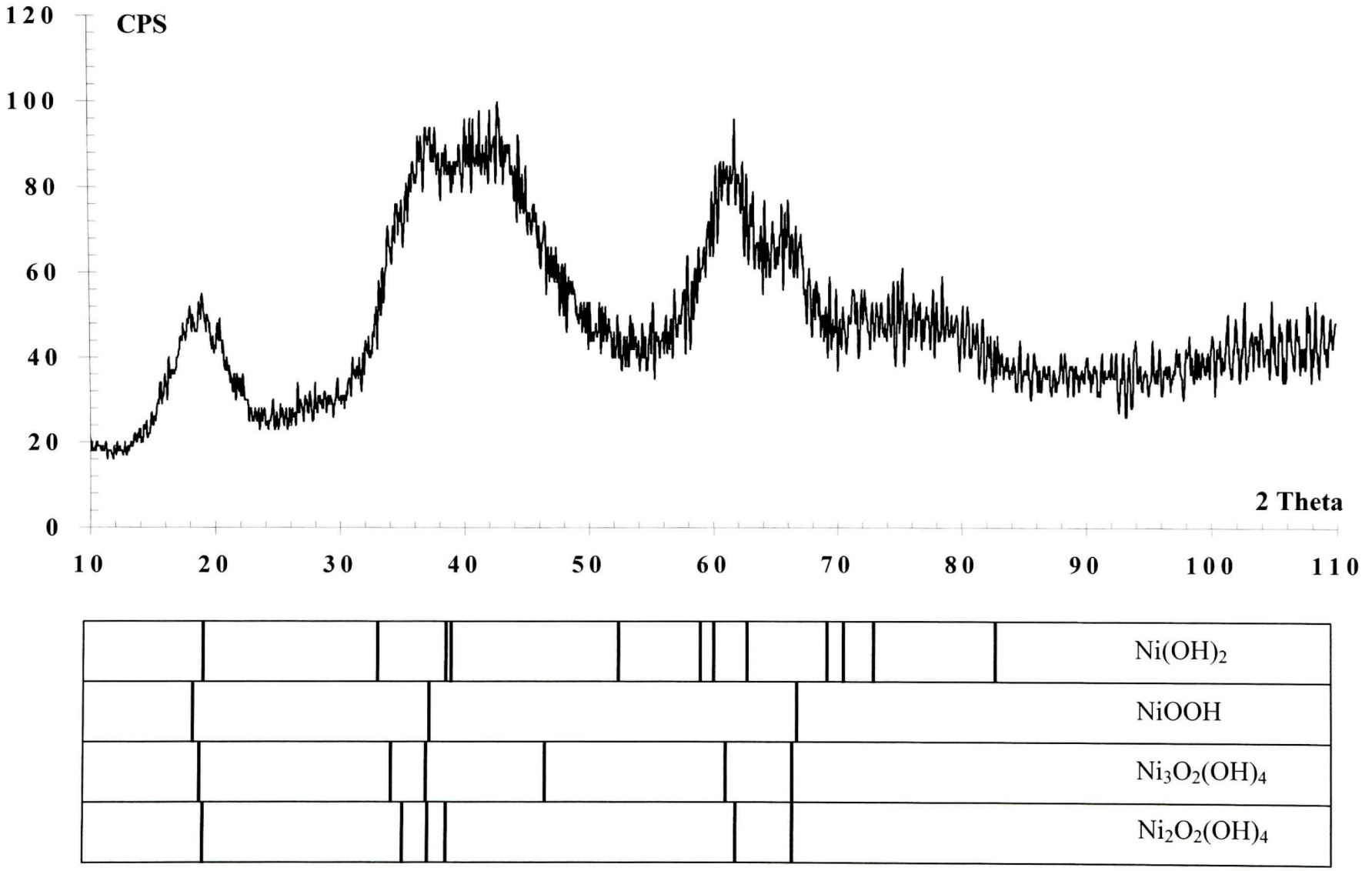

Figure 6.22. Nickel precipitate X-ray diffraction (test at $[O_3]_g = 9.17x10^{-4}$ mol/L), pH = 7.14

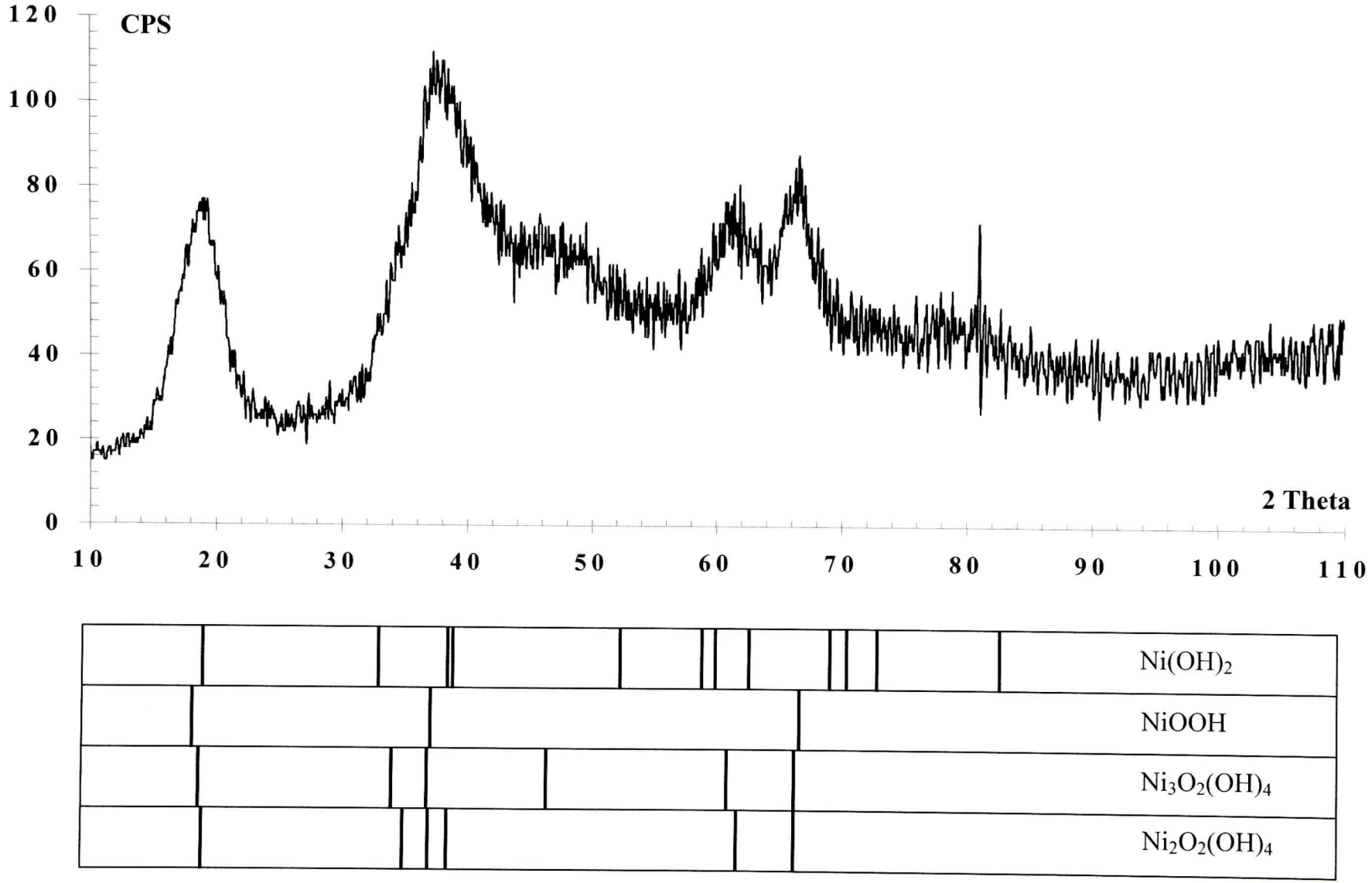

Figure 6.23. Nickel precipitate X-ray diffraction (test at [Ni] = 1.67×10^{-3} mol/L), pH = 7.23

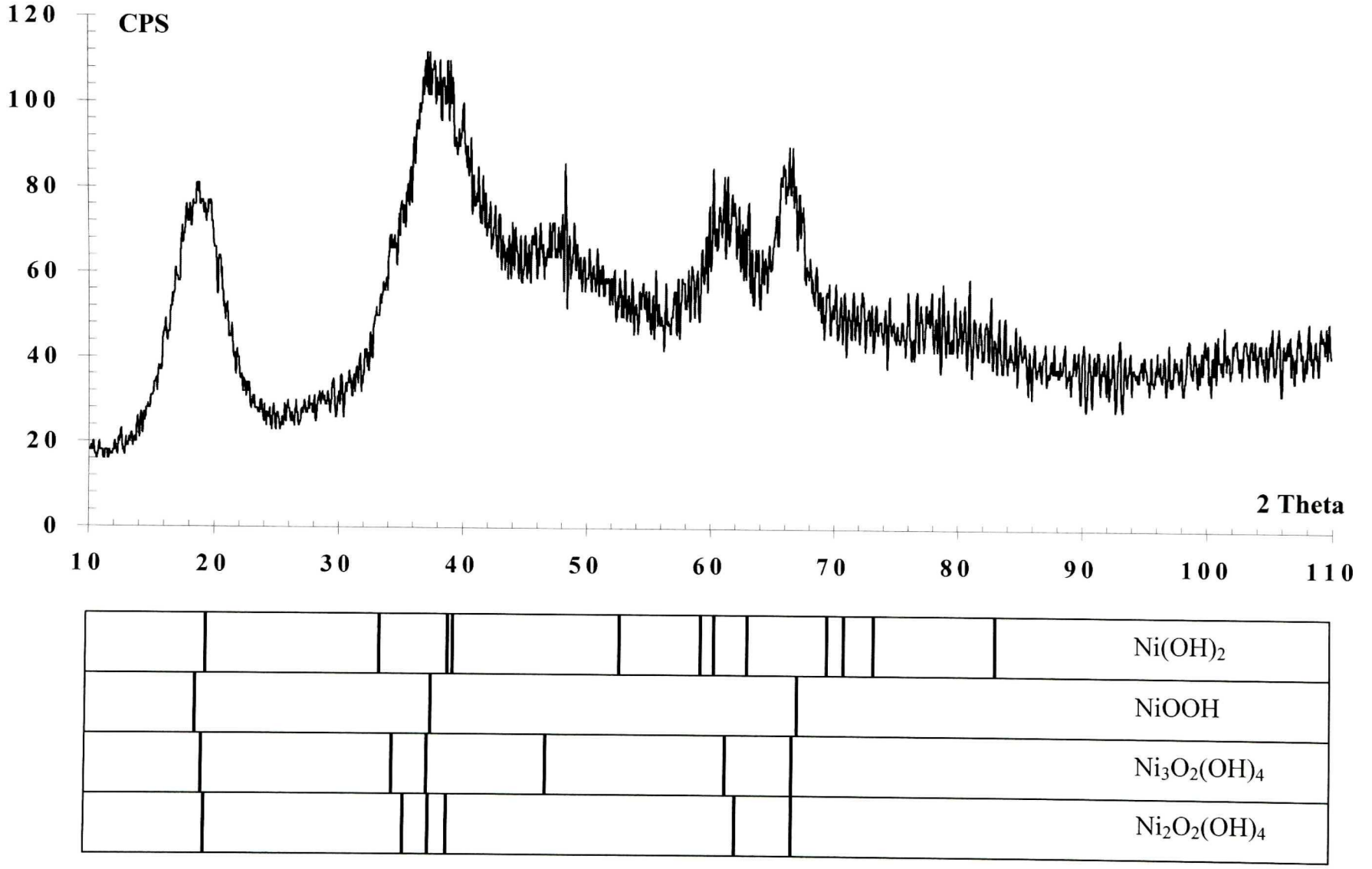

Figure 6.24. Nickel precipitate X-ray diffraction (test at [Ni] = 8.87×10^{-3} mol/L), pH = 7.18

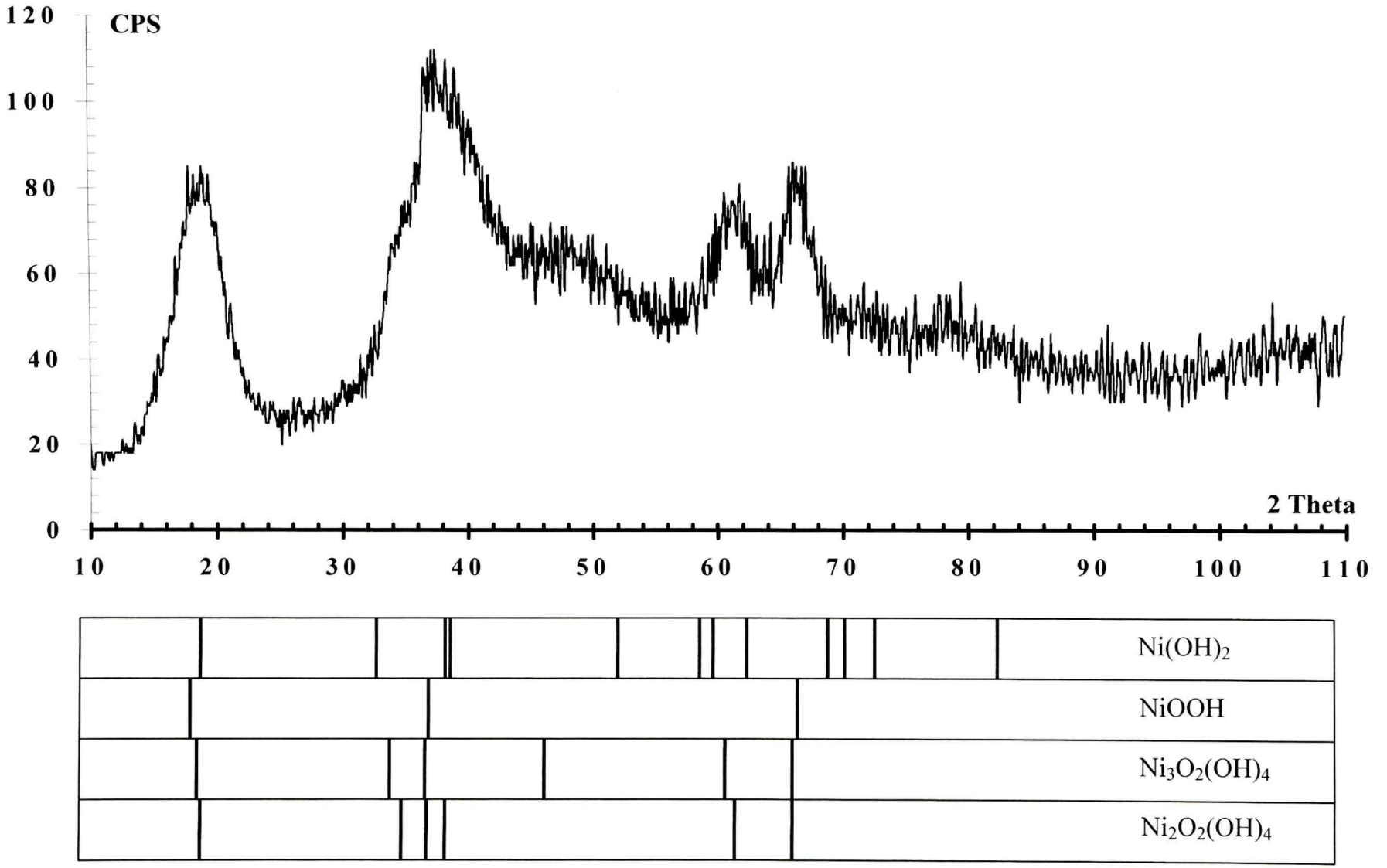

Figure 6.25. Nickel precipitate X-ray diffraction (test at [Ni] = 18.8×10^{-3} mol/L), pH = 7.06

X-ray diffraction detected $Ni_3O_2(OH)_4$, which can be written as $2NiOOH{\cdot}Ni(OH)_2$, i.e,. a combination of nickel oxide hydroxide (2/3) and nickel hydroxide (1/3).

Figures 6.20 and 6.21 indicate that the precipitate was the ozone consumer. X-ray diffraction detected nickel as Ni(IV), indicating continued solid state oxidation transforming some NiOOH to $Ni_2O_2(OH)_4$. The literature does not present thermodynamic data for $Ni_2O_2(OH)_4$ produced from NiOOH, but the FACT program can be used to investigate the following reaction:

$$2NiOOH + O_3 + H_2O \rightarrow 2NiO_2(H_2O) + 4O_2 \qquad (6.12)$$

Figure 6.27 shows the comparison of free energy formation to produce NiOOH and $NiO_2(H_2O)$.

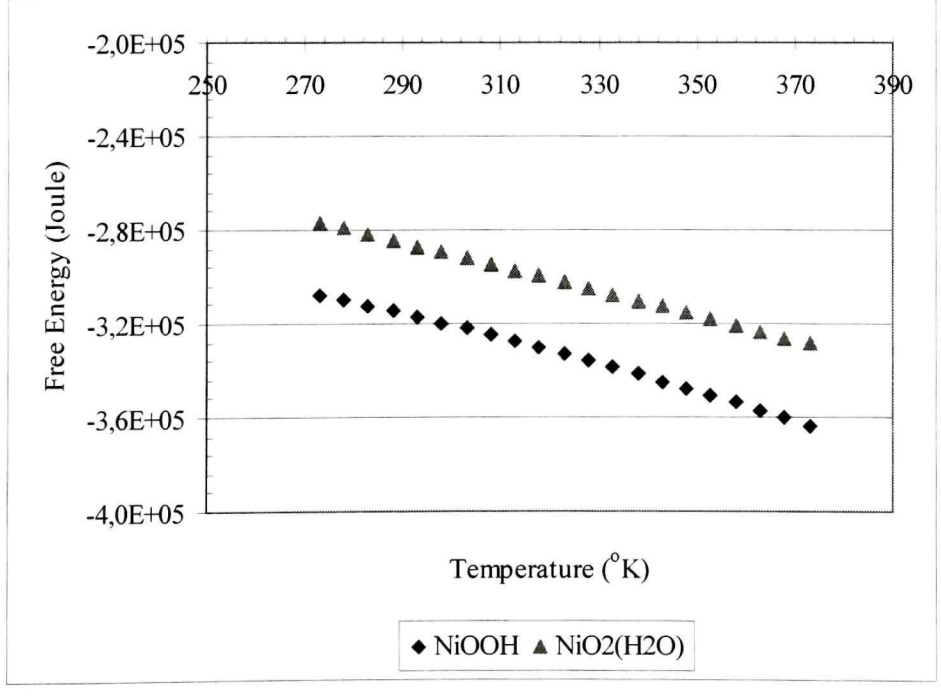

Figure 6.27. Thermodynamics of NiOOH and $NiO_2(H_2O)$ formation

Formation of Ni(III) and Ni(IV) compounds do not have any thermodynamic limitation and are spontaneous at room temperature. Figure 2.7 and 2.7a proposed by Pourbaix (1974) and FACT also support the oxidation of solid NiOOH because the potential required, according to Figure 6.8, is a value over 980 mV, which is already attained here.

CHAPTER 7

Conclusions and Suggestions

7.1 Conclusions

7.1.1 Ozone mass transfer

The methodology devised to estimate "k_La" from data collected in a semi-batch bubble column reactor proved successful. The key was the dynamic ozone mass balance allowed by the column instrumentation. The volumetric mass transfer coefficient was on the high side of the range compared with published data.

The calculation of interfacial area from gas holdup (differential pressure method) and bubble size distribution (bubble viewer technique) enabled the mass transfer coefficient to be calculated.

The ozone mass transfer coefficient from gas to water was constant for variations in diffuser porosity, solution volume, and gas velocity. The value measured was 6.7 x 10^{-4} m s^{-1} with a standard deviation of 0.1 x 10^{-4}.

7.1.2 Ozone decomposition by hydroxide

For the pH range 9.9 – 7.4 and temperature ca. 20 °C, sodium carbonate inhibits formation of hydroxide radical and ozone decomposition is reduced. The decomposition equation can be represented as:

$$-\frac{d[O_3]}{dt} = k_1 [OH^-]^{0.41} [O_3]^{0.90}$$

where $k_1 = 0.8$ L mol^{-1} s^{-1}

Over a similar pH range but with no carbonate (or carbonate concentration < 7.077×10^{-5} mol/L), ozone decomposition is increased and the decomposition equation is the following:

$$-\frac{d[O_3]}{dt} = k_2 [OH]^{0.36} [O_3]^{1.05}$$

where $k_2 = 1.7$ L mol^{-1} s^{-1}. That is, the order remains the same but a different rate constant is produced.

At pH < 7.2 ozone decomposition can be assumed low and constant (ca. 2.34×10^{-7} mol L^{-1} s^{-1}).

7.1.3 Nickel oxidation

The oxidative precipitation of nickel from sulfate solutions with ozone was investigated at room temperature and pH ~7. A solid black product was produced with similar characteristics to NiOOH signaled in the literature.

The kinetic equation of nickel precipitation was determined and the total order found was ~1.5 and rate constant 37.5 L^2 mol^{-2} s^{-1}. Determination of the kinetic equation of ozone consumption was not possible as more than one oxidation reaction occurred (Ni(II) → Ni(III) → Ni(IV)). Continued oxidation in the solid state (i.e., of the precipitate) was identified. X-ray diffraction analysis detected the following compounds:

$Ni(OH)_2$, NiOOH --- $Ni_3O_2(OH)_4$ and $Ni_2O_2(OH)_4$ confirming the continued oxidation. A hydrolysis/precipitation ($Ni(II) \rightarrow Ni(OH)_2$) – oxidation ($Ni(OH)_2 \rightarrow NiOOH \rightarrow Ni...$) mechanism was suggested.

7.2 Claims to originality

The work described in this thesis aimed to study the ozonation process for nickel recovery from dilute aqueous solution. A reactor was designed for this purpose and the three principal steps of the process were characterized: ozone mass transfer gas-liquid, ozone decomposition in water, and nickel oxidation-precipitation. The following are considered original contributions to knowledge:

- The equipment and methodology devised to perform a mass balance for ozone around the reactor.
- The methodology devised to study the ozone gas-liquid mass transfer process for a semi-batch reactor.
- The use of a bubble sizing technique developed in-house (the "bubble viewer") for the case of non-spherical gas bubbles to calculate the interfacial area.
- Determination of ozone gas-liquid mass transfer coefficient.
- The methodology devised to determine the kinetic parameters (reaction order and kinetic constant) for ozone decomposition in water from on-line measurement of ozone decomposition rate and reactant composition.
- The proposal, based on the trend in ozone consumption during nickel precipitation and X-ray diffraction analysis of the product, of the mechanism of Ni(II) oxidation by ozone namely, hydrolysis – precipitation - oxidation.

7.3 Suggestions for future work

Suggestions for future work are in two areas: equipment improvement and further testing:

In the case of equipment modifications, it is recommended to:

- Replace the ozone generator with a more stable and wider range unit in terms of gas flow and ozone concentration.
- Install probes and electrodes directly into the reactor and not in the sampling loop to avoid measurement delays.
- Operate with conditions that promote a thorough mixing of the liquid in the reactor.

In the case of further testing:

- Use diffusers, which produce smaller bubbles to have significant increases in ozone mass transfer rate.
- Complete a more exhaustive characterization of the effect of carbonate ions on ozone decomposition rate in water. The potential savings in ozone are important.
- Determine whether catalytic decomposition on the surface of the precipitated particles also contributes to ozone consumption.
- Perform similar studies on other metals in solution and to mixtures of metals. Thorough characterization of the precipitates should be undertaken to determine if any products provide "added value" potential.

REFERENCES

Adamec, J. B. and Kihlgren, T. E., (1967) "Encyclopedia of Chemical Technology", Kirk R. E. and Othmer D. E. Eds., pp. 735-753.

Alder, G. A. and Hill, G. R., (1950) "The Kinetics and Mechanism of Hydroxide Ion Catalyzed Ozone Decomposition in Aqueous Solution", Journal of American Chemical Society, Vol. 72, pp. 1884-1886.

Allan, R. J., (1995) "Impact of Mining Activities on the Terrestrial and Aquatic Environment with Emphasis on Mitigation and Remedial Measures", Mader, P. Editions.

Bader, H. and Hoigné, J., (1982) "Determination of Ozone in Water by the Indigo Method; a Submitted Standard Method", Ozone Science and Engineering, Vol. 4, pp. 169-176.

Bard, A. J., Parsons, R. and Jordan, J., (1985) "Standard Potentials in Aqueous Solution", International Union of Pure and Applied Chemistry (IUPAC), pp. 58-59.

Beenackers, A. A. C. M. and Van Swaaij, W. P. M. (1993), "Mass Transfer in Gas-Liquid Slurry Reactors", Chemical Engineering Science, Vol. 48, No 18, pp. 3109-3139.

Beltran, F. J., Garcia-Araya, J., Encinar, J. (1997), " Henry and Mass Transfer Coefficients in the Ozonation of Wastewater", Ozone; Science and Engineering, Vol. 19, No 3, pp. 281-296.

Bin, A. K., Duczmal, B. and Machniewski, P., (2001), "Hydrodynamics and Ozone Mass Transfer in a Tall Bubble Column", Chemical Engineering Science, Pergamom Press, V. 56, pp. 6233-6240.

Boldt, J. R., (1967) "The Winning of Nickel. Its Geology, Mining and Extractive Metallurgy", Van Nostrand, New York.

Centre de Recherche en Calcul Thermochimique. Ecole Polytechnique de Montreal, (2002) "FACT (Formulation Analytique en Calcul Thermodynamique)".

Charpentier, J. C., (1981) "Mass-Transfer Rates in Gas-Liquid Absorbers and Reactors" in Advances in Chemical Engineering, Vol. 11, Edit. Academic Press Inc.

Cohen, B. S. and Hering, S. V., (1995) "Air Sampling Instruments for Evaluation of Atmospheric Contaminants", 8th ed. American Conference of Governmental Industrial Hygienists, Inc. Cincinnati, Ohio.

Cotton, F. A., (1966) "Advanced Inorganic Chemistry a Comprehensive Text", Second edition, Geofrey Wilkinson, F.R.S., Interscience Publishers.

Dobbins, W. E., (1964), "Mechanism of Gas Absorption by Turbulent Liquids", Proceedings of the International Conference Water Pollution Research, London, Pergamom Press, pp. 61-76.

Durrant, P. J. and Durrant, B., (1970) "Introduction to Advanced Inorganic Chemistry", Second Edition, William Cloves and Sons, Limited.

Dyer, J. A. and Scrivner, N. C., (Spring 1998) "A Practical Guide for Determining the Solubility of Metal Hydroxides and Oxides in Water", Environmental Progress, Vol. 17, No 1, pp. 1-8.

El-Ammouri, E., (2000) "Heavy Metals Removal from Effluents by Adsorption in Activated Silica Sols", Thesis for the Degree of Doctor of Philosophy, McGill University, pp. 121-122.

Emsley, J., (1991) "The elements", Second edition, Printed in Great Britain, pp.126-127.

Gomez, C. O., Escudero, R. and Finch, J. A., (2000) "Determining Equivalent Pore Diameter for Rigid Porous Sparger", The Canadian Journal of Chemical Engineering, Vol. 78, pp. 785-792.

Gottschalk, C., Libra, J. A., Saupe, A., (2000) "Ozonation of Water and Waste-Water. A Practical Guide to Understanding Ozone and its Applications", Edited by Wiley-VCH Verlag GmbH, pp. 81-108.

Gurol, M. D. and Singer, P. C., (1982) "Kinetics of Ozone Decomposition: a Dynamic Approach", Environmental Science and Technology, Vol. 16, No 7, pp. 377-383.

Hernandez-Aguilar, J. R., Gomez, C. O., Finch, J. A., (2002) "A Technique for the Direct Measurement of Bubble Size Distributions in Industrial Flotation Cells", Proceedings 2002, 34th Annual Meeting of the Canadian Mineral Processors, January 22-24, 2002 Ottawa, Canada.

Hewes, C. G. and Davison, R. R., (1971) "Kinetics of Ozone Decomposition and Reaction with Organics in Water", AIChE Journal, Vol. 36, No 3, pp. 449-456.

Hoigné, J., Bader, H., Haag, W. R. and Staehelin, J., (1985) "Rate Constants of Reactions of Ozone with Organic and Inorganic Compounds in Water – III", Water Research, Vol. 19, No 8, pp. 993-1004.

JCPDS International Centre for Diffraction Data, (1979) " Inorganic Materials – Search Manual (Hanawalt)".

Kakness, K., Gordon, G., Langlais, B., Masschelein, W., Matsumoto, N., Richard, Y., Robson, C. M. and Somiya, I., (1996) "Guideline for Measurement of Ozone Concentration in the Process Gas from an Ozone Generator", Ozone Science and Engineering, Vol. 18, pp. 209-229.

Kinman, R. N., (1972) "Ozone in Water Desinfection" in Ozone in Water and Waste-Water Treatment by Evans, F.L., edited by Ann Arbor Science Publishers Inc., pp. 123-143.

Langlais, B., Reckhow, D. A. and Brink, D. R., (1991), "Ozone in Water Treatment. Application and Engineering", American Water Works Association Research Foundation and Lewis Publishers, Inc.

Le Sauze, N., Laplanche, A., Martin, N., Martin, G., (1993) " Modeling of Ozone Transfer in a Bubble Column", Water Research, Vol. 27, No 6, pp. 1071-1083.

Levenspiel, O., (1999) "Chemical Reaction Engineering" 3rd ed. Willey, New York.

Lewis W. K., Whitman W. G., (1924), "Principles of Gas Absorption", Industrial and Engineering Chemistry, Vol. 16, pp. 1215-1219.

Mallevialle, J., (1982) "Theoretical Aspects of Ozone Transfer into Water" in Ozonation Manual for Water and Wastewater Treatment, Edited by Masschelein, W. J., pp. 53-55.

Morris J.C. (1988) "The Aqueous Solubility of Ozone", Ozone News, Vol. 1, pp. 14-16.

Nikolic, C., Queneau, P. B., Sherwood, W. G., Barlow, C. B., (1978) " Nickel-Cobalt Separation by Ozonation", CIM Bulletin, October, pp. 121-127.

Nishimura, T., Umetsu, Y., (1992) "Separation of Cobalt and Nickel by Ozone Oxidation", Hydrometallurgy, 30, pp. 483-497.

Orsat, V., Vigneault, C., Raghavan, G. S. V., (1993) "Air Diffusers Characterization Using Digitized Image Analysis System", American Society of Agricultural Engineers, January, pp. 115-121.

Peleg, M., (1976) "Review Paper - The Chemistry of Ozone in the Treatment of Water", Water Research, Vol. 10, pp. 361-365.

Pourbaix, M., (1974) "Atlas of Electrochemical Equilibria in Aqueous Solutions", National Association of Corrosion Engineers, Houston, Texas, pp. 330-341.

Rackness, k., Gordon, G., Langlais, B., Masschelein, W., Matsumoto, N., Richard, Y., Robson, C. M., (1991), "Ozone in Water Treatment – Application in Engineering", 2nd ed. Lewis Publishers, Inc.

Reckhow, D., Brink, D., "Ozone in Water Treatment Applications and Engineering" in American Water Works Association, edit. Bruno Blank, Second Edition, 199, pp 112-116.

Reed, B. E., in Robert A. Meyers, ed., (1998), "Waste Water Treatment, Heavy Metals", Environmental Analysis and Remediation, John Wiley & Sons, U.S.A., Vol. 8, pp 5220-5225.

Rice, W. J., (1990) "The Dispersion Model Differential Equation for Packed Beds", Chemical Engineering Education, Vol. 24, pp 224-227.

Roth, J. A., Sullivan, D. E., (1981) "Solubility of Ozone in Water", Ind. Eng. Chem. Fundam. Vol.20, pp.137-140.

Roustan, M., Mallevialle, J., (1982) "Stability of Ozone in Water" in Ozonation Manual for Water and Wastewater Treatment, Edited by Masschelein, W.J., pp. 47-52.

Roustan, M., Wang, R. Y., Wolbert, D., (1996) "Modeling Hydrodynamics and Mass Transfer Parameters in a Continuous Ozone Bubble Columns", Ozone; Science and Engineering, Vol. 18, No 2, pp. 99-115.

Sato, M., Robbins, E. I., (2000) "Recovery/Removal of Metallic Elements from Acid Mine Drainage Using Ozone", ICARD 2000, Proceedings from the Fifth International Conference on Acid Mine. Published by the Society for Mining, Metallurgy and Exploration, Inc., Vol. 2, pp. 1095-1100.

Sennewald, K., (1933) Zeitschrift für physikalische Chemie. Abteilung A, Chemische Thermodynamik, Kinetik, Elektrochemie, Eigenschaftslehre. Vol. A164, pp. 305- Published by Leipzig : Akademische Verlagsgesellschaft

Somiya, I., (1996) "Guideline for Measurement of Ozone Concentration in the Process Gas from an Ozone Generator", Ozone Science & Engineering, Vol. 18, pp. 209-229.

Song, G. H. and Fan, L. S., (1990) " Gas-Liquid Mass Transfer from a Single Bubble in Liquid-Solid Fluidized Beds", AIChE Journal, Vol. 36, No. 3, pp 439-449.

Sotelo, J. L., Beltran, F. J., Benitez, F. J. and Beltran-Heredia,J., (1989) "Henry's Law Constant for the Ozone-Water System", Wat. Res. Vol. 23 No 10 pp. 1239-1246.

Staehelin, J. and Hoigné J., (1982), "Decomposition of Ozone in Water: Rate of Initiation by Hydroxide Ions and Hydrogen Peroxide", Environmental Science and Technology, Vol. 16, No 10, pp. 676-681.

Staehelin, J., Bahler R. F. and Hoigne, J., (1984) "Ozone Decomposition in Water Studied by Pulse Radiolysis. 2. OH and HO_4 as Chain Intermediates", J. Phys. Chem., Vol. 88, pp. 5999-6004.

Stenstrom, M. K. and Gilbert, R. G., (1981) "Review Paper: Effects of Alpha, Beta and Theta Factor Upon the Design Specification and Operation of Aeration Systems", Water Research, Vol. 15, pp. 643-654

Stephenson, T. in J. N. Lester, ed., (1987) "Heavy Metals in Wastewater and Sludge Treatment Processes", Vol. I, Sources Analysis, and Legislation, CRC Press, Boca Raton, Fla., pp. 31-34.

Stumm, W., (1954) "de Zerfall von Ozon in Wassriger Losung (Decoposition of Ozone in Aqueous Suspension)", Helvetica Chemical Acta, Vol. 37, pp. 773-775

Sullivan, D. E., Roth, J. A., (1980) AIChE Symp. Ser. 76, 142, 142-149.

Tatterson, G. B., (1991) "Fluid Mixing and Gas Dispersion in Agitated Tanks", McGraw-Hill, Inc.

Tomiyasu, H., Fukutomi, H. and Gordon, G., (1985) "Kinetics and Mechanism of Ozone Decomposition in Basic Aqueous Solution", Vol. 24, pp. 2962-2966.

Treybal, R. E., (1980) "Mass Transfer Operations", Third Edition, McGraw Hill Chemical Engineering Series.

Wesselingh, J. A. and Krishna, R., (1990) "Mass Transfer", Ellis Horwood Series in Chemical Engineering.

Weissenhorn, F. J., (1984) "Removal of Iron and Manganese by Ozone During Drinking Water Treatment in Dusseldorf", Handbook of Ozone Technology and Applications, V. II, pp.21-29.

Weiss, J., (1935) "Investigations on the Radical HO_2 in Solution", Journal Transaction Faraday Society, Vol. 31, pp. 668-681.

Yurteri, C. and Gurol, M. D., (1988) " Ozone Consumption in Natural Waters: Effects of Background Organic Matter, pH and Carbonate Species" Ozone Science and Engineering, Vol. 10, pp. 277-290.

APPENDIX 1

Chemical properties

Standard reduction potentials E^o/V

	VI		IV		II		0
Acid solution	NiO_4^{2-}	$\xleftrightarrow{>1.8}$	NiO_2	$\xleftrightarrow{1.593}$	Ni^{2+}	$\xleftrightarrow{-0.257}$	Ni
Alkaline solution	NiO_4^{2-}	$\xleftrightarrow{>0.4}$	NiO_2	$\xleftrightarrow{0.490}$	$Ni(OH)_2$	$\xleftrightarrow{-0.720}$	Ni

Oxidation States/Examples

Ni^{-I}	$[Ni_2(CO)_6]^{2-}$
Ni^{o}	$Ni(CO)_4$, $K_4[Ni(CN)_4]$
Ni^{I}	$[Ni(PPh_3Br]$
Ni^{II}	NiO, $Ni(OH)_2$
Ni^{III}	NiO(OH), NiF_3 ?
Ni^{IV}	NiO_2 ?
Ni^{VI}	K_2NiO_4 ?

Physical properties

ΔH_{fusion}/kJ mol^{-1}: 17.6

ΔH_{evp}/kj mol^{-1}: 371.8

Thermodynamic properties (298.15 K, 0.1 M Pa)

State	ΔH^o/kJ mol^{-1}	ΔG^o/kJ mol^{-1}	S^o/J K^{-1} mol^{-1}	C_p/J K^{-1} mol^{-1}
Solid	0	0	29.87	26.07
Gas	429.7	384.5	182.193	23.359

Density/ Kg m^{-3}: 8902 [298 K]; 7780 [liquid at m.p.]

Molar volume/ cm^3: 6.59

Source: The Elements (1991), Advanced Inorganic Chemistry (1966), Referenced Book of Inorganic Chemistry (1951).

APPENDIX 2

Ozone Generator Characteristics

Model	Griffin GTC
Ozone Output Ratings:	Maximum 9.17×10^{-4} mol/L (at 9.434×10^{4} Pa, 6.84 L/min of dry oxygen feed and 3 amp.)
Dimensions:	0.51 m (w) x 0.58 m (d) x 0.58 m (h)
Power required:	120V, 60 Hz, single phase, 10 amp

Ozone Gas Phase Monitor

Model:	API M 454
Measurement range	100, 200, 400 g/Nm3
Proof pressure	115 psig
Flow	0.5 – 5 L/min
Temperature range	5 to 45 °C
Repeatability	1% of full scale
Response Time	2 sec. To 95%

Ozone Liquid Phase Monitor

Model	ATI A15/64
Electronic Unit	
Measurement range	0 – 20 PPM
Repeatability	± 0.01 PPM
Temperature compensation	Automatic from –2 °C to +52 °C

Sensor

Response Time	90% in 45 seconds
Temperature Limit	from –5 °C to +55 °C

MASS TRANSFER TESTS

WORKSHEET 1

CONDITIONS												
Run	**Sol. Vol. (L)**		**Sol. Temp. (°C)**		**Gas in (mol O_3/ mol O_2)**		**Element. Vol. (L)**		**Column sect. Area (cm^2)**			
1	8		18		0.012		0.20		81.07			
RESULTS												
Time	0.00	0.53	1.07	1.60	2.13	2.67	3.20	3.73	4.27	4.80	5.33	5.87
pH	5.32	5.11	5.07	5.11	5.16	5.19	5.24	5.27	5.31	5.32	5.34	5.39
Vol. gas flow (L/min)	1.08	3.18	3.20	3.20	3.20	3.20	3.21	3.20	3.20	3.20	3.21	3.20
Mass gas flow (g O_2/min)	1.45	4.26	4.27	4.26	4.26	4.25	4.26	4.25	4.25	4.26	4.26	4.25
$[O_3]_g$ out (mg O_3/L)	0.00	7.69	15.01	17.79	20.04	22.36	22.88	23.12	23.21	23.35	23.89	23.90
Gas out molar ratio O_3/ O_2	0.00	0.00	0.01	0.01	0.01	0.01	0.01	0.01	0.01	0.01	0.01	0.01
$[O_3]_g$ out (mg O_3/g O_2)	0.00	5.79	11.35	13.48	15.20	16.97	17.38	17.56	17.63	17.74	18.15	18.16
$[O_3]_l$ (mg O_3/L)	0.00	1.58	3.62	5.01	5.89	6.62	7.05	7.39	7.57	7.61	7.74	7.95
$[O_3]_g$ out comparison using 40 elements of volume and k_La = 0.0266												
$[O_3]_g$ out measured (mg O_3/g O_2)	0.00	5.79	11.35	13.48	15.20	16.97	17.38	17.56	17.63	17.74	18.15	18.16
$[O_3]_g$ out calculated (mg O_3/g O_2)	0.00	7.53	10.94	13.24	14.71	15.93	16.65	17.22	17.52	17.58	17.80	17.98

WORKSHEET 2

CONDITIONS												
Run	**Sol. Vol. (L)**		**Sol. Temp. (°C)**		**Gas in (mol O_3/ mol O_2)**		**Element. Vol. (L)**		**Column sect. Area (cm^2)**			
2	8		18		0.012		0.20		81.07			
RESULTS												
Time	0.00	0.53	1.07	1.60	2.13	2.67	3.20	3.73	4.27	4.80	5.33	5.87
pH	5.88	5.83	5.84	5.82	5.82	5.80	5.78	5.78	5.74	5.73	5.71	5.69
Vol. gas flow (L/min)	3.04	3.21	3.21	3.20	3.20	3.20	3.20	3.20	3.20	3.21	3.20	3.21
Mass gas flow (g O_2/min)	4.09	4.30	4.28	4.27	4.26	4.26	4.26	4.26	4.25	4.26	4.26	4.26
$[O_3]_g$ out (mg O_3/L)	0.00	8.06	14.05	17.48	19.67	21.21	21.98	22.42	22.74	22.98	23.18	23.65
Out molar ratio O_3/ O_2	0.00	0.00	0.01	0.01	0.01	0.01	0.01	0.01	0.01	0.01	0.01	0.01
$[O_3]_g$ out (mg O_3/g O_2)	0.00	6.08	10.62	13.24	14.92	16.10	16.69	17.02	17.26	17.45	17.61	17.97
$[O_3]_l$ (mg O_3/L)	0.00	1.61	3.23	4.42	5.31	5.90	6.32	6.54	6.84	6.87	6.96	7.09
$[O_3]_g$ out comparison using 40 elements of volume and k_La = 0.0258												
$[O_3]_g$ out measured (mg O_3/g O_2)	0.00	8.45	11.21	13.23	14.77	15.79	16.50	16.88	17.40	17.45	17.61	17.83
$[O_3]_g$ out calculated (mg O_3/g O_2)	0.00	7.53	10.94	13.24	14.71	15.93	16.65	17.22	17.52	17.58	17.80	17.98

WORKSHEET 3

CONDITIONS												
Run	**Sol. Vol. (L)**	**Sol. Temp. (°C)**		**Gas in (mol O_3/ mol O_2)**		**Element. Vol. (L)**		**Column sect. Area (cm^2)**			
3	8	18		0.012		0.20		81.07			
RESULTS												
Time	0.00	0.53	1.07	1.60	2.13	2.67	3.20	3.73	4.27	4.80	5.33	5.87
pH	5.88	5.83	5.84	5.82	5.82	5.80	5.78	5.78	5.74	5.73	5.71	5.69
Vol. gas flow (L/min)	3.04	3.21	3.21	3.20	3.20	3.20	3.20	3.20	3.20	3.21	3.20	3.21
Mass gas flow (g O_2/min)	4.09	4.30	4.28	4.27	4.26	4.26	4.26	4.26	4.25	4.26	4.26	4.26
$[O_3]_g$ out (mg O_3/L)	0.00	8.06	14.05	17.48	19.67	21.21	21.98	22.42	22.74	22.98	23.18	23.65
Out molar ratio O_3/ O_2	0.00	0.00	0.01	0.01	0.01	0.01	0.01	0.01	0.01	0.01	0.01	0.01
$[O_3]_g$ out (mg O_3/g O_2)	0.00	6.08	10.62	13.24	14.92	16.10	16.69	17.02	17.26	17.45	17.61	17.97
$[O_3]_l$ (mg O_3/L)	0.00	1.61	3.23	4.42	5.31	5.90	6.32	6.54	6.84	6.87	6.96	7.09
$[O_3]_g$ out comparison using 40 elements of volume and k_La = 0.0250												
$[O_3]_g$ out measured (mg O_3/g O_2)	0.00	6.08	10.62	13.24	14.92	16.10	16.69	17.02	17.26	17.45	17.61	17.97
$[O_3]_g$ out calculated (mg O_3/g O_2)	0.00	8.45	11.21	13.23	14.77	15.79	16.50	16.88	17.40	17.45	17.61	17.83

WORKSHEET 4

CONDITIONS												
Run	**Sol. Vol. (L)**		**Sol. Temp. (^oC)**		**Gas in (mol O_3/ mol O_2)**		**Element. Vol. (L)**		**Column sect. Area (cm^2)**			
4	8		17.5		0.011		0.20		81.07			
RESULTS												
Time	0.00	0.53	1.07	1.60	2.13	2.67	3.20	3.73	4.27	4.80	5.33	5.87
pH	5.01	4.83	4.77	4.80	4.83	4.84	4.87	4.93	4.95	4.98	5.03	5.02
Vol. gas flow (L/min)	0.12	1.72	1.71	1.71	1.71	1.71	1.71	1.72	1.72	1.70	1.71	1.72
Mass gas flow (g O_2/min)	0.16	2.31	2.29	2.29	2.28	2.28	2.28	2.28	2.28	2.26	2.28	2.28
$[O_3]_g$ out (mg O_3/L)	0.00	3.20	10.21	13.67	15.65	17.23	18.41	19.59	20.42	20.97	21.47	21.83
Out molar ratio O_3/ O_2	0.00	0.00	0.01	0.01	0.01	0.01	0.01	0.01	0.01	0.01	0.01	0.01
$[O_3]_g$ out (mg O_3/g O_2)	0.00	2.40	7.70	10.34	11.84	13.04	13.95	14.85	15.49	15.91	16.29	16.57
$[O_3]_l$ (mg O_3/L)	0.00	0.87	2.11	3.15	3.99	4.76	5.34	5.82	6.13	6.43	6.53	6.70
$[O_3]_g$ out comparison using 40 elements of volume and k_La = 0.0161												
$[O_3]_g$ out measured (mg O_3/g O_2)	0.00	2.40	7.70	10.34	11.84	13.04	13.95	14.85	15.49	15.91	16.29	16.57
$[O_3]_g$ out calculated (mg O_3/g O_2)	0.00	5.93	8.16	10.06	11.60	13.01	14.08	14.97	15.53	16.08	16.27	16.59

WORKSHEET 5

CONDITIONS												
Run	**Sol. Vol. (L)**		**Sol. Temp. (°C)**		**Gas in (mol O_3/ mol O_2)**		**Element. Vol. (L)**		**Column sect. Area (cm^2)**			
5	8		18		0.012		0.20		81.07			
RESULTS												
Time	0.00	0.53	1.07	1.60	2.13	2.67	3.20	3.73	4.27	4.80	5.33	5.87
pH	5.88	5.83	5.84	5.82	5.82	5.80	5.78	5.78	5.74	5.73	5.71	5.69
Vol. gas flow (L/min)	3.04	3.21	3.21	3.20	3.20	3.20	3.20	3.20	3.20	3.21	3.20	3.21
Mass gas flow (g O_2/min)	4.09	4.30	4.28	4.27	4.26	4.26	4.26	4.26	4.25	4.26	4.26	4.26
$[O_3]_g$ out (mg O_3/L)	0.00	8.06	14.05	17.48	19.67	21.21	21.98	22.42	22.74	22.98	23.18	23.65
Out molar ratio O_3/ O_2	0.00	0.00	0.01	0.01	0.01	0.01	0.01	0.01	0.01	0.01	0.01	0.01
$[O_3]_g$ out (mg O_3/g O_2)	0.00	6.08	10.62	13.24	14.92	16.10	16.69	17.02	17.26	17.45	17.61	17.97
$[O_3]_l$ (mg O_3/L)	0.00	1.61	3.23	4.42	5.31	5.90	6.32	6.54	6.84	6.87	6.96	7.09
$[O_3]_g$ out comparison using 40 elements of volume and k_La = 0.0258												
$[O_3]_g$ out measured (mg O_3/g O_2)	0.00	8.45	11.21	13.23	14.77	15.79	16.50	16.88	17.40	17.45	17.61	17.83
$[O_3]_g$ out calculated (mg O_3/g O_2)	0.00	7.53	10.94	13.24	14.71	15.93	16.65	17.22	17.52	17.58	17.80	17.98

WORKSHEET 6

CONDITIONS												
Run	**Sol. Vol. (L)**		**Sol. Temp. (°C)**		**Gas in (mol O_3/ mol O_2)**		**Element. Vol. (L)**		**Column sect. Area (cm^2)**			
6	8		18		0.012		0.20		81.07			
RESULTS												
Time	0.00	0.53	1.07	1.60	2.13	2.67	3.20	3.73	4.27	4.80	5.33	5.87
pH	5.80	5.19	5.12	5.12	5.16	5.20	5.24	5.29	5.33	5.34	5.36	5.38
Vol. gas flow (L/min)	3.95	6.26	6.32	6.33	6.34	6.34	6.34	6.33	6.33	6.33	6.33	6.33
Mass gas flow (g O_2/min)	5.32	8.38	8.44	8.43	8.44	8.44	8.44	8.43	8.43	8.43	8.43	8.43
$[O_3]_g$ out (mg O_3/L)	0.00	13.83	19.33	21.63	22.80	23.44	23.87	24.11	24.27	24.18	24.15	24.17
Out molar ratio O_3/ O_2	0.00	0.01	0.01	0.01	0.01	0.01	0.01	0.01	0.01	0.01	0.01	0.01
$[O_3]_g$ out (mg O_3/g O_2)	0.00	10.46	14.65	16.42	17.32	17.81	18.14	18.32	18.44	18.37	18.35	18.37
$[O_3]_l$ (mg O_3/L)	0.00	2.67	5.30	6.72	7.51	7.85	8.09	8.19	8.31	8.43	8.24	8.28
$[O_3]_g$ out comparison using 40 elements of volume and k_La = 0.0436												
$[O_3]_g$ out measured (mg O_3/g O_2)	0.00	10.46	14.65	16.42	17.32	17.81	18.14	18.32	18.44	18.37	18.35	18.37
$[O_3]_g$ out calculated (mg O_3/g O_2)	0.00	9.87	13.82	15.93	17.11	17.62	17.98	18.14	18.31	18.49	18.21	18.26

WORKSHEET 7

CONDITIONS												
Run	**Sol. Vol. (L)**		**Sol. Temp. (^oC)**		**Gas in (mol O_3/ mol O_2)**		**Element. Vol. (L)**		**Column sect. Area (cm^2)**			
7	4		18		0.012		0.10		81.07			
RESULTS												
Time	0.00	0.53	1.07	1.60	2.13	2.67	3.20	3.73	4.27	4.80	5.33	5.87
pH												
Vol. gas flow (L/min)	2.53	3.19	3.20	3.21	3.19	3.20	3.21	3.20	3.21	3.18	3.19	3.19
Mass gas flow (g O_2/min)	3.40	4.27	4.27	4.27	4.25	4.26	4.26	4.26	4.26	4.23	4.24	4.25
$[O_3]_g$ out (mg O_3/L)	0.00	11.99	17.50	20.17	21.43	22.29	22.63	22.72	22.75	22.81	23.15	23.14
Out molar ratio O_3/ O_2	0.00	0.01	0.01	0.01	0.01	0.01	0.01	0.01	0.01	0.01	0.01	0.01
$[O_3]_g$ out (mg O_3/g O_2)	0.00	9.06	13.25	15.30	16.26	16.92	17.19	17.25	17.28	17.32	17.58	17.57
$[O_3]_l$ (mg O_3/L)	0.00	1.65	3.98	5.31	6.06	6.57	6.92	7.00	7.09	7.07	7.14	7.20
$[O_3]_g$ out comparison using 40 elements of volume and k_La = 0.0321												
$[O_3]_g$ out measured (mg O_3/g O_2)	0.00	9.06	13.25	15.30	16.26	16.92	17.19	17.25	17.28	17.32	17.58	17.57
$[O_3]_g$ out calculated (mg O_3/g O_2)	0.00	10.35	13.33	15.04	15.99	16.65	17.10	17.19	17.31	17.28	17.37	17.45

WORKSHEET 8

CONDITIONS												
Run	**Sol. Vol. (L)**		**Sol. Temp. (°C)**		**Gas in (mol O_3/ mol O_2)**		**Element. Vol. (L)**		**Column sect. Area (cm^2)**			
8	8		18		0.012		0.20		81.07			
RESULTS												
Time	0.00	0.53	1.07	1.60	2.13	2.67	3.20	3.73	4.27	4.80	5.33	5.87
pH	5.88	5.83	5.84	5.82	5.82	5.80	5.78	5.78	5.74	5.73	5.71	5.69
Vol. gas flow (L/min)	3.04	3.21	3.21	3.20	3.20	3.20	3.20	3.20	3.20	3.21	3.20	3.21
Mass gas flow (g O_2/min)	4.09	4.30	4.28	4.27	4.26	4.26	4.26	4.26	4.25	4.26	4.26	4.26
$[O_3]_g$ out (mg O_3/L)	0.00	8.06	14.05	17.48	19.67	21.21	21.98	22.42	22.74	22.98	23.18	23.65
Out molar ratio O_3/ O_2	0.00	0.00	0.01	0.01	0.01	0.01	0.01	0.01	0.01	0.01	0.01	0.01
$[O_3]_g$ out (mg O_3/g O_2)	0.00	6.08	10.62	13.24	14.92	16.10	16.69	17.02	17.26	17.45	17.61	17.97
$[O_3]_l$ (mg O_3/L)	0.00	1.61	3.23	4.42	5.31	5.90	6.32	6.54	6.84	6.87	6.96	7.09
$[O_3]_g$ out comparison using 40 elements of volume and k_La = 0.0258												
$[O_3]_g$ out measured (mg O_3/g O_2)	0.00	8.45	11.21	13.23	14.77	15.79	16.50	16.88	17.40	17.45	17.61	17.83
$[O_3]_g$ out calculated (mg O_3/g O_2)	0.00	7.53	10.94	13.24	14.71	15.93	16.65	17.22	17.52	17.58	17.80	17.98

WORKSHEET 9

CONDITIONS												
Run	**Sol. Vol. (L)**		**Sol. Temp. (°C)**		**Gas in (mol O_3/ mol O_2)**		**Element. Vol. (L)**		**Column sect. Area (cm^2)**			
9	12		18		0.011		0.30		81.07			
RESULTS												
Time	0.00	0.53	1.07	1.60	2.13	2.67	3.20	3.73	4.27	4.80	5.33	5.87
pH	5.31	5.03	4.89	4.90	4.94	5.00	5.05	5.07	5.10	5.14	5.15	5.17
Vol. gas flow (L/min)	3.32	3.20	3.19	3.19	3.19	3.20	3.20	3.20	3.20	3.20	3.20	3.21
Mass gas flow (g O_2/min)	4.52	4.34	4.32	4.32	4.32	4.32	4.32	4.32	4.32	4.32	4.32	4.32
$[O_3]_g$ out (mg O_3/L)	0.00	7.44	11.51	14.25	16.61	18.32	19.63	20.67	21.38	21.86	22.32	22.58
Out molar ratio O_3/ O_2	0.00	0.00	0.01	0.01	0.01	0.01	0.01	0.01	0.01	0.01	0.01	0.01
$[O_3]_g$ out (mg O_3/g O_2)	0.00	5.22	8.10	10.04	11.71	12.93	13.86	14.60	15.11	15.45	15.78	15.96
$[O_3]_l$ (mg O_3/L)	0.00	2.05	3.21	4.03	4.70	5.28	5.76	5.99	6.23	6.35	6.49	6.60
$[O_3]_g$ out comparison using 40 elements of volume and k_La = 0.0256												
$[O_3]_g$ out measured (mg O_3/g O_2)			8.92	10.52	11.85	12.98	13.94	14.39	14.87	15.12	15.40	15.60
$[O_3]_g$ out calculated (mg O_3/g O_2)	0.00	8.45	11.21	13.23	14.77	15.79	16.50	16.88	17.40	17.45	17.61	17.83

OZONE DECOMPOSITION TESTS

WORKSHEET RUN 1

RESULTS									
Time (min)	$[O_3]_l$ (mol/L)	$[O_3]_g$ (mol/L)	pH	ORP (mV)	Gas flow (L/min)	Jg (cm/s)	Holdup (%)	Ozone decomposition	
								Measured rate (mol L^{-1} s^{-1})	Calculated rate (mol L^{-1} s^{-1})
0	0.00	0.00	9.86	258.2	0.00	0.00	0.00		
1	2.40E-5	2.05E-4	9.74	879.3	3.11	0.64	1.99		
2	3.83E-5	2.57E-4	9.63	911.7	3.19	0.66	1.96		
3	4.41E-5	2.64E-4	9.59	921.1	3.20	0.66	2.02		
4	4.85E-5	2.70E-4	9.50	925.8	3.20	0.66	1.98		
5	5.22E-5	2.80E-4	9.47	931.5	3.20	0.66	2.03		
6	5.44E-5	2.87E-4	9.42	929.3	3.20	0.66	1.97		
7	5.88E-5	2.97E-4	9.38	930.9	3.21	0.66	1.99		
8	6.08E-5	3.01E-4	9.33	937.0	3.20	0.66	2.02		
9	6.19E-5	3.03E-4	9.30	940.0	3.20	0.66	2.03	1.30E-06	1.25E-06
10	6.49E-5	3.07E-4	9.24	939.3	3.19	0.66	2.08	1.28E-06	1.25E-06
11	6.64E-5	3.08E-4	9.23	946.1	3.20	0.66	2.08	1.28E-06	1.27E-06
12	6.77E-5	3.13E-4	9.17	946.7	3.20	0.66	2.03	1.25E-06	1.23E-06
13	6.92E-5	3.17E-4	9.12	947.4	3.21	0.66	2.07	1.23E-06	1.20E-06
14	7.17E-5	3.22E-4	9.08	947.1	3.20	0.66	2.01	1.20E-06	1.20E-06

15	7.37E-5	3.25E-4	9.06	945.7	3.20	0.66	2.03	1.19E-06	1.22E-06
16	7.53E-5	3.26E-4	9.05	950.9	3.20	0.66	1.99	1.18E-06	1.24E-06
17	7.62E-5	3.29E-4	8.97	958.1	3.21	0.66	2.04	1.17E-06	1.16E-06
18	7.81E-5	3.32E-4	8.95	958.1	3.20	0.66	1.97	1.14E-06	1.18E-06
19	7.86E-5	3.34E-4	8.91	952.6	3.19	0.66	1.99	1.13E-06	1.14E-06
20	7.97E-5	3.37E-4	8.87	964.4	3.19	0.66	2.00	1.12E-06	1.11E-06
21	8.22E-5	3.42E-4	8.82	963.8	3.20	0.66	1.98	1.09E-06	1.10E-06
22	8.56E-5	3.48E-4	8.79	961.0	3.20	0.66	1.94	1.06E-06	1.12E-06
23	8.52E-5	3.49E-4	8.74	967.5	3.20	0.66	1.96	1.05E-06	1.06E-06
24	8.76E-5	3.52E-4	8.72	961.0	3.20	0.66	1.94	1.04E-06	1.07E-06
25	8.71E-5	3.54E-4	8.68	967.1	3.21	0.66	1.92	1.03E-06	1.03E-06
26	8.89E-5	3.58E-4	8.63	969.4	3.20	0.66	1.90	1.00E-06	1.01E-06
27	9.26E-5	3.61E-4	8.58	975.4	3.20	0.66	1.96	9.86E-07	1.01E-06
28	9.24E-5	3.65E-4	8.54	977.0	3.20	0.66	2.00	9.67E-07	9.69E-07
29	9.50E-5	3.67E-4	8.51	980.6	3.20	0.66	1.96	9.55E-07	9.66E-07
30	9.60E-5	3.68E-4	8.48	983.5	3.20	0.66	1.99	9.51E-07	9.54E-07
31	9.86E-5	3.73E-4	8.40	984.9	3.20	0.66	2.01	9.20E-07	9.13E-07
32	1.01E-4	3.77E-4	8.34	985.0	3.20	0.66	2.01	8.97E-07	8.76E-07
33	1.02E-4	3.81E-4	8.29	983.7	3.20	0.66	1.99	8.76E-07	8.48E-07
34	1.04E-4	3.87E-4	8.27	992.1	3.20	0.66	1.95	8.47E-07	8.56E-07
35	1.06E-4	3.91E-0	8.22	988.1	3.21	0.66	1.96	8.23E-07	8.29E-07
36	1.09E-4	3.94E-4	8.16	996.0	3.20	0.66	2.01	8.08E-07	8.13E-07
37	1.11E-4	3.96E-4	8.14	999.7	3.20	0.66	1.95		
38	1.12E-4	4.00E-4	8.10	1002.0	3.20	0.66	1.96		
39	1.15E-4	4.05E-4	8.04	1003.2	3.20	0.66	1.96		
40	1.18E-4	4.10E-4	7.99	1005.1	3.20	0.66	2.01		
41	1.20E-4	4.16E-4	7.97	1011.7	3.20	0.66	1.99		

42	1.21E-4	4.19E-4	7.91	1013.8	3.20	0.66	1.96		
43	1.23E-4	4.24E-4	7.88	1017.8	3.20	0.66	1.97		
44	1.25E-4	4.26E-4	7.84	1017.3	3.20	0.66	1.99		
45	1.28E-4	4.32E-4	7.81	1023.9	3.20	0.66	1.97		
46	1.30E-4	4.36E-4	7.77	1023.2	3.20	0.66	1.97		
47	1.30E-4	4.37E-4	7.75	1027.1	3.20	0.66	1.97		
48	1.32E-4	4.39E-4	7.73	1031.3	3.20	0.66	1.97		
49	1.34E-4	4.42E-4	7.71	1029.9	3.20	0.66	1.93		
50	1.35E-4	4.46E-4	7.68	1030.0	3.20	0.66	1.97		
51	1.37E-4	4.49E-4	7.67	1035.3	3.20	0.66	1.97		
52	1.37E-4	4.53E-4	7.65	1030.8	3.20	0.66	2.01		
53	1.39E-4	4.55E-4	7.62	1035.0	3.20	0.66	1.97		
54	1.39E-4	4.56E-4	7.62	1038.7	3.20	0.66	1.97		
55	1.40E-4	4.58E-4	7.62	1041.9	3.20	0.66	1.95		
56	1.41E-4	4.61E-4	7.59	1041.4	3.20	0.66	1.98		
57	1.42E-4	4.61E-4	7.59	1039.5	3.20	0.66	2.00		
58	1.43E-4	4.61E-4	7.57	1039.8	3.20	0.66	2.05		
59	1.41E-4	4.62E-4	7.56	1040.9	3.20	0.66	2.04		
60	1.44E-4	4.62E-4	7.56	1042.8	3.20	0.66	2.05		
61	1.46E-4	4.65E-4	7.54	1047.5	3.20	0.66	2.05		
62	1.44E-4	4.64E-4	7.54	1043.0	3.20	0.66	1.99		

WORKSHEET RUN 2

RESULTS									
Time (min)	$[O_3]_l$ (mol/L)	$[O_3]_g$ (mol/L)	pH	ORP (mV)	Gas flow (L/min)	Jg (cm/s)	Holdup (%)	Ozone decomposition	
								Measured rate (mol L^{-1} s^{-1})	Calculated rate (mol L^{-1} s^{-1})
0	0.00	0.00	9.75	310.1	0.00	0.00	0.00		
1	3.21E-5	2.13E-4	9.61	905.0	3.20	0.66	2.16		
2	4.45E-5	2.57E-4	9.55	937.3	3.20	0.66	2.09		
3	5.21E-5	2.75E-4	9.47	948.1	3.20	0.66	2.09		
4	5.56E-5	2.86E-4	9.39	953.8	3.20	0.66	2.03		
5	5.99E-5	2.92E-4	9.38	950.1	3.20	0.66	2.08		
6	6.05E-5	3.00E-4	9.33	956.9	3.20	0.66	2.14		
7	6.25E-5	3.04E-4	9.30	958.3	3.20	0.66	2.02		
8	6.49E-5	3.09E-4	9.26	958.1	3.20	0.66	2.06		
9	6.66E-5	3.10E-4	9.21	960.4	3.20	0.66	2.02	1.27E-06	1.25E-06
10	6.78E-5	3.12E-4	9.19	959.6	3.21	0.66	2.02	1.26E-06	1.24E-06
11	6.93E-5	3.17E-4	9.17	959.2	3.20	0.66	2.04	1.23E-06	1.26E-06
12	7.02E-5	3.18E-4	9.12	966.1	3.20	0.66	2.07	1.23E-06	1.21E-06
13	7.24E-5	3.19E-4	9.08	966.2	3.20	0.66	2.01	1.22E-06	1.22E-06
14	7.42E-5	3.22E-4	9.07	968.5	3.20	0.66	2.06	1.21E-06	1.24E-06
15	7.53E-5	3.24E-4	9.04	967.8	3.20	0.66	2.03	1.19E-06	1.22E-06
16	7.56E-5	3.26E-4	8.98	968.9	3.20	0.66	2.02	1.18E-06	1.16E-06

17	7.70E-5	3.28E-4	8.98	971.0	3.19	0.66	2.07	1.17E-06	1.18E-06
18	7.84E-5	3.28E-4	8.94	969.0	3.20	0.66	2.01	1.17E-06	1.17E-06
19	7.94E-5	3.30E-4	8.90	975.2	3.20	0.66	2.06	1.16E-06	1.14E-06
20	8.10E-5	3.29E-4	8.86	975.7	3.20	0.66	2.03	1.16E-06	1.12E-06
21	8.17E-5	3.32E-4	8.84	978.1	3.20	0.66	2.05	1.15E-06	1.11E-06
22	8.33E-5	3.36E-4	8.80	980.0	3.20	0.66	2.03	1.13E-06	1.10E-06
23	8.54E-5	3.41E-4	8.76	981.9	3.20	0.66	2.06	1.10E-06	1.08E-06
24	8.81E-5	3.49E-4	8.76	983.0	3.20	0.66	2.07	1.05E-06	1.12E-06
25	8.83E-5	3.50E-4	8.71	981.6	3.20	0.66	2.08	1.05E-06	1.07E-06
26	8.89E-5	3.54E-4	8.65	986.1	3.20	0.66	2.04	1.03E-06	1.02E-06
27	9.24E-5	3.56E-4	8.61	988.5	3.20	0.66	2.07	1.01E-06	1.03E-06
28	9.34E-5	3.60E-4	8.56	990.2	3.20	0.66	2.10	9.93E-07	9.99E-07
29	9.47E-5	3.63E-4	8.51	990.4	3.20	0.66	2.11	9.74E-07	9.60E-07
30	9.44E-5	3.62E-4	8.47	993.7	3.20	0.66	2.13	9.80E-07	9.20E-07
31	9.52E-5	3.63E-4	8.45	996.0	3.20	0.66	2.11	9.76E-07	9.14E-07
32	9.74E-5	3.67E-4	8.38	999.4	3.20	0.66	1.97	9.53E-07	8.78E-07
33	1.02E-4	3.76E-4	8.31	1000.4	3.20	0.66	2.05	9.06E-07	8.64E-07
34	1.03E-4	3.81E-4	8.29	999.2	3.20	0.66	2.03	8.76E-07	8.63E-07
35	1.05E-4	3.85E-4	8.24	1004.0	3.21	0.66	2.05	8.53E-07	8.38E-07
36	1.06E-4	3.87E-4	8.20	1009.1	3.20	0.66	2.04	8.44E-07	8.14E-07
37	1.07E-4	3.90E-4	8.16	1009.6	3.20	0.66	2.10		
38	1.10E-4	3.95E-4	8.12	1004.6	3.20	0.66	2.07		
39	1.12E-4	4.03E-4	8.08	1009.0	3.20	0.66	2.06		
40	1.15E-4	4.09E-4	8.02	1020.1	3.20	0.66	2.03		
41	1.18E-4	4.16E-4	7.98	1023.7	3.20	0.66	2.07		
42	1.20E-4	4.20E-4	7.93	1026.1	3.20	0.66	2.08		
43	1.20E-4	4.25E-4	7.90	1028.0	3.20	0.66	2.07		

44	1.24E-4	4.28E-4	7.85	1031.5	3.20	0.66	2.03		
45	1.26E-0	4.33E-4	7.80	1034.4	3.20	0.66	2.09		
46	1.29E-4	4.37E-4	7.78	1033.6	3.20	0.66	2.06		
47	1.28E-4	4.41E-4	7.76	1036.3	3.20	0.66	2.05		
48	1.31E-4	4.43E-4	7.72	1035.5	3.19	0.66	2.01		
49	1.32E-4	4.45E-4	7.70	1036.0	3.19	0.66	2.04		
50	1.33E-4	4.46E-4	7.68	1038.1	3.20	0.66	2.08		
51	1.33E-4	4.48E-4	7.66	1043.6	3.20	0.66	2.05		
52	1.35E-4	4.48E-4	7.66	1040.2	3.20	0.66	2.08		
53	1.34E-4	4.50E-4	7.63	1042.0	3.20	0.66	2.06		
54	1.35E-4	4.52E-4	7.61	1041.9	3.20	0.66	2.06		
55	1.34E-4	4.51E-4	7.61	1041.3	3.20	0.66	2.06		
56	1.35E-4	4.51E-4	7.60	1045.0	3.20	0.66	2.03		
57	1.37E-4	4.53E-4	7.59	1049.0	3.20	0.66	2.07		
58	1.37E-4	4.53E-4	7.57	1048.4	3.20	0.66	2.03		
59	1.38E-4	4.54E-4	7.58	1048.6	3.20	0.66	2.09		
60	1.39E-4	4.60E-4	7.57	1047.1	3.20	0.66	2.05		
61	1.40E-4	4.65E-4	7.57	1043.8	3.20	0.66	2.08		
62	1.41E-4	4.64E-4	7.56	1044.6	3.20	0.66	2.06		
63	1.41E-4	4.65E-4	7.59	1048.9	3.20	0.66	2.08		
64	1.40E-4	4.64E-4	7.55	1049.7	3.20	0.66	2.10		
65	1.42E-4	4.66E-4	7.55	1051.2	3.20	0.66	2.09		
66	1.41E-4	4.67E-4	7.54	1052.6	3.20	0.66	2.05		
67	1.42E-4	4.68E-4	7.53	1051.8	3.20	0.66	2.04		
68	1.41E-4	4.68E-4	7.54	1051.1	3.20	0.66	2.06		
69	1.41E-4	4.69E-4	7.52	1051.9	3.20	0.66	2.05		
70	1.43E-4	4.61E-4	7.53	1053.7	3.20	0.66	2.05		

WORKSHEET RUN 3

RESULTS									
Time (min)	$[O_3]_l$ (mol/L)	$[O_3]_g$ (mol/L)	pH	ORP (mV)	Gas flow (L/min)	Jg (cm/s)	Holdup (%)	Ozone decomposition	
								Measured rate (mol L^{-1} s^{-1})	Calculated rate (mol L^{-1} s^{-1})
0	0.00	0.00	9.52	285.7	0.00	0.00	0.00		
1	3.65E-5	1.64E-4	9.42	628.7	3.19	0.66	2.35		
2	5.21E-5	2.53E-4	9.24	838.3	3.21	0.66	2.07		
3	6.69E-5	2.81E-4	9.03	908.7	3.21	0.66	2.00		
4	8.03E-5	3.04E-4	8.78	940.5	3.22	0.66	1.94		
5	9.25E-5	3.35E-4	8.48	964.8	3.20	0.66	1.90		
6	1.04E-4	3.58E-4	8.22	985.7	3.20	0.66	1.90		
7	1.15E-4	3.79E-4	7.95	1006.8	3.19	0.66	1.87		
8	1.24E-4	4.04E-4	7.73	1026.0	3.20	0.66	1.85		
9	1.32E-4	4.27E-4	7.52	1037.5	3.19	0.66	1.87	1.21E-06	1.20E-06
10	1.38E-4	4.43E-4	7.44	1043.4	3.20	0.66	1.87	1.11E-06	1.14E-06
11	1.40E-4	4.51E-4	7.40	1047.5	3.20	0.66	1.84	9.51E-07	9.76E-07
12	1.41E-4	4.55E-4	7.38	1051.2	3.21	0.66	1.89	8.52E-07	8.47E-07
13	1.42E-4	4.59E-4	7.35	1052.5	3.20	0.66	1.87	7.52E-07	7.16E-07
14	1.43E-4	4.60E-4	7.34	1052.2	3.20	0.66	1.89	6.39E-07	6.13E-07
15	1.43E-4	4.60E-4	7.34	1053.7	3.20	0.66	1.86	5.31E-07	5.26E-07
16	1.42E-4	4.62E-4	7.33	1052.2	3.21	0.66	1.89	4.69E-07	5.11E-07

17	1.42E-4	4.63E-4	7.33	1054.6	3.19	0.66	1.88		
18	1.42E-4	4.64E-4	7.35	1053.5	3.19	0.66	1.88		
19	1.43E-4	4.65E-4	7.35	1054.2	3.20	0.66	1.89		
20	1.42E-4	4.65E-4	7.35	1052.4	3.20	0.66	1.87		
21	1.43E-4	4.65E-4	7.34	1053.5	3.20	0.66	1.85		
22	1.44E-4	4.65E-4	7.35	1053.6	3.20	0.66	1.87		
23	1.44E-4	4.66E-4	7.36	1052.8	3.20	0.66	1.87		
24	1.43E-4	4.66E-4	7.35	1053.7	3.20	0.66	1.87		
25	1.44E-4	4.67E-4	7.36	1052.2	3.20	0.66	1.89		
26	1.43E-4	4.67E-4	7.35	1052.9	3.20	0.66	1.87		
27	1.44E-4	4.67E-4	7.37	1053.7	3.20	0.66	1.87		
28	1.43E-4	4.66E-4	7.34	1053.4	3.20	0.66	1.88		
29	1.44E-4	4.66E-4	7.36	1052.1	3.20	0.66	1.87		
30	1.44E-4	4.67E-4	7.36	1053.1	3.20	0.66	1.87		
31	1.44E-4	4.67E-4	7.36	1052.6	3.20	0.66	1.82		
32	1.43E-4	4.67E-4	7.35	1051.4	3.20	0.66	1.87		
33	1.43E-4	4.67E-4	7.36	1053.1	3.20	0.66	1.90		
34	1.43E-4	4.67E-4	7.38	1050.9	3.20	0.66	1.87		
35	1.44E-4	4.67E-4	7.38	1052.5	3.20	0.66	1.92		
36	1.44E-4	4.68E-4	7.39	1049.2	3.20	0.66	1.90		
37	1.43E-4	4.68E-4	7.39	1051.5	3.20	0.66	1.92		
38	1.43E-4	4.67E-4	7.38	1052.9	3.20	0.66	1.91		
39	1.44E-4	4.68E-4	7.39	1050.9	3.20	0.66	1.87		
40	1.43E-4	4.68E-4	7.41	1051.8	3.20	0.66	1.87		
41	1.44E-4	4.66E-4	7.40	1050.2	3.20	0.66	1.86		
42	1.44E-4	4.66E-4	7.40	1051.2	3.19	0.66	1.85		
43	1.43E-4	4.68E-4	7.40	1050.6	3.20	0.66	1.89		

44	1.43E-4	4.66E-4	7.41	1049.7	3.20	0.66	1.87		
45	1.43E-4	4.66E-4	7.41	1051.2	3.20	0.66	1.87		
46	1.43E-4	4.67E-4	7.41	1049.8	3.20	0.66	1.90		
47	1.43E-4	4.66E-4	7.43	1049.8	3.20	0.66	1.91		
48	1.43E-4	4.66E-4	7.42	1049.0	3.20	0.66	1.90		
49	1.42E-4	4.67E-4	7.43	1049.1	3.19	0.66	1.90		
50	1.42E-4	4.67E-4	7.43	1048.8	3.20	0.66	1.90		
51	1.42E-4	4.67E-4	7.42	1049.1	3.20	0.66	1.85		
52	1.41E-4	4.67E-4	7.42	1047.1	3.20	0.66	1.87		
53	1.42E-4	4.66E-4	7.44	1049.5	3.20	0.66	1.92		
54	1.42E-4	4.66E-4	7.44	1047.9	3.19	0.66	1.90		
55	1.42E-4	4.67E-4	7.42	1049.4	3.20	0.66	1.89		

WORKSHEET RUN 4

RESULTS									
Time (min)	$[O_3]_l$ (mol/L)	$[O_3]_g$ (mol/L)	pH	ORP (mV)	Gas flow (L/min)	Jg (cm/s)	Holdup (%)	Ozone decomposition	
								Measured rate (mol L^{-1} s^{-1})	Calculated rate (mol L^{-1} s^{-1})
0	0.00	0.00	9.74	268.2	0.00	0.00	0.00		
1	1.20E-5	9.16E-5	9.64	845.5	3.18	0.66	2.22		
2	1.78E-5	1.06E-4	9.59	887.9	3.20	0.66	2.08		
3	2.16E-5	1.13E-4	9.54	902.7	3.20	0.66	2.01		
4	2.42E-5	1.17E-4	9.48	905.0	3.20	0.66	2.03		
5	2.69E-5	1.22E-4	9.43	900.1	3.20	0.66	2.01		
6	2.90E-5	1.23E-4	9.41	911.6	3.20	0.66	2.02		
7	2.94E-5	1.28E-4	9.32	919.1	3.21	0.66	2.05		
8	3.10E-5	1.30E-4	9.31	918.9	3.20	0.66	2.07		
9	3.20E-5	1.32E-4	9.29	921.1	3.20	0.66	2.04		
10	3.33E-5	1.35E-4	9.23	914.6	3.20	0.66	1.96		
11	3.42E-5	1.37E-4	9.20	922.4	3.20	0.66	2.07		
12	3.50E-5	1.38E-4	9.17	922.9	3.20	0.66	2.00		
13	3.63E-5	1.41E-4	9.14	927.5	3.20	0.66	2.02		
14	3.74E-5	1.43E-4	9.09	931.8	3.20	0.66	2.02		
15	3.85E-5	1.45E-4	9.05	933.0	3.21	0.66	2.03		
16	3.97E-5	1.46E-4	9.04	932.2	3.21	0.66	1.97	8.86E-07	8.63E-07

17	4.02E-5	1.48E-4	9.00	935.9	3.20	0.66	1.97	8.74E-07	8.52E-07
18	4.15E-5	1.50E-4	8.94	941.1	3.21	0.66	2.00	8.65E-07	8.48E-07
19	4.18E-5	1.52E-4	8.94	943.7	3.20	0.66	2.01	8.53E-07	8.50E-07
20	4.27E-5	1.54E-4	8.91	944.3	3.20	0.66	1.99	8.46E-07	8.54E-07
21	4.37E-5	1.55E-4	8.86	942.8	3.20	0.66	2.00	8.4E-07	8.43E-07
22	4.40E-5	1.56E-4	8.82	942.1	3.20	0.66	1.99	8.33E-07	8.31E-07
23	4.46E-5	1.57E-4	8.77	942.9	3.20	0.66	2.01	8.3E-07	8.11E-07
24	4.56E-5	1.59E-4	8.73	951.2	3.20	0.66	2.01	8.2E-07	8.10E-07
25	4.77E-5	1.61E-4	8.70	944.3	3.20	0.66	2.02	8.09E-07	8.34E-07
26	4.84E-5	1.62E-4	8.64	954.0	3.20	0.66	1.98	8.01E-07	8.16E-07
27	4.93E-5	1.63E-4	8.62	956.7	3.20	0.66	2.01	7.97E-07	8.19E-07
28	5.05E-5	1.66E-4	8.61	951.4	3.20	0.66	1.96	7.8E-07	8.36E-07
29	5.08E-5	1.68E-4	8.55	956.6	3.20	0.66	1.96	7.68E-07	8.09E-07
30	5.12E-5	1.70E-4	8.49	957.8	3.20	0.66	1.94	7.59E-07	7.79E-07
31	5.20E-5	1.72E-4	8.44	956.4	3.21	0.66	1.94	7.51E-07	7.67E-07
32	5.22E-5	1.72E-4	8.42	952.8	3.20	0.66	1.97	7.48E-07	7.58E-07
33	5.27E-5	1.74E-4	8.36	960.0	3.19	0.66	1.94	7.37E-07	7.35E-07
34	5.42E-5	1.76E-4	8.34	968.5	3.19	0.66	2.01	7.3E-07	7.46E-07
35	5.43E-5	1.78E-4	8.25	973.8	3.20	0.66	2.02	7.18E-07	7.02E-07
36	5.57E-5	1.81E-4	8.23	977.4	3.20	0.66	2.01	7.05E-07	7.08E-07
37	5.67E-5	1.82E-4	8.19	979.7	3.20	0.66	1.95	6.96E-07	7.04E-07
38	5.73E-5	1.83E-4	8.16	981.5	3.20	0.66	1.98	6.9E-07	6.97E-07
39	5.74E-5	1.86E-4	8.13	982.9	3.20	0.66	2.01	6.76E-07	6.83E-07
40	5.91E-5	1.87E-4	8.08	985.7	3.20	0.66	1.97	6.74E-07	6.85E-07
41	6.00E-5	1.90E-4	8.03	987.1	3.21	0.66	2.01	6.59E-07	6.72E-07
42	5.99E-5	1.89E-4	8.00	986.0	3.19	0.66	2.03	6.58E-07	6.53E-07
43	6.02E-5	1.92E-4	7.97	986.4	3.20	0.66	2.05	6.42E-07	6.43E-07

44	6.12E-5	1.95E-4	7.94	994.5	3.20	0.66	2.02	6.31E-07	6.41E-07
45	6.15E-5	1.96E-4	7.91	996.3	3.20	0.66	2.05	6.23E-07	6.32E-07
46	6.23E-5	1.95E-4	7.86	997.5	3.20	0.66	2.02	6.3E-07	6.19E-07
47	6.30E-5	1.97E-4	7.84	1001.9	3.20	0.66	1.96	6.18E-07	6.18E-07
48	6.42E-5	2.00E-4	7.79	1002.5	3.20	0.66	1.96	6.06E-07	6.10E-07
49	6.41E-5	2.00E-4	7.79	1005.9	3.20	0.66	2.03	6.06E-07	6.08E-07
50	6.34E-5	2.00E-4	7.75	1005.6	3.20	0.66	1.99	6.05E-07	5.81E-07
51	6.41E-5	2.01E-4	7.72	1010.2	3.20	0.66	1.97	5.99E-07	5.78E-07
52	6.47E-5	2.03E-4	7.72	1008.8	3.20	0.66	1.99	5.88E-07	5.82E-07
53	6.49E-5	2.05E-4	7.70	1011.9	3.20	0.66	1.96	5.80E-07	5.76E-07
54	6.52E-5	2.05E-4	7.67	1012.5	3.20	0.66	1.96	5.78E-07	5.68E-07
55	6.56E-5	2.06E-4	7.69	1011.2	3.20	0.66	2.02	5.73E-07	5.80E-07
56	6.66E-5	2.07E-4	7.66	1014.1	3.21	0.66	2.07		
57	6.73E-5	2.08E-4	7.64	1018.5	3.20	0.66	2.02		
58	6.75E-5	2.08E-4	7.65	1016.3	3.20	0.66	2.03		
59	6.83E-5	2.08E-4	7.63	1016.7	3.19	0.66	2.01		
60	6.85E-5	2.08E-4	7.64	1017.8	3.19	0.66	1.95		
61	6.77E-5	2.09E-4	7.62	1017.6	3.20	0.66	1.99		
62	6.81E-5	2.10E-4	7.61	1016.0	3.19	0.66	1.99		
63	6.79E-5	2.11E-4	7.60	1016.6	3.20	0.66	1.98		
64	6.88E-5	2.12E-4	7.60	1020.8	3.20	0.66	1.97		
65	6.90E-5	2.13E-4	7.59	1015.0	3.20	0.66	2.01		
66	7.00E-5	2.13E-4	7.59	1017.2	3.20	0.66	1.99		
67	6.98E-5	2.12E-4	7.59	1005.2	3.20	0.66	2.02		
68	6.95E-5	2.14E-4	7.58	1011.8	3.20	0.66	2.03		
69	7.00E-5	2.14E-4	7.59	1019.2	3.20	0.66	2.07		
70	7.02E-5	2.14E-4	7.56	1017.1	3.19	0.66	2.04		

WORKSHEET RUN 5

RESULTS									
Time (min)	$[O_3]_l$ (mol/L)	$[O_3]_g$ (mol/L)	pH	ORP (mV)	Gas flow (L/min)	Jg (cm/s)	Holdup (%)	Ozone decomposition	
								Measured rate (mol L^{-1} s^{-1})	Calculated rate (mol L^{-1} s^{-1})
0	0.00	0.00	9.86	258.2	0.00	0.00	0.00		
1	2.40E-5	2.05E-4	9.74	879.3	3.11	0.64	1.99		
2	3.83E-5	2.57E-4	9.63	911.7	3.19	0.66	1.96		
3	4.41E-5	2.64E-4	9.59	921.1	3.20	0.66	2.02		
4	4.85E-5	2.70E-4	9.50	925.8	3.20	0.66	1.98		
5	5.22E-5	2.80E-4	9.47	931.5	3.20	0.66	2.03		
6	5.44E-5	2.87E-4	9.42	929.3	3.20	0.66	1.97		
7	5.88E-5	2.97E-4	9.38	930.9	3.21	0.66	1.99		
8	6.08E-5	3.01E-4	9.33	937.0	3.20	0.66	2.02		
9	6.19E-5	3.03E-4	9.30	940.0	3.20	0.66	2.03	1.30E-06	1.25E-06
10	6.49E-5	3.07E-4	9.24	939.3	3.19	0.66	2.08	1.28E-06	1.25E-06
11	6.64E-5	3.08E-4	9.23	946.1	3.20	0.66	2.08	1.28E-06	1.27E-06
12	6.77E-5	3.13E-4	9.17	946.7	3.20	0.66	2.03	1.25E-06	1.23E-06
13	6.92E-5	3.17E-4	9.12	947.4	3.21	0.66	2.07	1.23E-06	1.20E-06
14	7.17E-5	3.22E-4	9.08	947.1	3.20	0.66	2.01	1.20E-06	1.20E-06
15	7.37E-5	3.25E-4	9.06	945.7	3.20	0.66	2.03	1.19E-06	1.22E-06
16	7.53E-5	3.26E-4	9.05	950.9	3.20	0.66	1.99	1.18E-06	1.24E-06

17	7.62E-5	3.29E-4	8.97	958.1	3.21	0.66	2.04	1.17E-06	1.16E-06
18	7.81E-5	3.32E-4	8.95	958.1	3.20	0.66	1.97	1.14E-06	1.18E-06
19	7.86E-5	3.34E-4	8.91	952.6	3.19	0.66	1.99	1.13E-06	1.14E-06
20	7.97E-5	3.37E-4	8.87	964.4	3.19	0.66	2.00	1.12E-06	1.11E-06
21	8.22E-5	3.42E-4	8.82	963.8	3.20	0.66	1.98	1.09E-06	1.10E-06
22	8.56E-5	3.48E-4	8.79	961.0	3.20	0.66	1.94	1.06E-06	1.12E-06
23	8.52E-5	3.49E-4	8.74	967.5	3.20	0.66	1.96	1.05E-06	1.06E-06
24	8.76E-5	3.52E-4	8.72	961.0	3.20	0.66	1.94	1.04E-06	1.07E-06
25	8.71E-5	3.54E-4	8.68	967.1	3.21	0.66	1.92	1.03E-06	1.03E-06
26	8.89E-5	3.58E-4	8.63	969.4	3.20	0.66	1.90	1.00E-06	1.01E-06
27	9.26E-5	3.61E-4	8.58	975.4	3.20	0.66	1.96	9.86E-07	1.01E-06
28	9.24E-5	3.65E-4	8.54	977.0	3.20	0.66	2.00	9.67E-07	9.69E-07
29	9.50E-5	3.67E-4	8.51	980.6	3.20	0.66	1.96	9.55E-07	9.66E-07
30	9.60E-5	3.68E-4	8.48	983.5	3.20	0.66	1.99	9.51E-07	9.54E-07
31	9.86E-5	3.73E-4	8.40	984.9	3.20	0.66	2.01	9.20E-07	9.13E-07
32	1.01E-4	3.77E-4	8.34	985.0	3.20	0.66	2.01	8.97E-07	8.76E-07
33	1.02E-4	3.81E-4	8.29	983.7	3.20	0.66	1.99	8.76E-07	8.48E-07
34	1.04E-4	3.87E-4	8.27	992.1	3.20	0.66	1.95	8.47E-07	8.56E-07
35	1.06E-4	3.91E-0	8.22	988.1	3.21	0.66	1.96	8.23E-07	8.29E-07
36	1.09E-4	3.94E-4	8.16	996.0	3.20	0.66	2.01	8.08E-07	8.13E-07
37	1.11E-4	3.96E-4	8.14	999.7	3.20	0.66	1.95		
38	1.12E-4	4.00E-4	8.10	1002.0	3.20	0.66	1.96		
39	1.15E-4	4.05E-4	8.04	1003.2	3.20	0.66	1.96		
40	1.18E-4	4.10E-4	7.99	1005.1	3.20	0.66	2.01		
41	1.20E-4	4.16E-4	7.97	1011.7	3.20	0.66	1.99		
42	1.21E-4	4.19E-4	7.91	1013.8	3.20	0.66	1.96		
43	1.23E-4	4.24E-4	7.88	1017.8	3.20	0.66	1.97		

44	1.25E-4	4.26E-4	7.84	1017.3	3.20	0.66	1.99		
45	1.28E-4	4.32E-4	7.81	1023.9	3.20	0.66	1.97		
46	1.30E-4	4.36E-4	7.77	1023.2	3.20	0.66	1.97		
47	1.30E-4	4.37E-4	7.75	1027.1	3.20	0.66	1.97		
48	1.32E-4	4.39E-4	7.73	1031.3	3.20	0.66	1.97		
49	1.34E-4	4.42E-4	7.71	1029.9	3.20	0.66	1.93		
50	1.35E-4	4.46E-4	7.68	1030.0	3.20	0.66	1.97		
51	1.37E-4	4.49E-4	7.67	1035.3	3.20	0.66	1.97		
52	1.37E-4	4.53E-4	7.65	1030.8	3.20	0.66	2.01		
53	1.39E-4	4.55E-4	7.62	1035.0	3.20	0.66	1.97		
54	1.39E-4	4.56E-4	7.62	1038.7	3.20	0.66	1.97		
55	1.40E-4	4.58E-4	7.62	1041.9	3.20	0.66	1.95		
56	1.41E-4	4.61E-4	7.59	1041.4	3.20	0.66	1.98		
57	1.42E-4	4.61E-4	7.59	1039.5	3.20	0.66	2.00		
58	1.43E-4	4.61E-4	7.57	1039.8	3.20	0.66	2.05		
59	1.41E-4	4.62E-4	7.56	1040.9	3.20	0.66	2.04		
60	1.44E-4	4.62E-4	7.56	1042.8	3.20	0.66	2.05		
61	1.46E-4	4.65E-4	7.54	1047.5	3.20	0.66	2.05		
62	1.44E-4	4.64E-4	7.54	1043.0	3.20	0.66	1.99		

WORKSHEET RUN 6

RESULTS									
Time (min)	$[O_3]_l$ (mol/L)	$[O_3]_g$ (mol/L)	pH	ORP (mV)	Gas flow (L/min)	Jg (cm/s)	Holdup (%)	Ozone decomposition	
								Measured rate (mol L^{-1} s^{-1})	Calculated rate (mol L^{-1} s^{-1})
0	0.00	0.00	10.17	208.0	0.00	0.00	0.00		
1	3.64E-5	3.20E-4	10.05	901.0	3.19	0.66	1.96		
2	5.84E-5	3.73E-4	9.92	926.1	3.20	0.66	1.94		
3	6.80E-5	3.99E-4	9.82	932.4	3.21	0.66	1.93		
4	7.38E-5	4.14E-4	9.75	936.1	3.20	0.66	1.98		
5	8.13E-5	4.34E-4	9.69	944.2	3.21	0.66	1.95		
6	8.70E-5	4.53E-4	9.61	944.5	3.20	0.66	1.96		
7	8.91E-5	4.63E-4	9.61	939.7	3.20	0.66	1.91		
8	9.28E-5	4.63E-4	9.54	945.0	3.21	0.66	1.94		
9	9.66E-5	4.77E-4	9.48	949.4	3.20	0.66	1.89		
10	1.00E-4	4.83E-4	9.44	954.7	3.20	0.66	1.89		
11	1.02E-4	4.91E-4	9.39	958.4	3.20	0.66	1.91		
12	1.03E-4	4.94E-4	9.35	960.4	3.21	0.66	1.92		
13	1.03E-4	4.84E-4	9.32	961.9	3.22	0.66	1.96	2.34E-06	2.49E-06
14	1.05E-4	4.84E-4	9.26	964.2	3.20	0.66	1.94	2.32E-06	2.38E-06
15	1.09E-4	4.93E-4	9.25	962.4	3.20	0.66	1.96	2.27E-06	2.46E-06
16	1.10E-4	4.98E-4	9.18	969.3	3.20	0.66	1.92	2.25E-06	2.30E-06

17	1.13E-4	5.03E-4	9.14	971.3	3.20	0.66	1.92	2.22E-06	2.31E-06
18	1.16E-4	4.96E-4	9.13	970.0	3.20	0.66	1.92	2.30E-06	2.34E-06
19	1.20E-4	5.05E-4	9.07	969.9	3.20	0.66	1.92	2.21E-06	2.28E-06
20	1.21E-4	5.07E-4	9.05	977.3	3.21	0.66	1.90	2.19E-06	2.28E-06
21	1.25E-4	5.13E-4	8.99	980.6	3.20	0.66	1.91	2.16E-06	2.21E-06
22	1.29E-4	5.17E-4	8.95	981.8	3.20	0.66	1.91	2.14E-06	2.22E-06
24	1.31E-4	5.25E-4	8.87	986.6	3.20	0.66	1.92	2.09E-06	2.05E-06
25	1.32E-4	5.37E-4	8.82	990.1	3.20	0.66	1.92	2.03E-06	1.97E-06
26	1.36E-4	5.45E-4	8.79	991.5	3.20	0.66	1.92	1.98E-06	1.97E-06
27	1.37E-4	5.51E-4	8.72	993.7	3.20	0.66	1.91	1.95E-06	1.87E-06
28	1.40E-4	5.57E-4	8.71	998.7	3.21	0.66	1.97	1.92E-06	1.87E-06
29	1.44E-4	5.62E-4	8.63	999.7	3.21	0.66	1.92	1.89E-06	1.79E-06
30	1.49E-4	5.66E-4	8.56	1003.9	3.20	0.66	1.92	1.86E-06	1.74E-06
31	1.52E-4	5.76E-4	8.52	1002.8	3.19	0.66	1.92	1.81E-06	1.70E-06
32	1.56E-4	5.83E-4	8.46	1007.9	3.20	0.66	1.92	1.77E-06	1.65E-06
33	1.62E-4	5.90E-4	8.42	1008.5	3.19	0.66	1.92	1.73E-06	1.65E-06
34	1.63E-4	5.94E-4	8.35	1008.3	3.20	0.66	1.92	1.70E-06	1.56E-06
35	1.70E-4	6.03E-4	8.33	1014.9	3.20	0.66	1.92	1.65E-06	1.59E-06
36	1.73E-4	6.12E-4	8.27	1018.5	3.20	0.66	1.89	1.60E-06	1.53E-06
37	1.77E-4	6.19E-4	8.24	1022.2	3.19	0.66	1.88	1.56E-06	1.51E-06
38	1.83E-4	6.28E-4	8.20	1026.5	3.20	0.66	1.89	1.52E-06	1.51E-06
39	1.87E-4	6.36E-4	8.16	1029.3	3.19	0.66	1.92	1.47E-06	1.48E-06
40	1.88E-4	6.50E-4	8.11	1031.2	3.20	0.66	1.89		
41	1.93E-4	6.58E-4	8.07	1035.2	3.20	0.66	1.92		
42	1.95E-4	6.62E-4	8.01	1035.1	3.19	0.66	1.91		
43	1.94E-4	6.70E-4	7.97	1038.3	3.19	0.66	1.92		

44	1.99E-4	6.78E-4	7.97	1040.6	3.20	0.66	1.92		
45	2.03E-4	6.87E-4	7.93	1040.8	3.20	0.66	1.94		
46	2.08E-4	6.94E-4	7.90	1042.3	3.20	0.66	1.96		
47	2.12E-4	7.02E-4	7.88	1048.1	3.20	0.66	1.94		
48	2.14E-4	7.11E-4	7.84	1046.2	3.20	0.66	1.92		
49	2.17E-4	7.17E-4	7.80	1051.1	3.20	0.66	1.93		
50	2.20E-4	7.24E-4	7.77	1052.9	3.20	0.66	1.97		
51	2.22E-4	7.29E-4	7.77	1056.0	3.20	0.66	1.94		
53	2.28E-4	7.44E-4	7.73	1057.5	3.20	0.66	1.93		
54	2.29E-4	7.48E-4	7.68	1053.0	3.20	0.66	1.96		
55	2.31E-4	7.50E-4	7.69	1055.1	3.20	0.66	1.96		
56	2.32E-4	7.57E-4	7.71	1057.1	3.20	0.66	1.96		
57	2.33E-4	7.62E-4	7.67	1055.6	3.20	0.66	1.96		
58	2.34E-4	7.65E-4	7.67	1059.3	3.20	0.66	1.99		
59	2.31E-4	7.66E-4	7.65	1045.0	3.20	0.66	1.95		
60	2.42E-4	7.68E-4	7.65	1061.3	3.20	0.66	1.97		
61	2.39E-4	7.69E-4	7.65	1051.7	3.20	0.66	1.97		

WORKSHEET RUN 7

RESULTS									
Time (min)	$[O_3]_l$ (mol/L)	$[O_3]_g$ (mol/L)	pH	ORP (mV)	Gas flow (L/min)	Jg (cm/s)	Holdup (%)	Ozone decomposition	
								Measured rate (mol L^{-1} s^{-1})	Calculated rate (mol L^{-1} s^{-1})
0	0.00	0.00	7.18	380.1	0.00	0.00	0.00		
1	6.32E-5	2.71E-4	7.03	1033.0	3.17	0.65	2.12		
2	1.11E-4	3.99E-4	6.96	1066.7	3.20	0.66	2.07	4.31E-07	
3	1.33E-4	4.53E-4	6.85	1076.8	3.21	0.66	2.01	2.56E-07	
4	1.44E-4	4.86E-4	6.78	1082.0	3.20	0.66	2.00	2.03E-07	
5	1.50E-4	5.04E-4	6.73	1082.3	3.20	0.66	2.00	2.24E-07	
6	1.54E-4	5.07E-4	6.68	1085.3	3.20	0.66	1.97	2.34E-07	
7	1.54E-4	5.11E-4	6.64	1088.5	3.20	0.66	1.97	2.34E-07	
8									
9	1.57E-4	5.11E-4	6.61	1088.2	3.20	0.66	1.93		
10	1.59E-4	5.12E-4	6.59	1092.3	3.20	0.66	1.91		
11	1.58E-4	5.12E-4	6.56	1089.8	3.20	0.66	1.88		
12	1.58E-4	5.12E-4	6.56	1091.5	3.20	0.66	1.87		
13	1.57E-4	5.11E-4	6.52	1092.6	3.20	0.66	1.92		
14	1.57E-4	5.09E-4	6.53	1093.6	3.21	0.66	1.91		
15	1.57E-4	5.07E-4	6.50	1091.4	3.21	0.66	1.91		
16	1.58E-4	5.05E-4	6.50	1093.0	3.20	0.66	1.91		

17	1.57E-4	5.04E-4	6.51	1095.0	3.21	0.66	1.91		
18	1.57E-4	5.04E-4	6.49	1093.6	3.21	0.66	1.89		
19	1.56E-4	5.07E-4	6.48	1093.6	3.21	0.66	1.91		
20	1.57E-4	5.09E-4	6.46	1093.6	3.20	0.66	1.86		
21	1.57E-4	5.10E-4	6.46	1094.9	3.20	0.66	1.88		
22	1.57E-4	5.09E4	6.47	1094.7	3.20	0.66	1.88		
23	1.57E-4	5.08E-4	6.45	1094.1	3.20	0.66	1.89		
24									
25	1.57E-4	5.07E-4	6.44	1092.9	3.20	0.66	1.93		
26	1.57E-4	5.06E-4	6.45	1094.8	3.20	0.66	1.93		
27	1.57E-4	5.06E-4	6.45	1095.1	3.20	0.66	1.88		
28	1.57E-4	5.08E-4	6.44	1095.8	3.20	0.66	1.88		
29	1.56E-4	5.09E-4	6.45	1094.0	3.20	0.66	1.88		
30	1.57E-4	5.07E-4	6.43	1093.8	3.20	0.66	1.88		
31	1.57E-4	5.07E-4	6.41	1094.3	3.20	0.66	1.84		
32	1.57E-4	5.06E-4	6.43	1091.9	3.20	0.66	1.90		
33	1.57E-4	5.07E-4	6.42	1091.5	3.20	0.66	1.84		
34	1.57E-4	5.06E-4	6.45	1092.9	3.20	0.66	1.88		
35	1.57E-4	5.10E-4	6.44	1093.1	3.20	0.66	1.89		
36	1.56E-4	5.07E-4	6.43	1094.6	3.20	0.66	1.88		
37	1.57E-4	5.04E-4	6.43	1093.5	3.20	0.66	1.91		
38	1.56E-4	5.03E-4	6.42	1093.6	3.20	0.66	1.90		
39	1.57E-4	5.05E-4	6.43	1092.7	3.20	0.66	1.87		
40									
41	1.57E-4	4.97E-4	6.44	1092.2	3.20	0.66	1.98		
42	1.57E-4	4.98E-4	6.41	1091.1	3.20	0.66	1.91		
43	1.57E-4	5.01E-4	6.43	1090.9	3.20	0.66	1.88		

WORKSHEET RUN 8

RESULTS									
Time (min)	$[O_3]_l$ (mol/L)	$[O_3]_g$ (mol/L)	pH	ORP (mV)	Gas flow (L/min)	Jg (cm/s)	Holdup (%)	Ozone decomposition	
								Measured rate (mol L^{-1} s^{-1})	Calculated rate (mol L^{-1} s^{-1})
0	0.00	0.00	9.86	258.2	0.00	0.00	0.00		
1	2.40E-5	2.05E-4	9.74	879.3	3.11	0.64	1.99		
2	3.83E-5	2.57E-4	9.63	911.7	3.19	0.66	1.96		
3	4.41E-5	2.64E-4	9.59	921.1	3.20	0.66	2.02		
4	4.85E-5	2.70E-4	9.50	925.8	3.20	0.66	1.98		
5	5.22E-5	2.80E-4	9.47	931.5	3.20	0.66	2.03		
6	5.44E-5	2.87E-4	9.42	929.3	3.20	0.66	1.97		
7	5.88E-5	2.97E-4	9.38	930.9	3.21	0.66	1.99		
8	6.08E-5	3.01E-4	9.33	937.0	3.20	0.66	2.02		
9	6.19E-5	3.03E-4	9.30	940.0	3.20	0.66	2.03	1.30E-06	1.25E-06
10	6.49E-5	3.07E-4	9.24	939.3	3.19	0.66	2.08	1.28E-06	1.25E-06
11	6.64E-5	3.08E-4	9.23	946.1	3.20	0.66	2.08	1.28E-06	1.27E-06
12	6.77E-5	3.13E-4	9.17	946.7	3.20	0.66	2.03	1.25E-06	1.23E-06
13	6.92E-5	3.17E-4	9.12	947.4	3.21	0.66	2.07	1.23E-06	1.20E-06
14	7.17E-5	3.22E-4	9.08	947.1	3.20	0.66	2.01	1.20E-06	1.20E-06
15	7.37E-5	3.25E-4	9.06	945.7	3.20	0.66	2.03	1.19E-06	1.22E-06
16	7.53E-5	3.26E-4	9.05	950.9	3.20	0.66	1.99	1.18E-06	1.24E-06

17	7.62E-5	3.29E-4	8.97	958.1	3.21	0.66	2.04	1.17E-06	1.16E-06
18	7.81E-5	3.32E-4	8.95	958.1	3.20	0.66	1.97	1.14E-06	1.18E-06
19	7.86E-5	3.34E-4	8.91	952.6	3.19	0.66	1.99	1.13E-06	1.14E-06
20	7.97E-5	3.37E-4	8.87	964.4	3.19	0.66	2.00	1.12E-06	1.11E-06
21	8.22E-5	3.42E-4	8.82	963.8	3.20	0.66	1.98	1.09E-06	1.10E-06
22	8.56E-5	3.48E-4	8.79	961.0	3.20	0.66	1.94	1.06E-06	1.12E-06
23	8.52E-5	3.49E-4	8.74	967.5	3.20	0.66	1.96	1.05E-06	1.06E-06
24	8.76E-5	3.52E-4	8.72	961.0	3.20	0.66	1.94	1.04E-06	1.07E-06
25	8.71E-5	3.54E-4	8.68	967.1	3.21	0.66	1.92	1.03E-06	1.03E-06
26	8.89E-5	3.58E-4	8.63	969.4	3.20	0.66	1.90	1.00E-06	1.01E-06
27	9.26E-5	3.61E-4	8.58	975.4	3.20	0.66	1.96	9.86E-07	1.01E-06
28	9.24E-5	3.65E-4	8.54	977.0	3.20	0.66	2.00	9.67E-07	9.69E-07
29	9.50E-5	3.67E-4	8.51	980.6	3.20	0.66	1.96	9.55E-07	9.66E-07
30	9.60E-5	3.68E-4	8.48	983.5	3.20	0.66	1.99	9.51E-07	9.54E-07
31	9.86E-5	3.73E-4	8.40	984.9	3.20	0.66	2.01	9.20E-07	9.13E-07
32	1.01E-4	3.77E-4	8.34	985.0	3.20	0.66	2.01	8.97E-07	8.76E-07
33	1.02E-4	3.81E-4	8.29	983.7	3.20	0.66	1.99	8.76E-07	8.48E-07
34	1.04E-4	3.87E-4	8.27	992.1	3.20	0.66	1.95	8.47E-07	8.56E-07
35	1.06E-4	3.91E-0	8.22	988.1	3.21	0.66	1.96	8.23E-07	8.29E-07
36	1.09E-4	3.94E-4	8.16	996.0	3.20	0.66	2.01	8.08E-07	8.13E-07
37	1.11E-4	3.96E-4	8.14	999.7	3.20	0.66	1.95		
38	1.12E-4	4.00E-4	8.10	1002.0	3.20	0.66	1.96		
39	1.15E-4	4.05E-4	8.04	1003.2	3.20	0.66	1.96		
40	1.18E-4	4.10E-4	7.99	1005.1	3.20	0.66	2.01		
41	1.20E-4	4.16E-4	7.97	1011.7	3.20	0.66	1.99		
42	1.21E-4	4.19E-4	7.91	1013.8	3.20	0.66	1.96		
43	1.23E-4	4.24E-4	7.88	1017.8	3.20	0.66	1.97		

44	1.25E-4	4.26E-4	7.84	1017.3	3.20	0.66	1.99		
45	1.28E-4	4.32E-4	7.81	1023.9	3.20	0.66	1.97		
46	1.30E-4	4.36E-4	7.77	1023.2	3.20	0.66	1.97		
47	1.30E-4	4.37E-4	7.75	1027.1	3.20	0.66	1.97		
48	1.32E-4	4.39E-4	7.73	1031.3	3.20	0.66	1.97		
49	1.34E-4	4.42E-4	7.71	1029.9	3.20	0.66	1.93		
50	1.35E-4	4.46E-4	7.68	1030.0	3.20	0.66	1.97		
51	1.37E-4	4.49E-4	7.67	1035.3	3.20	0.66	1.97		
52	1.37E-4	4.53E-4	7.65	1030.8	3.20	0.66	2.01		
53	1.39E-4	4.55E-4	7.62	1035.0	3.20	0.66	1.97		
54	1.39E-4	4.56E-4	7.62	1038.7	3.20	0.66	1.97		
55	1.40E-4	4.58E-4	7.62	1041.9	3.20	0.66	1.95		
56	1.41E-4	4.61E-4	7.59	1041.4	3.20	0.66	1.98		
57	1.42E-4	4.61E-4	7.59	1039.5	3.20	0.66	2.00		
58	1.43E-4	4.61E-4	7.57	1039.8	3.20	0.66	2.05		
59	1.41E-4	4.62E-4	7.56	1040.9	3.20	0.66	2.04		
60	1.44E-4	4.62E-4	7.56	1042.8	3.20	0.66	2.05		
61	1.46E-4	4.65E-4	7.54	1047.5	3.20	0.66	2.05		
62	1.44E-4	4.64E-4	7.54	1043.0	3.20	0.66	1.99		

NICKEL PRECIPITATION TESTS

WORKSHEET RUN 1

Time (min)	$[O_3]_l$ (mol/L)	$[O_3]_g$ (mol/L)	[Ni] (mol/L)	Gas flow (L/min)	Jg (cm/s)	Holdup (%)
0.0	0.00	0.00	0.0218	0.00	0.00	0.00
0.5	3.56E-5	1.21E-4		2.79	0.57	0.89
1.1	8.04E-5	2.77E-4		2.82	0.58	0.93
1.6	1.06E-4	3.57E-4		2.83	0.58	0.93
2.1	1.22E-4	4.10E-4		2.84	0.58	0.89
2.7	1.33E-4	4.41E-4		2.84	0.58	0.84
3.2	1.39E-4	4.67E-4		2.84	0.58	0.84
3.7	1.46E-4	4.82E-4		2.84	0.58	0.82
4.3	1.48E-4	4.89E-4	0.0201	2.86	0.59	0.79
4.8	1.48E-4	4.94E-4		2.85	0.59	0.77
5.3	1.46E-4	4.96E-4		2.86	0.59	0.76
5.9	1.48E-4	4.99E-4		2.86	0.59	0.78
6.4	1.48E-4	4.98E-4		2.86	0.59	0.78
6.9	1.46E-4	4.96E-4	0.0201	2.86	0.59	0.78
7.5	1.43E-4	4.93E-4		2.87	0.59	0.78
8.0	1.41E-4	4.89E-4		2.87	0.59	0.78
8.5	1.39E-4	4.83E-4		2.87	0.59	0.76
9.1	1.36E-4	4.77E-4		2.87	0.59	0.78
9.6	1.31E-4	4.68E-4		2.87	0.59	0.75
10.1	1.26E-4	4.59E-4	0.0197	2.88	0.59	0.76
10.7	1.22E-4	4.53E-4		2.88	0.59	0.78
11.2	1.22E-4	4.45E-4		2.87	0.59	0.77
11.7	1.18E-4	4.36E-4		2.88	0.59	0.77
12.3	1.12E-4	4.25E-4		2.88	0.59	0.76
12.8	1.08E-4	4.20E-4		2.88	0.59	0.76
13.3	1.07E-4	4.12E-4	0.0195	2.89	0.59	0.71
13.9	1.04E-4	4.06E-4		2.89	0.59	0.75
14.4	1.02E-4	4.02E-4		2.89	0.59	0.76
14.9	1.00E-4	3.92E-4		2.89	0.59	0.73
15.5	9.64E-5	3.87E-4		2.89	0.59	0.73
16.0	9.32E-5	3.70E-4	0.0193	2.90	0.60	0.73
16.5	9.02E-5	3.61E-4		2.90	0.60	0.79
17.1	8.81E-5	3.52E-4		2.90	0.60	0.79
17.6	8.16E-5	3.45E-4		2.89	0.60	0.77
18.1	7.97E-5	3.36E-4		2.89	0.60	0.71

18.7	7.66E-5	3.31E-4		2.89	0.60	0.75
19.2	7.30E-5	3.26E-4		2.89	0.60	0.78
19.7	6.95E-5	3.22E-4		2.89	0.60	0.79
20.3	6.74E-5	3.15E-4	0.0192	2.91	0.60	0.76
20.8	6.32E-5	3.07E-4		2.90	0.60	0.76
21.3	5.85E-5	3.00E-4		2.90	0.60	0.77
21.9	5.54E-5	2.94E-4		2.90	0.60	0.76
22.4	5.28E-5	2.89E-4		2.90	0.60	0.77
22.9	5.16E-5	2.84E-4		2.90	0.60	0.75
23.5	5.13E-5	2.80E-4	0.0191	2.90	0.60	0.77

WORKSHEET RUN 2

Time (min)	$[O_3]_l$ (mol/L)	$[O_3]_g$ (mol/L)	[Ni] (mol/L)	Gas flow (L/min)	Jg (cm/s)	Holdup (%)
0.0	0.00	0.00	0.0184	0.00	0.00	0.00
0.5	3.22E-5	5.00E-5		2.63	0.54	0.86
1.1	6.85E-5	2.20E-4		2.67	0.55	0.90
1.6	9.70E-5	3.14E-4		2.67	0.55	0.87
2.1	1.16E-4	3.82E-4		2.68	0.55	0.83
2.7	1.29E-4	4.29E-4		2.68	0.55	0.77
3.2	1.32E-4	4.41E-4	0.0179	2.70	0.56	0.72
3.7	1.27E-4	4.43E-4		2.69	0.55	0.72
4.3	1.21E-4	4.42E-4		2.70	0.56	0.69
4.8	1.18E-4	4.35E-4	0.0177	2.70	0.56	0.69
5.3	1.12E-4	4.23E-4		2.71	0.56	0.69
5.9	1.02E-4	4.10E-4		2.71	0.56	0.68
6.4	9.50E-5	3.92E-4		2.71	0.56	0.68
6.9	8.68E-5	3.73E-4	0.0176	2.71	0.56	0.69
7.5	8.31E-5	3.64E-4		2.72	0.56	0.70
8.0	7.84E-5	3.55E-4		2.71	0.56	0.67
8.5	7.10E-5	3.37E-4		2.71	0.56	0.69
9.1	6.70E-5	3.29E-4	0.0174	2.72	0.56	0.69
9.6	6.03E-5	3.24E-4		2.72	0.56	0.69
10.1	5.81E-5	3.09E-4		2.72	0.56	0.71
10.7	5.62E-5	3.00E-4		2.72	0.56	0.72
11.2	5.00E-5	2.91E-4		2.72	0.56	0.72
11.7	4.62E-5	2.75E-4		2.72	0.56	0.74
12.3	4.15E-5	2.71E-4		2.71	0.56	0.74
12.8	3.94E-5	2.59E-4	0.0168	2.72	0.56	0.74
13.3	3.55E-5	2.53E-4		2.72	0.56	0.69
13.9	3.32E-5	2.44E-4		2.72	0.56	0.75
14.4	3.08E-5	2.40E-4		2.72	0.56	0.74
14.9	2.95E-5	2.36E-4	0.0164	2.72	0.56	0.72
15.5	2.80E-5	2.28E-4		2.73	0.56	0.71
16.0	2.54E-5	2.24E-4		2.73	0.56	0.70
16.5	2.39E-5	2.21E-4		2.73	0.56	0.70
17.1	2.28E-5	2.18E-4		2.73	0.56	0.71
17.6	2.19E-5	2.15E-4		2.73	0.56	0.72
18.1	2.15E-5	2.13E-4		2.73	0.56	0.74
18.7	2.10E-5	2.11E-4		2.72	0.56	0.72
19.2	2.02E-5	2.09E-4	0.0157	2.73	0.56	0.74
19.7	1.99E-5	2.07E-4		2.73	0.56	0.73

20.3	1.92E-5	2.04E-4		2.73	0.56	0.74
20.8	1.89E-5	2.02E-4		2.73	0.56	0.70
21.3	1.76E-5	1.97E-4		2.73	0.56	0.69
21.9	1.65E-5	1.95E-4		2.73	0.56	0.69
22.4	1.52E-5	1.92E-4		2.73	0.56	0.66
22.9	1.43E-5	1.90E-4	0.0152	2.73	0.56	0.66
23.5	1.26E-5	1.88E-4	0.0149	2.74	0.56	0.74

WORKSHEET RUN 3

Time (min)	$[O_3]_l$ (mol/L)	$[O_3]_g$ (mol/L)	[Ni] (mol/L)	Gas flow (L/min)	Jg (cm/s)	Holdup (%)
0.0	0.00	0.00	0.0169	0.00	0.00	0.00
0.5	2.98E-5	3.69E-5		2.67	0.55	0.70
1.1	6.57E-5	9.58E-5		2.69	0.55	0.81
1.6	8.56E-5	2.46E-4		2.71	0.56	0.77
2.1	7.82E-5	3.14E-4	0.0166	2.71	0.56	0.75
2.7	5.70E-5	3.45E-4		2.72	0.56	0.71
3.2	4.44E-5	3.35E-4		2.72	0.56	0.67
3.7	3.27E-5	3.24E-4		2.72	0.56	0.68
4.3	2.95E-5	3.01E-4		2.72	0.56	0.72
4.8	2.35E-5	2.79E-4	0.0165	2.72	0.56	0.70
5.3	1.93E-5	2.50E-4		2.73	0.56	0.69
5.9	1.65E-5	2.36E-4		2.73	0.56	0.72
6.4	1.36E-5	2.17E-4		2.73	0.56	0.72
6.9	1.06E-5	2.11E-4	0.0154	2.73	0.56	0.73
7.5	8.92E-6	2.00E-4		2.74	0.56	0.71
8.0	7.97E-6	1.96E-4		2.74	0.56	0.69
8.5	7.03E-6	1.89E-4		2.73	0.56	0.70
9.1	6.21E-6	1.80E-4	0.0153	2.73	0.56	0.68
9.6	5.85E-6	1.80E-4		2.74	0.56	0.68
10.1	6.09E-6	1.75E-4		2.74	0.56	0.73
10.7	4.88E-6	1.70E-4		2.74	0.56	0.70
11.2	3.96E-6	1.69E-4	0.0144	2.75	0.57	0.70
11.7	3.80E-6	1.65E-4		2.75	0.56	0.73
12.3	3.79E-6	1.65E-4		2.74	0.56	0.72
12.8	3.73E-6	1.64E-4	0.0139	2.74	0.56	0.72
13.3	3.28E-6	1.61E-4		2.76	0.57	0.73
13.9	3.27E-6	1.60E-4		2.75	0.57	0.75
14.4	3.31E-6	1.59E-4		2.75	0.57	0.73
14.9	2.94E-6	1.59E-4	0.0134	2.75	0.57	0.72
15.5	2.81E-6	1.58E-4		2.76	0.57	0.69
16.0	2.56E-6	1.58E-4		2.76	0.57	0.68
16.5	2.38E-6	1.58E-4		2.76	0.57	0.69
17.1	2.25E-6	1.58E-4		2.75	0.57	0.69
17.6	2.18E-6	1.57E-4		2.75	0.57	0.70
18.1	2.11E-6	1.57E-4		2.75	0.57	0.73
18.7	2.11E-6	1.56E-4		2.75	0.57	0.74
19.2	1.72E-6	1.54E-4		2.75	0.57	0.74
19.7	1.96E-6	1.55E-4		2.75	0.57	0.72

20.3	1.92E-6	1.54E-4	0.0120	2.76	0.57	0.75
20.8	1.54E-6	1.55E-4		2.75	0.57	0.74
21.3	1.54E-6	1.53E-4		2.75	0.57	0.69
21.9	1.44E-6	1.52E-4		2.75	0.57	0.72
22.4	1.21E-6	1.43E-4		2.76	0.57	0.72
22.9	1.31E-6	1.46E-4		2.75	0.57	0.71
23.5	1.30E-6	1.44E-4	0.0107	2.75	0.57	0.70

WORKSHEET RUN 4

Time (min)	$[O_3]_l$ (mol/L)	$[O_3]_g$ (mol/L)	ORP (mV)	Gas flow (L/min)	Jg (cm/s)	Holdup (%)
0.00	0.00	0.00	426.1	0.00	0.00	0.00
0.53	2.44E-5	2.00E-5	739.2	3.12	0.64	1.99
1.07	6.94E-5	1.00E-4	991.4	3.15	0.65	1.96
1.47	9.76E-5	2.36E-4	1034.6	3.18	0.65	2.02
2.00	1.23E-4	3.66E-4	1060.1	3.19	0.66	1.98
2.53	1.37E-4	4.30E-4	1069.5	3.20	0.66	2.03
3.07	1.46E-4	4.57E-4	1075.1	3.20	0.66	1.97
3.47	1.50E-4	4.76E-4	1077.9	3.20	0.66	1.99
4.00	1.56E-4	4.88E-4	1082.2	3.20	0.66	2.02
4.53	1.58E-4	5.09E-4	1097.7	3.20	0.66	2.03
5.07	1.62E-4	5.14E-4	1087.5	3.20	0.66	2.08
5.47	1.64E-4	5.20E-4	1088.2	3.21	0.66	2.08
6.00	1.67E-4	5.26E-4	1115.3	3.20	0.66	2.03
6.53	1.66E-4	5.30E-4	1089.9	3.20	0.66	2.07
7.07	1.67E-4	5.35E-4	1092.3	3.21	0.66	2.01
7.47	1.69E-4	5.35E-4	1091.3	3.20	0.66	2.02
8.00	1.69E-4	5.37E-4	1093.7	3.21	0.66	1.99
8.53	1.70E-4	5.39E-4	1095.8	3.21	0.66	1.96
9.07	1.71E-4	5.42E-4	1109.1	3.21	0.66	2.02
9.47	1.72E-4	5.44E-4	1110.6	3.21	0.66	1.98
10.00	1.73E-4	5.44E-4	1098.1	3.21	0.66	2.03
10.53	1.72E-4	5.45E-4	1097.0	3.21	0.66	1.97
11.07	1.74E-4	5.44E-4	1099.2	3.21	0.66	1.99
11.47	1.73E-4	5.45E-4	1100.1	3.21	0.66	2.02
12.00	1.73E-4	5.49E-4	1100.3	3.21	0.66	2.03
12.53	1.73E-4	5.49E-4	1100.4	3.21	0.66	2.08
13.07	1.72E-4	5.49E-4	1099.1	3.20	0.66	2.08
13.47	1.74E-4	5.48E-4	1115.6	3.20	0.66	2.03
14.00	1.73E-4	5.49E-4	1103.4	3.20	0.66	2.07
14.53	1.74E-4	5.49E-4	1115.7	3.20	0.66	2.01
15.07	1.74E-4	5.49E-4	1104.3	3.20	0.66	2.00

WORKSHEET RUN 5

Time (min)	$[O_3]_l$ (mol/L)	$[O_3]_g$ (mol/L)	ORP (mV)	Gas flow (L/min)	Jg (cm/s)	Holdup (%)
0.00	0.00	0.00	465.5	0.00	0.00	0.00
0.53	1.53E-5	1.34E-4	787.2	3.13	0.64	1.99
1.07	6.28E-5	3.10E-4	1040.9	3.16	0.65	1.96
1.47	9.23E-5	3.74E-4	1076.0	3.19	0.66	2.02
2.00	1.21E-4	4.33E-4	1095.2	3.19	0.66	1.98
2.53	1.38E-4	4.66E-4	1101.3	3.20	0.66	2.03
3.07	1.50E-4	4.94E-4	1105.2	3.21	0.66	1.97
3.47	1.57E-4	5.08E-4	1107.2	3.21	0.66	1.99
4.00	1.65E-4	5.21E-4	1107.9	3.21	0.66	2.02
4.53	1.68E-4	5.26E-4	1107.7	3.21	0.66	2.03
5.07	1.68E-4	5.32E-4	1107.9	3.20	0.66	2.08
5.47	1.70E-4	5.35E-4	1106.4	3.20	0.66	2.08
6.00	1.71E-4	5.37E-4	1107.8	3.20	0.66	2.03
6.53	1.72E-4	5.39E-4	1106.4	3.20	0.66	2.07
7.07	1.72E-4	5.40E-4	1106.8	3.21	0.66	2.01
7.47	1.73E-4	5.40E-4	1108.1	3.20	0.66	2.03
8.00	1.73E-4	5.40E-4	1105.9	3.21	0.66	1.99
8.53	1.72E-4	5.39E-4	1105.8	3.19	0.66	1.96
9.07	1.72E-4	5.40E-4	1106.1	3.20	0.66	2.02
9.47	1.71E-4	5.38E-4	1106.5	3.20	0.66	1.98
10.00	1.72E-4	5.39E-4	1106.5	3.20	0.66	2.03
10.53	1.72E-4	5.39E-4	1117.2	3.20	0.66	1.97
11.07	1.72E-4	5.40E-4	1106.2	3.20	0.66	1.99
11.47	1.72E-4	5.40E-4	1118.7	3.20	0.66	2.02
12.00	1.72E-4	5.40E-4	1107.9	3.20	0.66	2.03
12.53	1.73E-4	5.40E-4	1108.0	3.20	0.66	2.08
13.07	1.73E-4	5.40E-4	1108.4	3.20	0.66	2.08
13.47	1.73E-4	5.40E-4	1106.7	3.20	0.66	2.03
14.00	1.74E-4	5.41E-4	1120.0	3.20	0.66	2.07
14.53	1.73E-4	5.42E-4	1120.2	3.20	0.66	2.01
15.07	1.75E-4	4.74E-4	1108.1	3.21	0.66	2.00

WORKSHEET RUN 6

Time (min)	$[O_3]_l$ (mol/L)	$[O_3]_g$ (mol/L)	ORP (mV)	Gas flow (L/min)	Jg (cm/s)	Holdup (%)
0.00	0.00	0.00	551.9	0.00	0.00	0.00
0.53	1.07E-5	1.33E-4	894.0	3.13	0.64	1.99
1.07	4.78E-5	3.07E-4	1088.3	3.16	0.65	1.96
1.47	7.34E-5	3.78E-4	1102.7	3.18	0.65	2.02
2.00	1.06E-4	4.25E-4	1145.2	3.20	0.66	1.98
2.53	1.30E-4	4.61E-4	1126.3	3.20	0.66	2.03
3.07	1.44E-4	4.89E-4	1128.0	3.20	0.66	1.97
3.47	1.51E-4	5.02E-4	1128.8	3.20	0.66	1.99
4.00	1.62E-4	5.19E-4	1130.7	3.20	0.66	2.01
4.53	1.66E-4	5.33E-4	1130.3	3.20	0.66	2.00
5.07	1.70E-4	5.41E-4	1129.9	3.21	0.66	2.03
5.47	1.74E-4	5.46E-4	1129.2	3.20	0.66	2.04
6.00	1.77E-4	5.52E-4	1130.4	3.20	0.66	2.03
6.53	1.78E-4	5.53E-4	1129.1	3.21	0.66	2.01
7.07	1.79E-4	5.54E-4	1128.1	3.21	0.66	2.01
7.47	1.80E-4	5.54E-4	1141.6	3.21	0.66	2.03
8.00	1.81E-4	5.55E-4	1126.6	3.21	0.66	200
8.53	1.80E-4	5.54E-4	1153.4	3.21	0.66	1.96
9.07	1.80E-4	5.55E-4	1128.0	3.21	0.66	2.02
9.47	1.79E-4	5.55E-4	1138.8	3.21	0.66	1.99
10.00	1.80E-4	5.54E-4	1151.9	3.21	0.66	2.03
10.53	1.79E-4	5.54E-4	1127.9	3.21	0.66	1.99
11.07	1.79E-4	5.54E-4	1125.4	3.20	0.66	1.99
11.47	1.81E-4	5.55E-4	1124.9	3.20	0.66	2.02
12.00	1.81E-4	5.54E-4	1125.7	3.20	0.66	2.03
12.53	1.79E-4	5.54E-4	1127.8	3.20	0.66	2.08
13.07	1.79E-4	5.53E-4	1127.1	3.20	0.66	2.08
13.47	1.79E-4	5.54E-4	1126.4	3.21	0.66	2.03
14.00	1.81E-4	5.54E-4	1153.5	3.21	0.66	2.07
14.53	1.81E-4	5.55E-4	1139.9	3.21	0.66	2.01
15.07	1.79E-4	5.39E-4	1140.8	3.20	0.66	2.00

WORKSHEET RUN 7

Time (min)	$[O_3]_l$ (mol/L)	$[O_3]_g$ (mol/L)	[Ni] (mol/L)	O_3 oxidation rate (mol/min	ORP (mV)	Gas flow (L/min)	Jg (cm/s)	Holdup (%)
0.00	0.00	0.00	1.084E-2		716.3	0.00	0.00	0.00
3.20	1.14E-4	3.89E-4	1.082E-2		814.5	3.27	0.67	1.88
6.40	8.67E-5	3.52E-4	1.080E-2	5.499E-4	894.8	3.26	0.67	1.79
9.07	6.40E-5	3.06E-4	1.076E-2	7.205E-4	939.3	3.26	0.67	1.76
12.27	3.61E-5	2.48E-4	9.870E-3	9.387E-4	1003.7	3.28	0.67	1.71
14.93	2.67E-5	2.23E-4	9.401E-3	1.032E-3	1068.0	3.24	0.67	1.75
18.13	2.03E-5	2.07E-4	8.603E-3	1.116E-3	1040.7	3.27	0.67	1.70
21.33	1.44E-5	1.92E-4	8.060E-3	1.170E-3	1021.6	3.26	0.67	1.73
24.00	1.42E-5	1.87E-4	7.485E-3	1.179E-3	1011.7	3.23	0.67	1.71
27.20	1.00E-5	1.80E-4	6.955E-3	1.214E-3	992.8	3.27	0.67	1.70
30.40	9.02E-6	1.77E-4	6.439E-3	1.216E-3	974.7	3.24	0.67	1.71
33.07	7.62E-6	1.74E-4	5.958E-3	1.232E-3	972.9	3.25	0.67	1.69
36.27	6.73E-6	1.72E-4	5.511E-3	1.236E-3	966.1	3.24	0.67	1.70
38.93	6.33E-6	1.72E-4	5.004E-3	1.231E-3	958.3	3.23	0.66	1.71
42.13	5.89E-6	1.72E-4	4.706E-3	1.244E-3	948.4	3.26	0.67	1.75
45.33	5.77E-6	1.71E-4	4.369E-3	1.243E-3	940.2	3.24	0.67	1.72

WORKSHEET RUN 8

Time (min)	$[O_3]_l$ (mol/L)	$[O_3]_g$ (mol/L)	[Ni] (mol/L)	O_3 oxidation rate (mol/min)	ORP (mV)	Gas flow (L/min)	Jg (cm/s)	Holdup (%)
0.00	0.00	0.00	1.069E-2		813.4	0.00	0.00	0.00
3.20	1.62E-4	5.57E-4	1.023E-2		1160.4	3.27	0.67	1.76
6.40	8.64E-5	4.21E-4	1.010E-2	1.177E-3	1148.0	3.28	0.68	1.71
9.07	6.09E-5	3.68E-4	9.210E-3	1.329E-3	1129.9	3.25	0.67	1.72
12.27	4.01E-5	3.11E-4	8.496E-3	1.501E-3	1100.8	3.25	0.67	1.71
14.93	3.51E-5	2.96E-4	7.549E-3	1.527E-3	1074.9	3.23	0.66	1.74
18.13	2.61E-5	2.79E-4	7.091E-3	1.573E-3	1068.6	3.25	0.67	1.71
21.33	2.00E-5	2.59E-4	6.505E-3	1.617E-3	1037.4	3.21	0.66	1.70
24.00	1.55E-5	2.48E-4	5.909E-3	1.649E-3	1006.0	3.20	0.66	1.69
27.20	1.27E-5	2.36E-4	5.213E-3	1.690E-3	997.9	3.21	0.66	1.72
30.40	9.02E-6	2.31E-4	4.616E-3	1.687E-3	987.4	3.18	0.65	1.69
33.07	7.47E-6	2.30E-4	4.088E-3	1.686E-3	961.2	3.17	0.65	1.70
36.27	7.49E-6	2.28E-4	3.935E-3	1.686E-3	953.5	3.16	0.65	1.68
38.93	5.72E-6	2.23E-4	3.437E-3	1.700E-3	936.8	3.16	0.65	1.63
42.13	4.92E-6	2.22E-4	3.215E-3	1.703E-3	913.4	3.16	0.65	1.69
45.33	4.38E-6	2.22E-4	3.049E-3	1.708E-3	918.7	3.17	0.65	1.70
48.00	4.31E-6	2.19E-4	2.755E-3	1.711E-3	916.6	3.17	0.65	1.68

WORKSHEET RUN 9

Time (min)	$[O_3]_l$ (mol/L)	$[O_3]_g$ (mol/L)	[Ni] (mol/L)	O_3 oxidation rate (mol/min)	ORP (mV)	Gas flow (L/min)	Jg (cm/s)	Holdup (%)
0.00	0.00	0.00	1.108E-2		793.4	0.00	0.00	0.00
3.20	1.35E-4	5.56E-4	1.052E-2		1162.9	3.30	0.68	1.59
6.40	7.46E-5	4.51E-4	8.901E-3	1.689E-3	1137.6	3.27	0.67	1.52
9.07	4.82E-5	3.89E-4	8.422E-3	1.836E-3	1116.4	3.24	0.67	1.50
12.27	3.27E-5	3.38E-4	7.304E-3	1.944E-3	1087.2	3.23	0.67	1.50
14.93	2.43E-5	3.17E-4	6.761E-3	1.986E-3	1073.7	3.22	0.66	1.46
18.13	2.00E-5	2.99E-4	6.047E-3	2.059E-3	1038.5	3.24	0.67	1.44
21.33	1.84E-5	2.97E-4	5.526E-3	2.060E-3	1023.5	3.23	0.66	1.46
24.00	1.42E-5	2.92E-4	4.695E-3	2.075E-3	1001.3	3.23	0.66	1.46
27.20	9.98E-6	2.84E-4	4.054E-3	2.096E-3	991.3	3.23	0.66	1.50
30.40	7.56E-6	2.86E-4	3.450E-3	2.092E-3	982.9	3.23	0.66	1.48
33.07	6.42E-6	2.87E-4	3.049E-3	2.099E-3	972.9	3.25	0.67	1.53
36.27	5.02E-6	2.80E-4	2.824E-3	2.116E-3	967.4	3.24	0.67	1.50
38.93	4.27E-6	2.77E-4	2.257E-3	2.122E-3	953.1	3.23	0.66	1.49
42.13	3.51E-6	2.77E-4	1.963E-3	2.139E-3	940.9	3.26	0.67	1.53
45.33	3.10E-6	2.77E-4	1.878E-3	2.130E-3	942.1	3.25	0.67	1.49
48.00	3.06E-6	2.66E-4	1.491E-3	2.138E-3	930.5	3.24	0.67	1.52

WORKSHEET RUN 10

Time (min)	$[O_3]_l$ (mol/L)	$[O_3]_g$ (mol/L)	[Ni] (mol/L)	O_3 oxidation rate (mol/min)	ORP (mV)	Gas flow (L/min)	Jg (cm/s)	Holdup (%)
0.00	0.00	0.00	1.936E-3		389.0	0.00	0.00	0.00
3.07	2.21E-4	6.93E-4	1.814E-3		1118.4	3.21	0.66	1.96
6.00	1.44E-4	5.64E-4	1.348E-3	5.246E-4	1137.3	3.19	0.66	1.89
9.07	1.01E-4	4.75E-4	1.161E-3	8.996E-4	1125.5	3.19	0.66	1.87
9.47	9.85E-5	4.66E-4						
12.00	7.79E-5	4.28E-4	9.688E-4	1.113E-3	1108.3	3.20	0.66	1.85
15.07	5.78E-5	3.84E-4	8.333E-4	1.270E-3	1087.6	3.21	0.66	1.89
18.00	4.76E-5	3.70E-4						
19.07	4.10E-5	3.53E-4	6.518E-4	1.379E-3	1063.2	3.22	0.66	1.83
21.07	3.47E-5	3.38E-4	5.309E-4	1.396E-3	1043.0	3.19	0.66	1.79
24.00	3.34E-5	3.43E-4	4.549E-4	1.424E-3	1029.5	3.20	0.66	1.86
27.07	3.01E-5	3.37E-4	3.765E-4	1.452E-3	1013.2	3.22	0.66	1.88
30.00	2.74E-5	3.36E-4	3.137E-4	1.467E-3	1007.7	3.20	0.66	1.81
33.07	2.53E-5	3.34E-4	2.778E-4	1.482E-3	956.3	3.21	0.66	1.82
36.00	2.35E-5	3.29E-4			975.2	3.20	0.66	1.86

WORKSHEET RUN 11

Time (min)	$[O_3]_l$ (mol/L)	$[O_3]_g$ (mol/L)	[Ni] (mol/L)	O_3 oxidation rate (mol/min)	ORP (mV)	Gas flow (L/min)	Jg (cm/s)	Holdup (%)
0.00	0.00	0.00	8.866E-3		575.1	1.53	0.32	0.00
3.07	2.02E-4	6.85E-4	8.830E-3		1146.2	3.20	0.66	1.92
6.00	1.73E-4	6.45E-4	8.486E-3	3.091E-4	1160.3	3.19	0.66	1.81
9.07	1.26E-4	5.29E-4						
9.47	1.19E-4	5.17E-4	8.025E-3	7.560E-4	1154.8	3.19	0.66	1.80
12.00	7.84E-5	4.18E-4	7.799E-3	1.103E-3	1135.9	3.20	0.66	1.76
15.07	6.07E-5	3.80E-4	7.040E-3	1.255E-3	1121.5	3.21	0.66	1.75
18.00	4.53E-5	3.37E-4	6.914E-3	1.415E-3	1101.0	3.20	0.66	1.76
19.07	4.34E-5	3.30E-4						
21.07	3.60E-5	3.17E-4	6.308E-3	1.507E-3	1087.6	3.20	0.66	1.77
24.00	2.88E-5	3.04E-4	5.793E-3	1.558E-3	1046.6	3.20	0.66	1.74
27.07	2.39E-5	2.85E-4		1.622E-3	1041.6	3.20	0.66	1.77
30.00	2.15E-5	2.82E-4	5.235E-3	1.632E-3	1026.9	3.20	0.66	1.78
33.07	1.86E-5	2.79E-4	4.951E-3	1.642E-3	1035.5	3.20	0.66	1.79
36.00	1.70E-5	2.79E-4		1.644E-3	1026.4	3.20	0.66	1.72
39.07	1.57E-5	2.78E-4						
39.47	1.53E-5	2.75E-4	4.493E-3	1.657E-3	1009.6	3.20	0.66	1.77
42.00	1.34E-5	2.69E-4	4.422E-3	1.680E-3	981.8	3.20	0.66	1.81
44.00	1.25E-5	2.69E04						
45.07	1.22E-5	2.68E-4	4.157E-3	1.681E-3	1005.9	3.20	0.66	1.81
48.00	1.09E-5	2.66E-4	4.080E-3	1.689E-3	1012.1	3.19	0.66	1.80
51.07	1.10E-5	2.67E-4	3.809E-3	1.697E-3	991.7	3.21	0.66	1.81
52.00	1.06E-5	2.67E-4						

WORKSHEET RUN 12

Time (min)	$[O_3]_l$ (mol/L)	$[O_3]_g$ (mol/L)	[Ni] (mol/L)	O_3 oxidation rate (mol/min)	ORP (mV)	Gas flow (L/min)	Jg (cm/s)	Holdup (%)
0.00	0.00	0.00	1.880E-02		368.8	0.00	0.00	0.00
3.07	2.28E-4	7.13E-4						
6.00	2.13E-4	7.09E-4	1.768E-02	7.984E-5	1140.5	3.22	0.66	1.72
9.07	1.73E-4	6.27E-4	1.720E-02	3.749E-4	1155.9	3.22	0.66	1.67
9.47	1.71E-4	6.19E-4						
12.00	1.28E-4	5.35E-4	1.654E-02	6.937E-4	1152.0	3.19	0.66	1.65
15.07	8.92E-5	4.47E-4	1.588E-02	1.004E-3	1135.5	3.19	0.66	1.62
18.00	6.80E-5	3.95E-4	1.532E-02	1.201E-3	1130.2	3.20	0.66	1.63
19.07	5.86E-5	3.71E-4						
21.07	4.79E-5	3.44E-4	1.472E-02	1.386E-3	1109.3	3.20	0.66	1.59
24.00	3.93E-5	3.20E-4	1.399E-02	1.482E-3	1096.4	3.19	0.66	1.63
27.07	2.71E-5	2.81E-4	1.296E-02	1.632E-3	1074.0	3.20	0.66	1.63
30.00	1.99E-5	2.66E-4	1.272E-02	1.680E-3	1056.3	3.20	0.66	1.64
33.07	1.91E-5	2.63E-4	1.206E-02	1.697E-3	1057.1	3.21	0.66	1.64
36.00	1.40E-5	2.52E-4	1.160E-02	1.735E-3	1030.2	3.21	0.66	1.66
39.07	1.32E-5	2.50E-4	1.103E-02	1.736E-3	1027.1	3.20	0.66	1.68
39.47	1.24E-5	2.50E-4						
42.00	1.01E-5	2.45E-4						
44.00	1.01E-5	2.42E-4	1.052E-02	1.765E-3	1015.2	3.20	0.66	1.67
45.07	1.01E-5	2.42E-4						
48.00	7.83E-6	2.40E-4	9.716E-03	1.775E-3	1008.2	3.20	0.66	1.63
51.07	7.33E-6	2.39E-4						
52.00	7.12E-6	2.39E-4	9.122E-03	1.781E-3	995.5	3.20	0.66	1.71

ADDITIONAL OZONE CONSUMPTION

WORKSHEET RUN 13

Time (min)	$[O_3]_l$ (mol/L)	$[O_3]_g$ (mol/L)	[Ni] (mol/L)	pH	ORP (mV)
0.00	0.00	0.00	2.232E-3	6.85	978.3
4.90	2.12E-4	7.23E-4	2.135E-3	6.83	981.7
9.80	1.41E-4	5.83E-4	1.834E-3	6.81	995.4
14.70	1.12E-4	5.13E-4	1.611E-3	6.82	983.4
20.30	8.11E-5	4.47E-4	1.342E-3	6.81	982.6
25.20	7.30E-5	4.34E-4	1.180E-3	6.81	982.4
30.10	5.95E-5	4.05E-4	1.018E-3	6.81	990.8
35.00	5.23E-5	3.94E-4	8.992E-4	6.80	979.5
39.90	5.04E-5	3.99E-4	8.257E-4	6.79	982.7
44.80	4.44E-5	3.76E-4	8.057E-4	6.79	981.1
50.05	3.98E-5	3.75E-4	7.800E-4	6.77	987.0
54.95	4.03E-5	3.74E-4	8.292E-4	6.77	984.7
60.20	3.90E-5	3.74E-4	7.705E-4	6.76	986.6
65.80	3.99E-5	3.79E-4	7.705E-4	6.78	986.5
71.05	3.60E-5	3.68E-4	7.686E-4	6.77	981.4
74.90	3.72E-5	3.79E-4	8.424E-4	6.77	981.0

WORKSHEET RUN 14

Time (min)	$[O_3]_l$ (mol/L)	$[O_3]_g$ (mol/L)	pH
0	1.667E-7	4.361E-4	7.35
1	1.667E-7	1.012E-4	7.32
2	1.667E-7	5.946E-5	7.25
3	1.667E-7	1.571E-4	7.16
4	1.667E-7	1.491E-4	7.08
5	1.667E-7	1.624E-4	7.00
6	1.667E-7	1.982E-4	6.91
7	1.667E-7	2.018E-4	6.83
8	1.667E-7	2.026E-4	6.77
9	1.667E-7	2.029E-4	6.71
10	1.667E-7	2.032E-4	6.65
11	1.667E-7	2.015E-4	6.58
12	1.667E-7	2.000E-4	6.53
13	1.667E-7	2.000E-4	6.49
14	1.667E-7	1.982E-4	6.45
15	1.667E-7	1.955E-4	6.41
16	1.667E-7	1.917E-4	6.38
17	1.667E-7	1.908E-4	6.35
18	1.667E-7	1.920E-4	6.33
19	1.667E-7	1.914E-4	6.30
20	1.667E-7	1.899E-4	6.29
21	1.667E-7	1.896E-4	6.27
22	1.667E-7	1.867E-4	6.25
23	1.667E-7	1.855E-4	6.23
24	1.667E-7	1.846E-4	6.22
25	1.667E-7	1.840E-4	6.20